TRIBHUVAN UNIVERSITY

INSTITUTE OF ENGINEERING

CENTRAL CAMPUS, PULCHOWK

THESIS NO: G12/071

Analysis of Landslides and Slopes Stabilized Using Single Row of Piles

by

Pravesh Regmi

A THESIS

SUBMITTED TO THE DEPARTMENT OF CIVIL ENGINEERING

IN PARTIAL FULFILLMENT OF THE REQUIREMENT FOR THE DEGREE

OF MASTER OF SCIENCE IN GEOTECHNICAL ENGINEERING

DEPARTMENT OF CIVIL ENGINEERING

LALITPUR, NEPAL

NOVEMBER, 2016

COPYRIGHT

TRIBHUVAN UNIVERSITY
INSTITUTE OF ENGINEERING
CENTRAL CAMPUS
DEPARTMENT OF CIVIL ENGINEERING

The undersigned certify that they have read, and recommended to the Institute of Engineering for acceptance, a thesis entitled "**Analysis of Landslides and Slopes Stabilized Using Single Row of Piles**" submitted by Mr. Pravesh Regmi (071/MSG/812) in partial fulfillment of the requirements for the degree of Master of Science in Geotechnical Engineering.

Supervisor: _____
Dr. Indra Prasad Acharya
Lecturer
Central Campus, Pulchowk, Lalitpur, Nepal.

External Examiner: _____
Prof. Dr. Akkal Bahadur Singh
Central Campus, Pulchowk, Lalitpur, Nepal.

Program Coordinator: _____
Dr. Indra Prasad Acharya
Lecturer
M. Sc. Program in Geotechnical Engineering
Department of Civil Engineering
Central Campus, Pulchowk, Lalitpur, Nepal.

November, 2016

ABSTRACT

Landslide and slope failure phenomenon is recurrent phenomenon in Nepalese Himalaya. The study area comprises the hill slopes along a road stretch of 155 m along Mirchaiya-Katari-Okhaldhunga-Salleri (F052) near Ch. 75+545 to 75+700 situated at right bank of Ghurmi Steel Truss Bridge, Udayapur. The main objective of the research work is to perform certain parametric analysis on general slope to find out optimum value of parameters affecting pile slope system and apply these results on actual pile slope simulation.

The research started with field mapping, data collection, soil sample collection. The material properties have been determined from laboratory and verified by various literatures. The stability analysis was performed in 3D slope stability analysis provided in RS3 and verified by 3D slope stability provided in Plaxis 3D Foundation and various literatures. A general slope is used to perform parametric analysis by varying different factors that affect the stability of pile stabilized slopes. After finding optimum parameters the slope stability analysis of particular slope at Ghurmi is done. The factor of safety of slope before and after using piles is compared.

ACKNOWLEDGEMENT

I wish to express my deepest and sincere appreciation to my supervisor and M. Sc. Geotechnical program coordinator Dr. Indra Prasad Acharya for his guidance, encouragement and critical suggestion throughout the course of this study without whom, this thesis couldn't come in this completion from. I highly appreciate his scholastic attitude and pragmatics thinking over thesis problems.

I can't stop thanking to Dr. Sanjay Kumar Jha for his encouragement and support for the completion of this work.

My sincere thanks goes to all the faculty members of Department of Civil Engineering, Master's Program in Geotechnical Engineering and the classmates of Geotechnical Engineering Batch 2071 for their kind support and suggestions during the entire thesis period.

In addition, I would like to thank all the staff of Central Material Testing Laboratory (CMTL) of Central Campus, Pulchowk, Lalitpur, Nepal for helping me in carrying out my experimental study.

I would like to extend further thanks to all individuals for their direct and indirect help.

At last but not the least, I am grateful to my parents and my wife Uma Sharma for their endless moral support and encouragement during my entire thesis study period. I owe all that I have accomplished up to this point of my life to them.

Pravesh Regmi
071/MSG/812
November, 2016

TABLE OF CONTENTS

LIST OF FIGURES

LIST OF TABLES

ABBREVIATION

Ch.	Chainage
PI	Plasticity Index
LL	Liquid Limit
PL	Plastic Limit
C	Cohesion of soil
Φ	Internal Friction angle of the soil
FEM	Finite Element Method
LEM	Limit Equilibrium Method
SSR	Shear Strength Reduction
SRF	Strength Reduction Factor
FOS	Factor of Safety
GL	Ground Level
USCS	Unified Soil Classification System
ASTM	American Society for Testing and Materials
SW	Strain Wedge
Cc	Coefficient of Curvature
Cu	Coefficient of Uniformity
E	Young's Modulus of Elasticity

CHAPTER 1: INTRODUCTION

1.1 Background

Nepal is located in the heart of the Himalayan arc and occupies nearly one third of the main mountain range. About 83 % of the country is mountainous terrain, and remaining 17 % in the south Indo-Gangetic Plain, the Terai. Owing to the rugged mountain topography, complex and fragile nature of the geological structures resulting from tectonic movement and the intensive rainfall during every monsoon season, serious slope failure has occurred frequently in Nepal. The rapidly increasing construction of infrastructures, such as roads, irrigation canals and dams, without due consideration given to natural hazards, is contributing considerably to triggering landslides. Every year especially during monsoon season, landslides cause a huge economic loss and damage of infrastructure. It imposes marked effect on the lives of local people and has been a cause of many socio-economic problems. Road transport is severely affected of blockade due to slopes failures. Though landslides and related disasters occur frequently in the fragile and young Himalayan region of Nepal, only a few and widely scattered studies has been carried out.

There are various methods for the slope stability analysis i.e. Limit Equilibrium approach and Finite Element method. LEM methods are based on various assumption. And it does not consider the stress-strain behaviour of the soil materials. Hence it could not reveal the progressive nature of the failure of slopes. On contrary Finite Element Methods represents one of the powerful alternative approaches for slope stability analysis which is accurate, versatile and requires fewer priori assumptions. Two dimensional slope stability methods are the most common used methods among engineers due to their simplicity. However, these methods are based on simplifying assumptions to reduce the three-dimensional problem to a two dimensional problem and therefore the accuracy of the analysis results vary. In this research author has attempted to study the stability of slopes by using three dimensional Finite Element Method which best represent actual slope condition.

Traditional geotechnical practices in Nepal were developed during medieval period. Although geotechnics was practiced in Nepal from early times but only a limited use of the modern geotechnics has been made till now.

Agencies which are involved in the field of landslide study and its stabilization are merely practicing same conventional methods for stabilizing the slopes. These approaches seem to be quite inefficient and uneconomic in many cases. Due to lack of research studies, there is suspicion to adopt new efficient and economic methods to stabilize the slopes over current status- quo. Pile stabilisation is a recent development in the field of slope stabilization. Slope stabilizing piles show significant promise however, very scatter research has been made on the field of pile slope stabilization. This thesis report attempts to explore various aspects of pile stabilized slopes so as to make them as engineered solution.

1.2 Landslide Location and Details

The study area comprises the hill slopes along a road stretch of 155 m along Mirchaiya-Katari-Okhaldhunga-Salleri (F052) near Ch. 75+545 to 75+700 situated at Right bank of Ghurmi Steel Truss Bridge, Udayapur. Others details of landslide are as follows:

Landslide location: 27° 10’ 16” N Latitude, 86° 24’ 2.5” E Longitude, Altitude: 376m at base (road) to 396.45m at top.

Geographical Description: Himalaya, Midland and Basin.

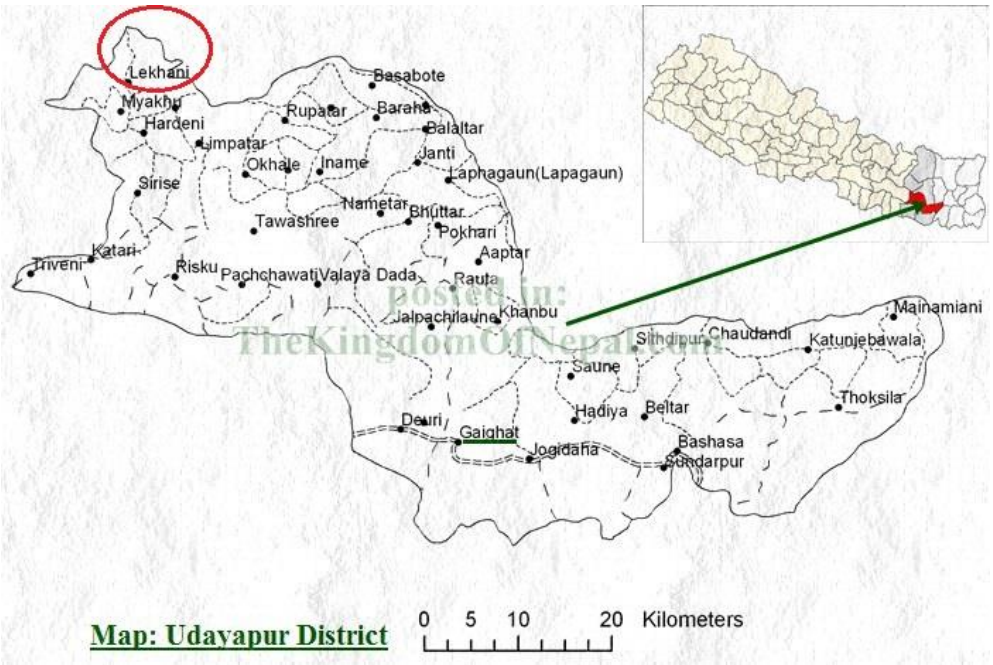

Figure 0.1 Location map of Udayapur district with landslide location at Ghurmi which lies in Lekhani VDC.

Figure 0.2 Google Image of the Landslide area at Ghurmi in 2014.

Figure 0.3 Landslide view from opposite bank (Left Bank) of Sunkoshi River

Figure 0.4 Landslide view which is on the Right bank of Sunkoshi river at Ghurmi Bridge

Figure 0.5 Close up view of Landslide area.

1.3 Objectives

The objective of this research are as follows:

(i) To study characteristics of landslide area.

(ii) To develop reliable 3D finite element model of homogenous soil slopes pertinent to the progressive failure for evaluation of Factor of Safety for the landslide zone.

(iii) To find optimum value of various parameters that affect the stability of pile stabilized sandy slopes.

(iv) Numerically simulate actual landslide with pile stabilization using obtained optimum value of various parameters.

1.4 Scope

When slope failures of highway-slopes are considered, the practical remedies are more limited as the slope crest is commonly the road grade, and the toe is typically at or near the right of- way boundary. In these cases, the crest cannot be modified without significant expense, additional mass cannot be added to the toe, the slope grade cannot be easily modified, and the shear strength of the ground typically cannot be improved without significant expense and traffic disruption. For such ground pile reinforcement techniques appear to be the most realistic approach to achieving stability. The piles can be installed quickly and provide immediate strength improvements. The installation of the piles does not significantly disrupt traffic flow, and they can be installed from the shoulder of the road without completely closing the highway.

This research work covers the analysis of the slope stability of the landslide area. Piles are chosen as the technique to reinforce the slopes over other practicing conventional methods. Improvement in stability of slopes after use of piles as stabilizing measure is analyzed by varying different parameters which influence the stability of pile slope system. Recommendations are made for future research in this subject area.

1.5 Organization of Thesis

The entire thesis is divided into six chapters along with the appendix included at the end of thesis. The first chapter consist of introduction, details of landslide, objective, scope of thesis work. The review of literature about the topic is shown in second chapter. The third consist of methods and steps for doing research work. Fourth include result and outcome of the study. The fifth one consist of verification of stability analysis followed by conclusion and recommendation at last. The conclusion is followed by appendix which consist of remaining chart and details from the research work.

CHAPTER 2: LITERATURE REVIEW

2.1 Landslide

A landslide or landslip is a geological phenomenon which includes a wide range of ground movement, such as rock falls, deep failure of slopes and shallow debris flows. The movement occurs when the shear stress exceeds the shear strength of the material. The causes of slope movement and failure are:

1. Increase in shear stress.
2. Decrease in shear strength.

The factors contributing to an increase of the shear stress are:

- Removal of lateral and underlying support (erosion, previous slides, road cuts and quarries)
- Increase of load (weight of rain/snow, fills, vegetation)
- Increase of lateral pressures (hydraulic pressures, roots, crystallization, swelling of clay)
- Transitory stresses (earthquakes, vibrations of trucks, machinery, blasting)
- Regional tilting (geological movements).

Factors related to the decrease of the material strength are:

- Decrease of material strength (weathering, change in state of consistency)
- Changes in inter-granular forces (pore water pressure, saturation)
- Changes in material structure (decrease strength in failure plane, fracturing due to unloading).

2.2 Types of Landslide

There are many classification schemes for landslides proposed by different authors like Campbell (1951), Hutchinson (1968, 1969, 1977), Crozier (1973), Sharpe (1938) and Varnes (1958, 1978). In which few of them are discussed in Table 2.1.

Falls

A fall starts with the detachment of soil or rock from a steep slope along a surface on which little or no shear displacement takes place. The material then descends mainly through the air by falling, bouncing, or rolling" (Varnes & Cruden, 1996). Typical slope angle of occurrence of falls is from 45-90 degrees. All types of falls are promoted by vibration, undercutting, differential weathering, excavation, or stream erosion.

Table 0.1 Varnes Classification for Landslide (1978)

Types of movement			Type of Material		
			Bedrock	Engineering Soils	
				Predominantly fine	Predominantly course
Falls			Rockfall	Earth fall	Debris fall
Topples			Rock topple	Earth topple	Debris topple
Slide	Rotational		Rock slump	Earth slump	Debris slump
	Translation	Few units	Rock block slide	Earth block slide	Debris block slide
		Many units	Rock slide	Earth slide	Debris slide
Lateral spread			Rock spread	Earth spread	Debris spread
Flows			Rock flow	Earth flow	Debris flow
			Rock avalanche		Debris avalanche
			Deep creep	Soil creep	
Complex and Compound			Combination in time and/or space of two or more principal types of movement.		

Topples

Topples is the forward rotation out of the slope of mass of soil or rock about a point or axis below the center of gravity of the displaced mass. Toppling is sometimes driven by gravity exerted by material upslope of the displaced mass and sometimes by water or ice in cracks in the mass" (Varnes & Cruden, 1996)

Slides

"A slide is a downslope movement of soil or rock mass occurring dominantly on the surface of rupture or on relatively thin zones of intense shear strain." (Varnes & Cruden, 1996).

Translational slide: In translational slides the mass displaces along a planar or undulating surface of rupture, sliding out over the original ground surface." (Varnes & Cruden, 1996)

Rotational Slides: Rotational slides move along a surface of rupture that is curved and concave" (Varnes & Cruden, 1996). The causes of rotational slide are vibration, undercutting, differential weathering, excavation, or stream erosion.

Spread

Spread is defined as an extension of a cohesive soil or rock mass combined with a general subsidence of the fractured mass of cohesive material into softer underlying material." (Varnes & Cruden, 1996). “In spread, the dominant mode of movement is lateral extension accommodated by shear or tensile fractures" (Varnes, 1978). The causes of spread are vibration, undercutting, differential weathering, excavation, or stream erosion.

Flows

A flow is a spatially continuous movement in which surfaces of shear are short-lived, closely spaced, and usually not preserved.

Flows in rock

Rock Flow: "Flow movements in bedrock include deformations that are distributed among many large or small fractures, or even micro fracture, without concentration of displacement along a through-going fracture" (Varnes, 1978). Its causes are Vibration, undercutting, differential weathering, excavation, or stream erosion.

Rock avalanche (Sturzstrom): Extremely rapid, massive, flow-like motion of fragmented rock from a large rock slide or rock fall” (Hungr, 2001). Its causes are vibration, undercutting, differential weathering, excavation or stream erosion.

Flows in soil

Debris flow: Debris flow is a very rapid to extremely rapid flow of saturated non-plastic debris in a steep channel" (Hungr et al.,2001). Its main cause is high intensity rainfall.

Debris avalanche: Debris avalanche is a very rapid to extremely rapid shallow flow of partially or fully saturated debris on a steep slope, without confinement in an established channel. "(Hungr et al., 2001)

Earth flow: Earth flow is a rapid or slower, intermittent flow-like movement of plastic, clayey earth." (Hungr et al.,2001).

Mudflow: Mudflow is a very rapid to extremely rapid flow of saturated plastic debris in a channel, involving significantly greater water content relative to the source material (Plasticity index> 5%)." (Hungr et al.,2001). Its main cause is high intensity rainfall.

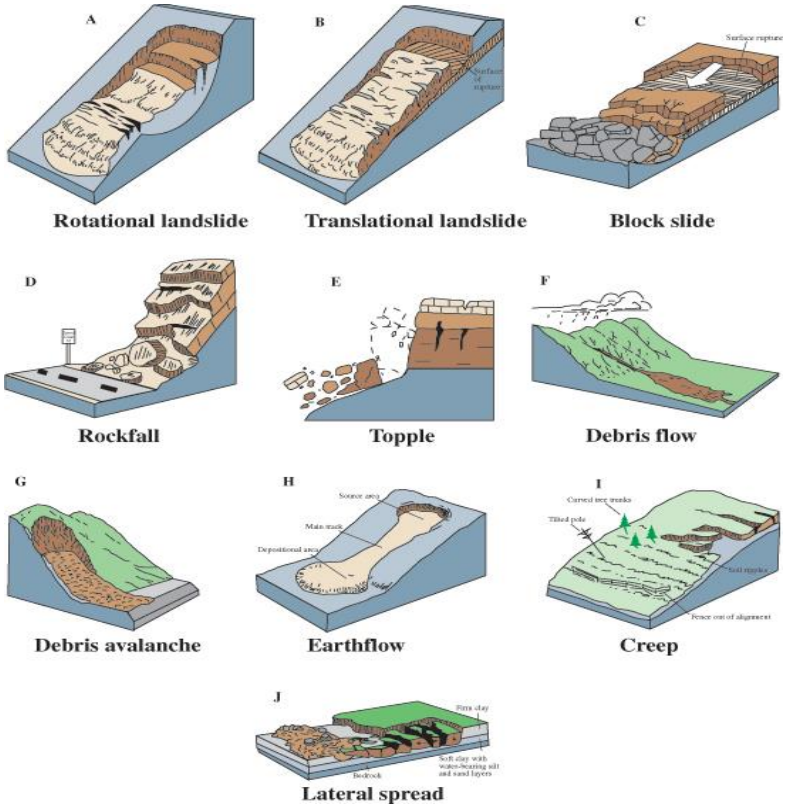

Figure 0.1 Types of landslide and slope failure.

2.3 Slope Stability Analysis

Slope stability analyses are mainly performed to assess the safety factor of a particular slope in a given geologic and physical conditions. For a slope to be stable the resisting forces in the slope must be sufficiently greater than the forces causing the failure (Duncan and Wright 2005). Stability analysis can be used for the following,

1) To assess the safety of a structure in terms of its stability.
2) To locate the critical failure surface and to know it shape of failure.
3) To understand and numerically evaluate the sensitivity of stability to its geologic parameters and climatic conditions.
4) To assess the movement of the slope.
5) To assess remedial measures and aid in their design.

To perform a slope stability analysis, the geometry of the slope, external and internal loading, soil stratigraphy and strength parameters and variation of the ground water table all along the slope must be defined. In the current state of practice, there are many number of slope stability analysis methods available. However, the scope of this report is limited to a discussion on the limit equilibrium methods and finite element methods.

2.4 Limit Equilibrium Methods

Limit equilibrium method is still mostly used for slope stability analysis. This method proceeds with assumption that failure occur by rotational slip by approximately circular failure. The method consists of cutting the slope into fine slices so that their base can be comparable with straight line than to write equilibrium equations (equilibrium of force and/or moment). According to assumption made on the effort between slices, the equilibrium equation considered. Many research work on slope stability analysis were done using this concept. Some of them are Ordinary method of slices (Fellenius 1927), Bishop's modified method (Bishop 1927), Janbu generalized procedure of slices (Janbu 1968), Morgenstern and price's method (Morgenstern and price's 1965), Spencer Method (Spencer 1967). This method does not utilize the stress versus strain parameters of the soils and need assumptions of failure surface shape (circular, log-spiral, piecewise linear, etc.) in advance. It is typically restricted to Mohr-Coulomb soil models.

Limitations of Limit Equilibrium Methods:

1. It is based on assumption that the failing soil mass can be divided into slices. This in turn necessitates further assumptions relating to side force directions between slices.
2. LEM does not consider the stress-strain behavior of the soil materials in slope. It only provides rough estimate of the stability of a slope but doesn't provide any information about the magnitude of movement of the slope.

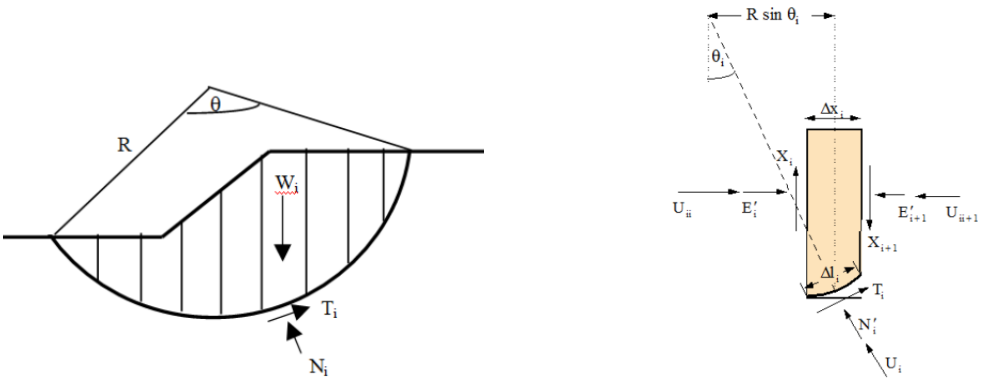

Figure 0.2 Typical representation of a circular slip surface subdivided into vertical slices and forces acting on it.

Table 0.2 : Summary of 2D Limit Equilibrium methods for slope stability analysis (Ducan & Wright , 2005)

Method	Accuracy and Limitations
Ordinary Method of slices (Fellenius 1927)	• Gives a very low Factor of safety value in case of effective stress analysis for flat slopes with high pore water pressures. • Accurate only when φ=0 analysis • Accurate in case of total stress analysis with circular slip surfaces.
Modified Swedish method (Corps of Engineers 1970)	• Applicable for all types of slip surfaces • Factor of safety values are generally higher than the methods which satisfy all the conditions of equilibrium.
Bishop's modified method (Bishop 1955)	• Accurate only when circular slip surfaces are involved • Factor of safety values differ 3% to 5% from the Ordinary method of slices.
Janbu's simplified method (Janbu 1968)	• Accurate method satisfying all equilibrium conditions. • Applicable to any shape of failure surface. • Results in a lower factor safety values than other method satisfying all equilibrium equations.
Spencer's method (Spencer 1967)	• Accurate method satisfying all equilibrium conditions. • Applicable to any shape of failure surface.
Morgenstern and Price Method (Morgenstern and Price 1965)	• Accurate method satisfying all equilibrium conditions. • Applicable to any shape of failure surface.

2.5 Finite Element Method

Majority of the slope stability problem was addressed using the limit equilibrium approaches, which is conventional, simple, and widely accepted to the practicing engineer over the decades. However, these classical techniques have limitations in handling material variation, varying geometry, etc., with large number of assumptions. Numerical techniques appear to be a better alternative to simulate the practical slope stability problem. Number of researchers applied different numerical techniques (continuum and discontinuum) to solve complex problems. The finite element method represents one of the powerful alternative approaches for slope stability analysis which is accurate, versatile, and requires fewer a priori assumptions. The method can be applied with complex slope configurations and soil deposits in two or three dimensions to model virtually all types of mechanisms. The method can be extended to account for seepage induced failures, brittle soil behaviors, random field soil properties, and engineering interventions such as geo-textiles, soil nailing, drains and retaining walls.

The advantages of a FE approach to slope stability analysis over traditional limit equilibrium methods can be summarized as follows.(Griffiths & Lane, 1999)

1. No assumption needs to be made in advance about shape or location of the failure surface. Failure occurs ‘naturally’ through the zones within the soil mass in which the soil shear strength is unable to sustain the applies shear stresses.
2. Since there is no concept of slices in the FE approach, there is no need for assumptions about slice side forces. The FE method preserves global equilibrium until ‘failure’ is reached.
3. If realistic soil compressibility data are available, the FE solutions will give information about deformations at working stress levels.
4. The FE method is able to monitor progressive failure up to and including overall shear failure.

2.6 Engineering measures for landslide disaster mitigation

Some of available **Landslide mitigation measures** listed under 4 titles, (Popescu, 2001).

A. Modification of Geometry

- Removing material from the area driving landslide.
- Adding material to the area maintaining stability.
- Reducing general slope angle.

B. Drainage

- Surface Drain (collecting ditch and pipe).
- Sub-Surface drain (deep drain trench with coarse granular filer material surrounded by geo-synthetic material)
- Buttress of coarse grained material.
- Pumping (Vacuum Dewatering)
- Electro-osmotic Dewatering.
- Vegetation (Hydrological Effect)
- Drainage tunnel, galleries or adits.

C. Retaining Structures

- Gravity retaining walls
- Crib block walls
- Gabion walls
- Passive piles, pier, cassions
- Cantilever R.C.C walls
- Reinforced earth wall (Geo-synthetic, Metallic strip etc.)
- Buttress, Counterfort of coarse grained material
- Rock fall attenuation.

D. Internal slope reinforcement

- Rock bolts
- Micro piles
- Soil nailing
- Geo-synthetics
- Anchors (pre-stressed or not)
- Grouting
- Stone or lime/cement columns
- Heat treatment
- Freezing
- Vegetation (Root Strength)

2.7 Stabilization of slopes using Piles

2.7.1 Suitability of use of piles as slope stabilizing measures

(a) Slope stabilizing piles can provide effective solutions to slope stabilization problems where space and access restrictions that typically occur in highway slopes render alternate approaches unfeasible.

(b) Slope stabilizing piles have not been thoroughly researched, and, while they show significant benefits over the current status- quo, they are not fully understood.

(c) Slope stabilizing piles have a cost similar to other low impact landslide mitigation techniques.

(d) Slope stabilizing piles modeled using finite elements show that piles can provide significant improvements to the factor of safety of a slope.

Slope stabilizing piles show significant promise however, not enough in currently understood about their behavior to make them as engineered solution.

2.7.2 Use of piles as mitigation measures

The use of piles to stabilize active landslides or to prevent instability in currently stable slopes have become one of the most important innovative slope reinforcement techniques over the last few decades. Piles have been used successfully in many situations in order to stabilize slopes or to improve slope stability, and numerous methods have been developed for the analysis of piled slopes (Ito et al., 1981; Poulos, 1995; Chen and Poulos, 1997; Zeng and Liang, 2002; Won et al., 2005).

The piles used in slope stabilization are usually subjected to lateral force through horizontal movements of the surrounding soil; hence they are considered to be passive piles. The interaction behavior between the piles and the soil is a complicated phenomenon due to its 3-dimensional nature and can be influenced by many factors, such as the characteristics of deformation and the strength parameters of both the pile and the soil. The interaction among piles installed in a slope is complex and depends on the pile and soil strength and stiffness properties, the length of the pile that is embedded in unstable (sliding) and stable soil layers, and the center-to-center pile spacing (S) in a row. Furthermore, the earth pressures applied to the piles are highly dependent upon the relative movement of the soil and the piles.

Landslides (slope failure) are critical and likely result from poor land management or seasonal change in the soil moisture conditions. Driven piles, drilled shafts, or micro piles can be installed to reduce the likelihood of slope failure or landslides. At present, simplified methods based on crude assumptions are used to design the driven piles/drilled shafts/micro piles needed to stabilize slopes of bridge embankments or to reduce the potential for landslides. The major challenge lies in the evaluation of lateral loads (pressure) acting on the piles/pile groups by the moving soil. The interaction among piles including the lateral effective range of pile resistance is complex and depends on soil and pile properties and the level of soil-induced driving force. The problem of landslides and the use of piles to improve the stability of such slopes require better characterization of the integrated effect of laterally loaded pile behavior, pile-structure interaction, and nonlinear behavior of pile materials (steel or concrete) on the resulting slope stability

condition. Slope stabilizing pile can be easily and accurately modeled using FEM and has shown significant improvements to FOS in previous researches.

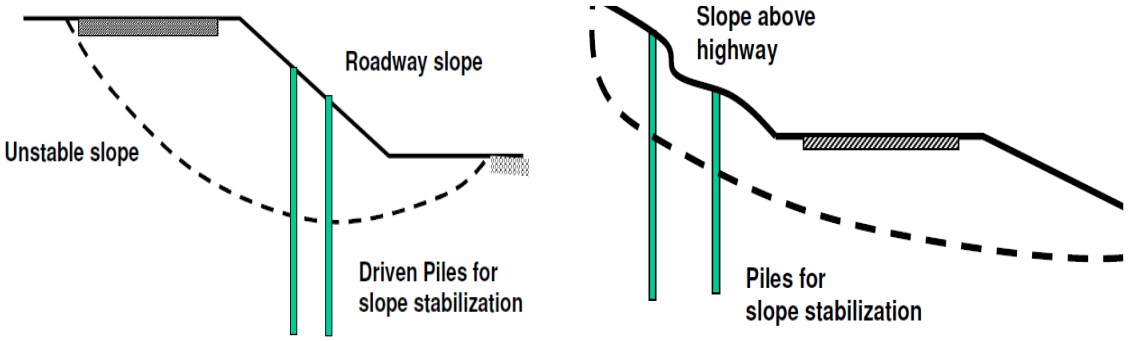

Figure 0.3 Different types of piles stabilized slopes

Figure 0.4 Slope being stabilized using concrete piles

2.7.3 Method of Analysis

Pressure Displacement Method

In this method, the pile is subjected to a presumed slope displacement. This, along with the distribution with depth of the soil modulus and the limiting values of pile-soil contact pressure, has to be pre-specified.

The pile is modeled as a beam connected with the soil through nonlinear springs, at the support of which the displacement of the slope is imposed. Hence, the assessment of pile lateral capacity is accomplished by solving two differential equations:

For the portion of pile above the sliding surface:

$EI\ (d^4y_1/dz^4) = q(z)$, for $z<0$ ……(2.1)

in which y_1 = pile deflection above the sliding surface (assumed to lie at z=0) and EI = pile's bending stiffness. The force intensity, q(z), is calculated using the principle of plastic deformation of soil.

For the portion of pile below the sliding surface:

$EI\ (d^4y_2/dz^4) = -Ky_2$, for $z\geq 0$ ……(2.2)

where y2 = pile deflection below the sliding surface and K is related to the modulus of subgrade reaction of soil.

Despite its simplicity, this approach requires predetermining the slope-displacement profile and the distribution of lateral soil modulus (the assessment of which may require extensive field measurements), as well as the limiting lateral pile-soil pressure with depth. A number of analytical approaches have been developed for the determination of the latter.

Among the most widely accepted are the approaches of Poulos (1973, 1999), Viggiani (1981), and Reese et al. (1992). These methods assume a single laterally loaded pile and correlate the ultimate soil-pile resistance with the undrained shear strength for clays and with the overburden stress and friction angle for sands. A drawback of these methods is that group effects are simplistically taken into account by the application of reduction factors (e.g., Chen and Poulos 1993; Poulos 1995; Guerpillon et al., 1999; Jeong et al., 2003).

Ito and Matsui (1975) developed a plastic extrusion-deformation model for rigid piles of infinite length (and not closely spaced) to estimate the shear resistance offered by a row of piles embedded in a slope. Their approach presumes that the soil is soft and deforms plastically around piles. Despite its rigor, the method neglects pile flexibility, pile limited length, and soil arching-phenomena that may all have a substantial effect (Zeng and Liang 2002; Liang and Yamin 2009). This approach has formed the basis of a number of design methods (Popescu 1991; Hassiotis et al., 1997).

Numerical Methods

In this method, the problem is analyzed by employing finite elements or finite differences. These methods can presently tackle the entire 3D problem, taking into account of the exact geometry, soil-structure interaction and pile group effects.

Because of the dramatic progress in computing and software power over the last few years, the finite element (FE) and finite difference (FD) methods are increasingly popular. These methods provide the ability to model complex geometries and soil-structure interaction phenomena such as pile-group effects. Moreover, they are able to model the three dimensionality of the problem, and may well capture soil and pile non-linearity.

As early as 1979, Rowe and Poulos (1979) developed a two dimensional (2D) finite element approach that, in a simplified way, accounted for the three dimensional (3D) effect of soil flowing through rows of piles.

A 3D elastic FE approach has been developed by Oakland and Chameau (1984) for the analysis of stabilization of surcharged slopes with drilled piles.

Chow (1996) presented a numerical model in which the piles are modeled using beam elements and the soil is modeled using a hybrid method of analysis, which simulates the soil response at individual piles (using the subgrade reaction modulus) and the pile-soil-pile interaction (using the theory of elasticity). This method has been recently used by Cai and Ugai (2000) to analyze the effect of piles on slope stability.

More recently, Kim et al., (2002) and Mujah et al. (2013) introduced a model based on the load-transfer approach to compute the load and deformations of piles subjected to lateral soil movement.

Despite their potential rigor, the application of numerical methods in three dimensions requires extensive computational resources, often becoming unattractive to practitioners (Kourkoulis et al., 2012).

Hybrid Method of Analysis

This method was proposed by Kourkoulis et al. (2012) which develop a hybrid method for designing slope-stabilizing piles, combining the accuracy of rigorous three dimensional (3D) finite elements (FE) simulation with the simplicity of widely accepted analytical techniques. It consists of two steps: (1) evaluation of the lateral resisting force (RF) needed to increase the safety factor of the precarious slope to the desired value, and (2) estimation of the optimum pile configuration that offers the required RF for a prescribed deformation level. The first step utilizes the results of conventional slope-stability analysis. A novel approach is proposed for the second step. This consists of decoupling the slope geometry from the computation of pile lateral capacity, which allows numerical simulation of only a limited region of soil around the piles. A comprehensive validation is presented against published experimental, field, and theoretical results from

fully coupled 3D nonlinear FE analyses. The proposed method provides a useful, computationally efficient tool for parametric analyses and design of slope stabilizing piles.

Uncoupled Method of Analysis

The uncoupled method of analysis for slope stabilizing piles stems for the fact that the pile response (i.e. pile displacement, bending moment, shear force and also pile deflection) and slope stability are considered separately according to their specified method of analysis. A study conducted by Jeong et al., (2003) describes a simplified numerical approach for analyzing the slope-pile system subjected to lateral soil movements. The lateral one-row pile response above and below the critical surface is computed by using load transfer approach. The response of groups was analyzed by developing interaction factors obtained from a three-dimensional nonlinear finite element study. The nonlinear characteristics of the soil-pile interaction in the stabilizing piles are modeled by hyperbolic load transfer curves. The Bishop's simplified method of slope stability analysis is extended to incorporate the soil-pile interaction and evaluate the safety factor of the reinforced slope. Numerical study is performed to illustrate the major influencing parameters on the pile-slope stability problem. Through comparative studies, it has been found that the factor of safety in slope is much more conservative for an uncoupled analysis than for a coupled analysis based on three-dimensional finite element analysis.

(i) The governing equation for the pile deflection can be expressed in separate forms for the pile segments along its z-axis at node, i above and below the interface.

$EI(d^4w/dz^4)_i = K_i[(y_s)_i - w_i]$ …….. (2.3)

$EI(d^4w/dz^4)_i = K_i w_i$ …….. (2.4)

Where, w=Lateral pile displacement

Y_s = free-field soil movement at each depth before pile installation

K_i = Elastic constant of soil

E_s = Initial tangent stiffness

EI = Pile's bending stiffness

δi = relative displacement between free-field soil movement (y_s) and lateral pile displacement (w).

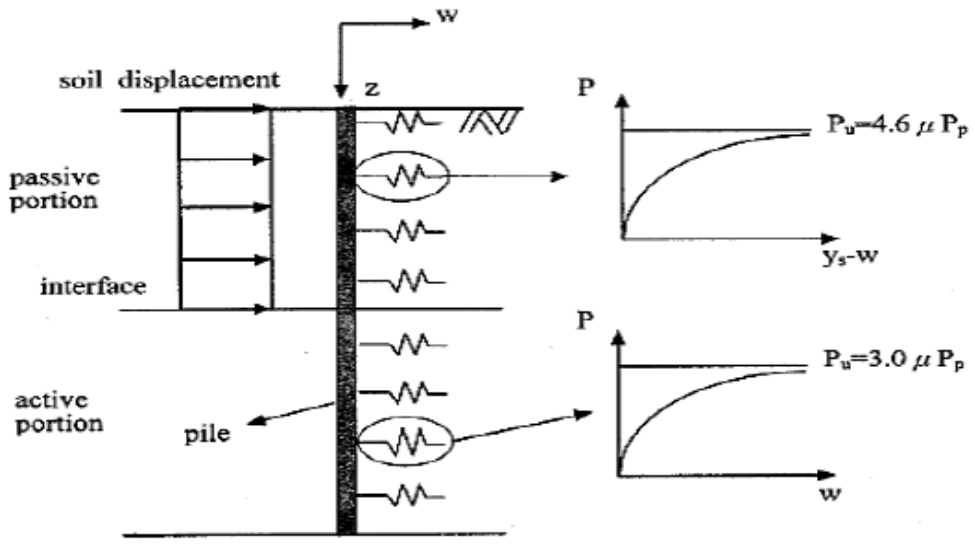

Figure 0.5 A pile subjected to lateral soil displacement (Jeong et al., 2003)

(ii) Safety factor of the reinforced slope with respect to circular sliding is calculated as:

$$F=F_i+\Delta F$$

$$= \frac{MR}{MD} + \frac{Vcr.R.cos\theta - Mcr + Vhead.Yhead}{MD}$$

Where, Fi = safety factor of un-stabilized slope

ΔF = increased safety factor of slope reinforced with pile

Mcr = bending moment at critical surface

Vcr = shear force at critical surface

Vhead = shear force at pile head.

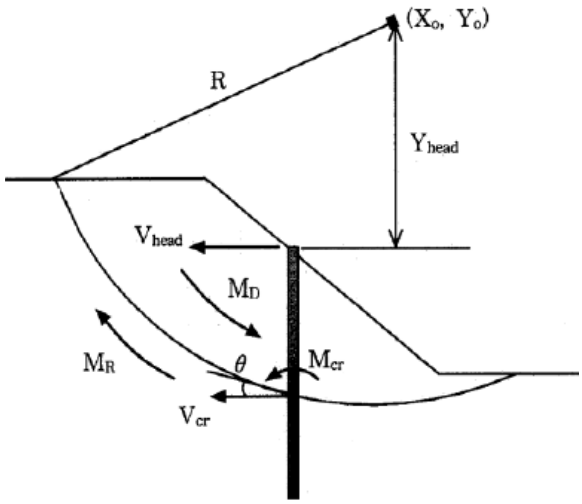

Figure 0.6 Forces on stabilizing piles and slope (Jeong et al., 2003)

Coupled Method of Analysis

Coupled method of analysis is used whenever both pile response and the slope safety factor are considered into account in the stability analysis of slope stabilizing piles. The applicability of this method recently was undertaken by Ashour and Ardalan (2012) in their paper which presents a new procedure for the analysis of slope stabilization using piles. It is the combination of Limit Equilibrium Analysis and Strain Wedge (SW) model technique. The developed method allows the assessment of soil pressure and its distribution along the pile segment above the slip surface based on soil-pile interaction. The proposed method accounts for the influence of pile spacing on the interaction between the pile and surrounding soils and pile capacity. The paper also studies the effect of soil type, and pile diameter, position and spacing on the safety factor of the stabilized slope. Specific criteria are adopted to evaluate the pile capacity, ultimate soil-pile pressure, development of soil flow-around failure and group action among adjacent piles in a pile row above and below the slip surface. The ability of the proposed method to predict the behavior of piles subject to lateral soil movements due to slope instability is verified through a number of full scale load tests.

The characterization of the problem of slope instability and the use of piles to improve the stability of such slopes requires better characterization of the integrated effect of laterally loaded pile behavior, pile-structure-interaction, and the nonlinear behavior of pile materials (steel and/or concrete) on the resultant slope stability condition. The driving force of the soil mass that acts along the pile segment above the slip surface is transmitted to the lower (stable) soil layers, as shown in Figure 2.7. Such a scenario requires representative modeling for the soil-pile interaction above the failure surface that reflects and describes actual distribution for the soil driving force along that particular portion of the pile. In addition, the installation of closely spaced pile row would create an interaction effect (group action) among adjacent piles not only below but also above the slip surface. The presented method allows the determination of the mobilized driving soil-pile pressure per unit length of the pile (PD) above the slip surface based on soil-pile interaction in an incremental fashion using the strain wedge (SW) model technique developed by Norris (1986) and Ashour et al., (1998). The buildup of PD along the pile segment above the slip surface should be coherent with the variation of stress/strain level that is developed in the resisting soil layers below the slip surface. The mobilized non-uniformly distributed soil pressure (PD) is governed by the soil-pile interaction (i.e. soil and pile properties) and developing flow-around failure above and below the slip surface. In addition, the

presented technique allows the calculation of the post-pile installation safety factor (i.e. stability improvement) for the whole stabilized slope, and the slope portions uphill and downhill the pile. The size of the mobilized passive wedge of sliding soil mass controls the magnitudes and distribution of the soil-pile pressure (PD) and the total amount of the driving force (PD) transferred via an individual pile in a pile row down to the stable soil layers. The presented technique also accounts for the interaction among adjacent piles (group effect) above and below the slip surface. Figure 2.8 shows the soil-pile model as employed in the proposed technique. The ability of this method to predict the behavior of piles subject to lateral soil movements due to slope instability is verified through a comparison with two case histories. Also, the efficiency of using stabilizing pile in a slope is discussed by examining the influence of pile location in the slope, pile spacing, pile diameter and stiffness.

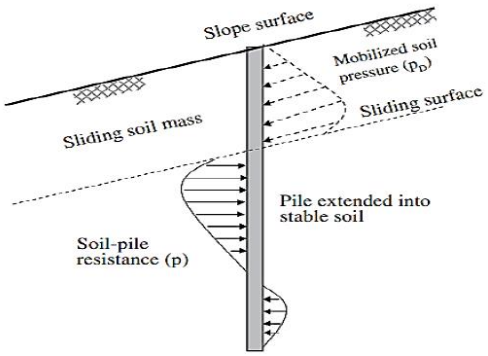

Figure 0.7 Driving force induced by displaced soil mass above sliding surface (Ashour & Ardalan, 2012)

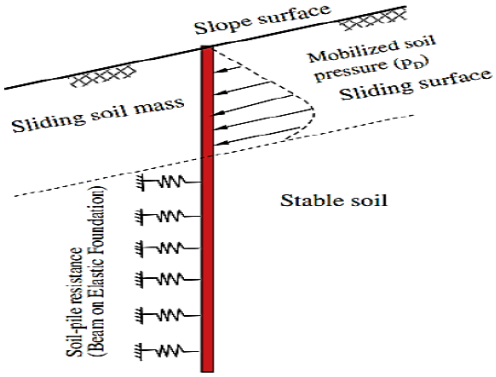

Figure 0.8 Proposed model for soil-pile analysis in pile stabilized slopes (Ashour & Ardalan, 2012)

2.7.4 Parameters affecting pile slope system

2.7.4.1 Effect of pile spacing

The principle of the proposed approach is illustrated in Fig.2.10 which gives the driving and resisting force acting on each pile in a row as a function of the non-dimensional pile interval ratio B/D. The driving force, FD, is the total horizontal force exerted by the sliding mass corresponding to a prescribed increase in the safety factor along the given failure surface. The resisting force, FR, is the lateral force corresponding to soil yield, adjacent to piles, in the hatched area shown in Fig 2.10. FD increases with the pile interval while FR decreases with the same interval. The intersection point of the two curves which

represent the two forces gives the pile interval ratio satisfying the equality between driving and resisting force.

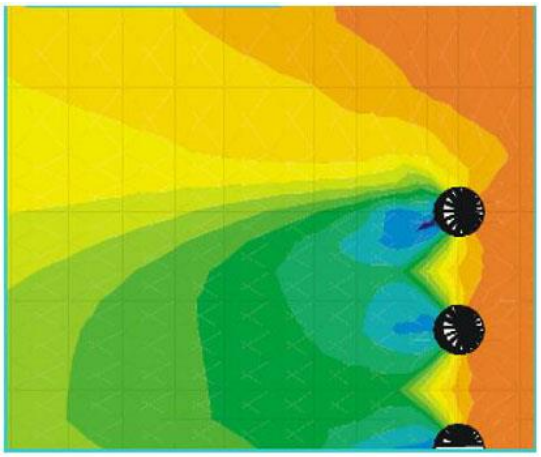

Figure 0.9 Arching of Soil Between two Piles

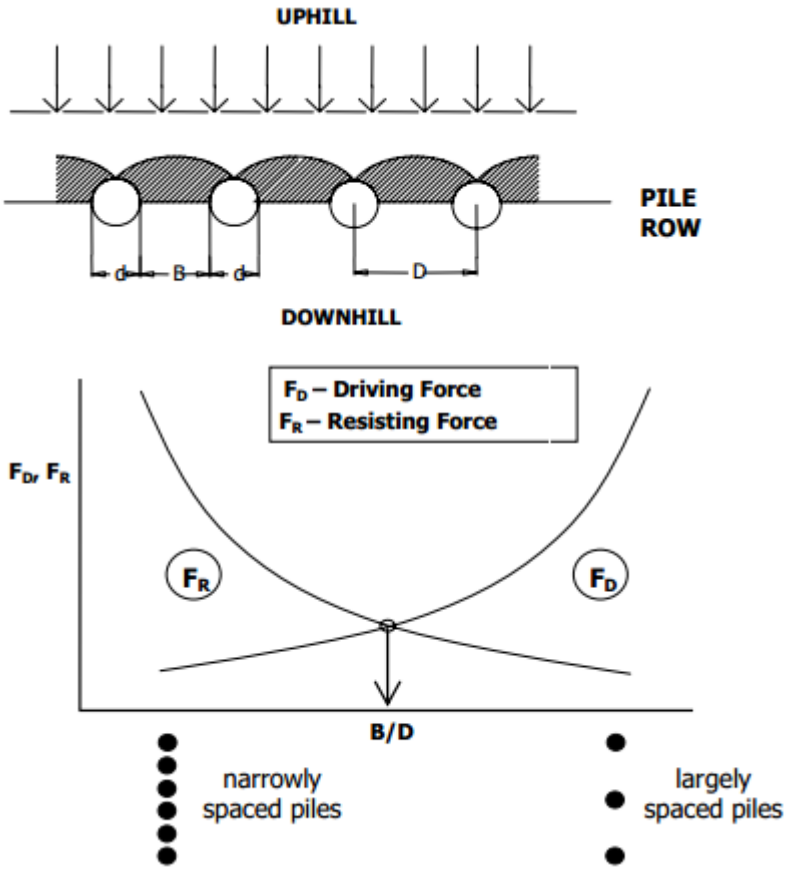

Figure 0.10 Both driving and resisting force acting on each pile in a row should be considered to derive the optimum non-dimensional pile interval ratio B/D.

In general, it has been observed that in sandy slope the safety factor increases up to pile spacing of 4D and there after it decreases on further increase in the spacing. Reason for

the increase in the factor of safety is due to arching of sand between the piles. When piles are at closer spacing they attract more force by resisting the movement of the soil. On increasing the spacing, the relative motion between the pile and soil develops arching of soil and this is effective till the spacing is 4D. Spacing more than 4D provide soil between the piles to move easily thus showing reduction in the factor of safety. The reduction in the factor of safety may be attributed to more loss in the arching effect due to increase in the spacing.

But in case of clay slope the safety factor is reduced marginally with increase in pile spacing.

2.7.4.2 Effect of Pile position

Guidelines for selection of the optimal location of piles in a slope are not well-established. However, there is evidence to suggest that, in order to be effective, stabilizing piles must have the following characteristics:

- they must be of relatively large diameter and relative stiffness
- they must extend well below the critical failure surface so that the failure surface is not merely shifted downwards below the pile tips with a factor of safety still less than the target value
- they should be located in the vicinity of the center of the critical failure circle (or wedge, etc.) to avoid merely relocating the failure surface behind, or in front of, the piles.

In general, it is found that the optimum location of pile is at the center of the slope in case of sandy slope. But in case of clayey soil slope the factor of safety is higher for the pile located towards the toe.

2.7.4.3 Effect of pile Length

In case of sandy soil slope, the length to depth ratio (L/H) (where L is length of pile and H is height of slope) is effective if the ratio lies between 1 and 1.5. Length to depth ratio more than 1.5 do not add factor of safety further. But in case of clayey soil slope, the length to the depth ratio is effective if the ratio lies between 1 and 2.5.

2.7.4.4 Effect of Pile Stiffness

The effect of stiffness of the pile in the soil slope are represented in terms of stiffness factor K=EpIp/EsIs. The stiffness of the pile mainly depends on the diameter of the pile and also depends on the elastic modulus of the pile (Ep) and the soil (Es). The safety factor increases with increase in stiffness of the pile but its contribution to factor of safety is insignificant irrespective of soil type and their strength particularly if stiffness factor is more than 0.002. Thus pile of high rigidity is not favorable to increase the safety.

2.7.4.5 Effect of slope angle

The safety factor increases with decrease in slope angle both in clay and sandy slopes.

CHAPTER 3: RESEARCH APPROACH AND METHODOLOGY

The research starts with desk study of article based on landslide research of similar slides. All the technical information was collected in the field. Primary and Secondary data were collected from different sources. Laboratory test were performed in CMTL lab and Soil lab of IOE, central campus to determine required parameters. From the contour data the slope profile is prepared in AutoCAD.

The numerical analysis is carried out using a 3D finite element formulation provided in the RS ^{3}(RS^3= Rock and soil 3 dimensional analysis) developed by Rocscience(2016).

3.1 Data Collection/Field visits/Surveys

It includes collection of technical information and facts regarding the landslide from field visit and from different literatures. The data to be collected are primary data, secondary data and other technical information.

The technical information such as approximate geological, geotechnical, hydrological information were gathered during field visit. Since the undisturbed sampling at the site is very tedious, disturbed but representative sample of debris from pit of 1ft deep 1×1×1 cu. ft. are taken from the site for the laboratory test.

Secondary data collection

This step mainly includes second hand data collection from related organizations. In this process existing maps of that area, geological maps, the concerned journals, books, correlated publications, various article, research papers etc. are beneficial.

Primary data collection

The primary data collection starts from field visit. The disturbed but representative samples are collected in the field. The primary data collection, in general, comprise the collection of technical information and facts regarding soil strength properties (cohesion and friction angle) during site visit from soil collected. The first hand data regarding properties of soil, geographical and geological data, are collected during this step which especially influences the stability of slope.

3.2 Laboratory tests

3.2.1 Grain Size Distribution/ Particle Size Distribution

The test is done to determine the percentage of different sized particle of soil/ debris remained in the landslide area. The sieve analysis is performed to determine the distribution of the coarser, larger-sized particles. The distribution of different grain sizes affects the engineering properties of soil and it is required in classifying the soil. Following results are obtained during the test from the three samples collected from site

which are tabulated. Sample of calculation table and graph is shown below and remaining tables and graph of different location are listed on annex A.

Table 0.1 Sample calculation of sieve Analysis of Sample 1

Sample No: 1		Location: Right Bank of Ghurmi Bridge, Udayapur			
Site: 1					
Depth of Sampling: 0.75 m from Ground					
Weight of sample for wet sieve: 2725 gm					
S.N.	Observation		Calculation		
	Sieve Opening (mm)	Wt. of Soil retained in gm	% Retained	Cumulative % Retained	% Passing
1	50.8	192.8	7.08	7.08	92.92
2	38.1	0	0.00	7.08	92.92
3	25.4	151.6	5.56	12.64	87.36
4	19.1	190.05	6.97	19.61	80.39
5	12.7	238.4	8.75	28.36	71.64
6	9.52	161.6	5.93	34.29	65.71
7	4.76	352.2	12.92	47.22	52.78
8	2	197.5	7.25	54.46	45.54
9	0.84	301.3	11.06	65.52	34.48
10	0.42	157.7	5.79	71.31	28.69
11	0.25	192.1	7.05	78.36	21.64
12	0.149	136.5	5.01	83.37	16.63
13	0.074	97.4	3.57	86.94	13.06
14	Pan	355.85	13.06	100.00	0.00
		2725	100.00		

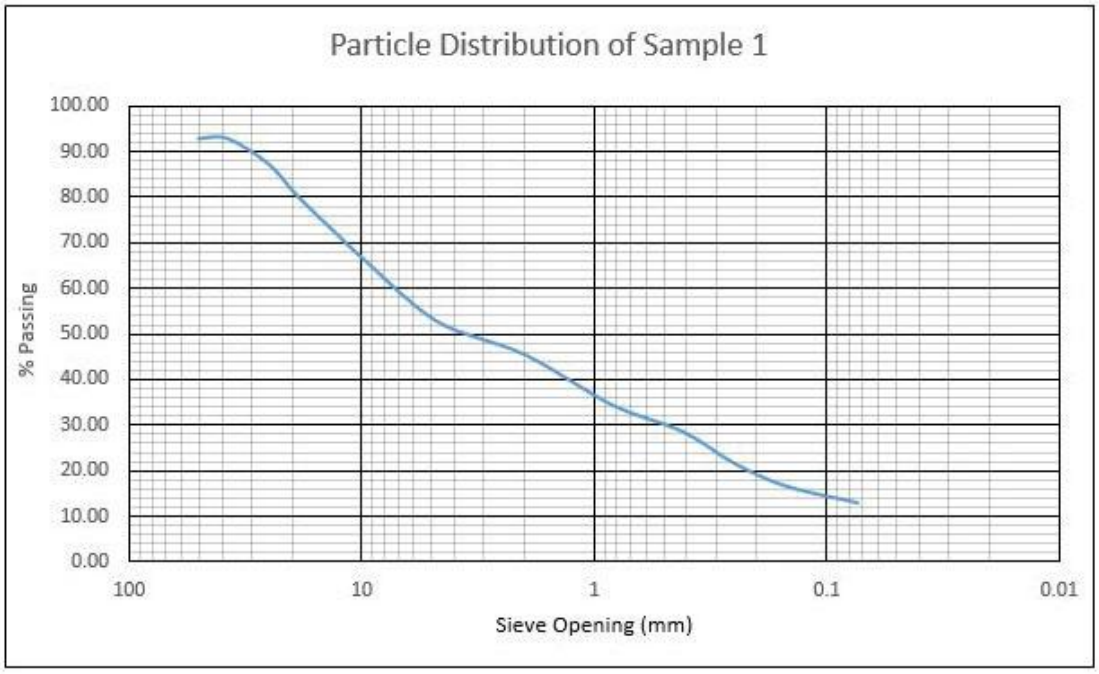

Figure 0.1 Particle Size Distribution of Sample 1

% Passing 75μ sieve = 13.06 % (Coarse Grained Soils)

% Passing 4.75 mm sieve = 52.78 % (Sands)

% Fines = 13.06 % (Sand with Fines)

PI = 0.73 (LL-20) = 0.73(20-20) =0 {PI= LL-PL=20-0=20} (Plots above A-Line) (SC)

% Gravel = 40.14 % (Clayey Sand with Gravel)

3.2.2 Liquid Limit and Plastic Limit test

The liquid limit and plastic limit is determined for fine contained in the soil. Liquid limit is percentage of water content required to close the soil 13mm (1/2 inch) in standard Casagrande apparatus by 25 number of blows with cup dropped from height of 10 mm in each drop. Plastic limit is the water content in which soil just start crumbling while rolled into 3.2 mm diameter threads. Plastic limit defines the water content in transition from plastic state to semi solid state whereas liquid limit defines the water content which is transition from liquid state to plastic state. Sample calculation table and graph of the one section is shown below.

Table 0.2 Liquid Limit and Plastic Limit Calculation

ATTERBERG LIMITS TEST						
Location: Ghurmi, Udayapur						
Liquid Limit						
SN	Determination	Unit	Observation and Calculation			
1	Container No.		PB	B9	3	3B
2	No. of Blows	no.	19	14	27	7
3	Wt. Cont. + Wet Soil	gm	38.62	36	40.21	36
4	Wt. Cont. + Dry Soil	gm	35.18	32.55	36.5	31.67
5	Wt. Water	gm	3.44	3.45	3.71	4.33
6	Wt. Container	gm	19.2	17.88	17.55	15.74
7	Wt. Dry Soil	gm	15.98	14.67	18.95	15.93
8	Water Content	%	21.52691	23.51738	19.57784	27.18142
Plastic Limit : Non-Plastic						

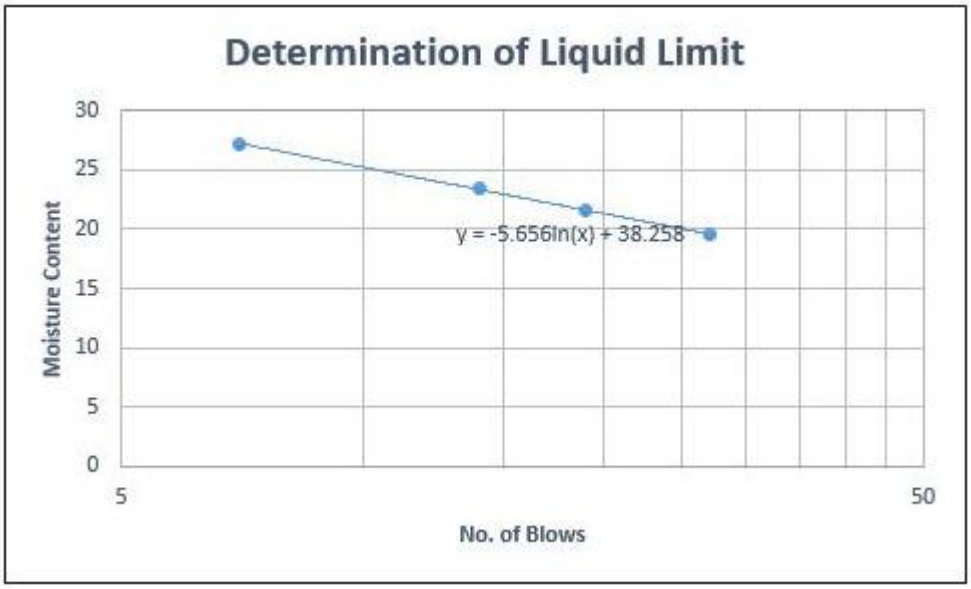

Figure 0.2 Chart of Liquid Limit and Number of Blows

From Chart LL = 20%

Average Plastic Limit = 0%

Plasticity Index = LL-PL = 20%

From equation of A Line, PI of A line = 0% (Since, PI=0.73(LL-20) from chart)

PI obtained is more than PI from chart therefore the soil is Clayey sand.

3.2.3 Shear Parameters (C, ϕ)

This test is performed to determine the consolidated -drained shear strength of a sandy to silty soil. The shear test is done to determine shear stress parameters.

A direct shear test apparatus was used to determine the shear strength parameter of the soil. In the apparatus on the variation of normal load (5kg, 10kg, 15 kg or 4kg, 8kg, 12 kg) applied and corresponding maximum shear stress is determined. On constant normal load shear stress increased with displacement at interval 20mm to determine maximum shear stress. Graph of horizontal shear stress versus displacement, shear stress versus normal stress of one sample is shown below and remaining are listed on annex A.

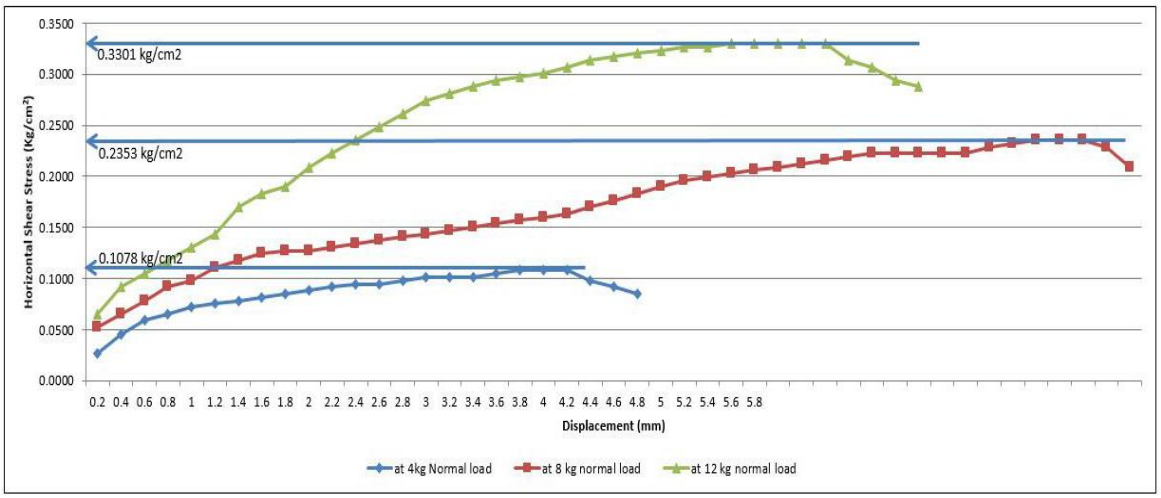

Figure 0.3 Horizontal Shear Stress versus Displacement of one sample

Table 0.3 Horizontal Shear Stress versus Displacement of one sample

S.No.	Normal Stress (kg/cm2)	Shear stress at failure (kg/cm2)	Displacement at failure (mm)
1	0.153787005	0.1078	4.2
2	0.30757401	0.2353	8.6
3	0.461361015	0.3301	6.4

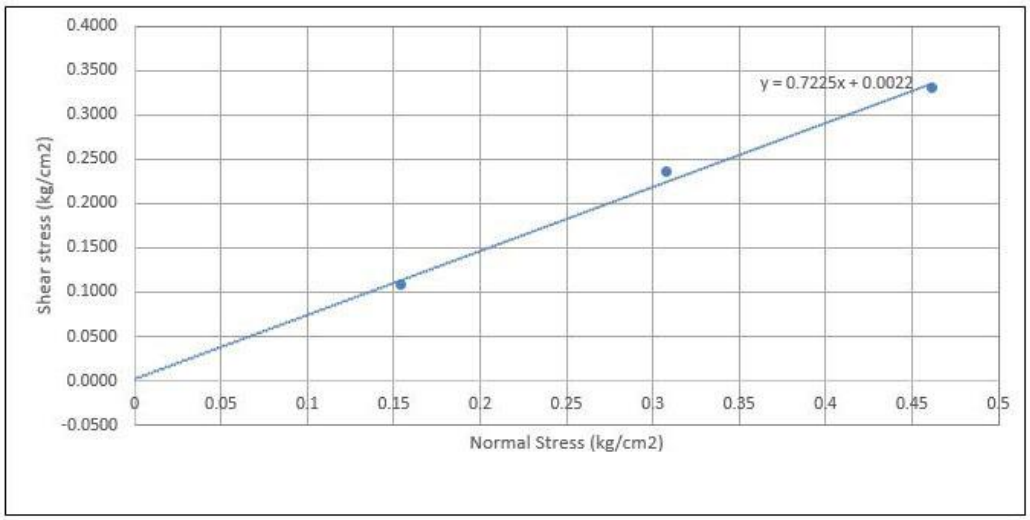

Figure 0.4 Horizontal Shear Stress versus Displacement of one Sample.

Table 0.4 Soil Properties obtained from different samples

Sample No.	Gravel %	Sand %	Fines %	USCS Classification	Dry Density (KN/m^3)
1	40.14	52.78	13.06	Clayey Sand with Gravel	18
2	51.94	48.06	12.03	Clayey Sand with Gravel	18
3	31.32	41.06	9.74	Poorly Graded Gravel with Clay and Sand	18

Table 0.5 Shear parameters obtained from different samples

Sample	Cohesion (kg/cm^2)	Friction Angle (°)
1	0.02	35.848
2	0.02	39.505
3	0.02	42.28

3.3 Finite Element Modelling

3.3.1 Brief description of the finite element model

The soil is initially assumed to be elastic and the model generates normal and shear stresses at all Gauss Points within the mesh. These stresses are then compared with the Mohr-Coulomb failure criterion. If the stresses at a particular Gauss point lie within the Mohr-Coulomb failure envelope, then that location is assumed to remain elastic. If the stresses lie on or outside the failure envelope, then that location is assumed to be yielding. Yielding stresses are redistributed throughout the mesh utilizing the visco-plastic algorithm (Perzyna,1966; Zienkiewicz & Cormeau, 1974). Overall shear failure occurs when a sufficient number of Gauss points have yielded to allow a mechanism to develop.

Soil Model

The model commonly used is six parameter model

Φ'-Friction Angle

C'-Cohesion

Ψ- Dilation angle

E- Young's modulus

υ-Poisson's ratio

γ - Unit Weight

If a value of Poisson's ratio is assumed (typical drained values lie in the range $0.2<\upsilon'<0.3$), the value of Young's modulus can be related to the compressibility of the soil as measured in a one-dimensional oedometer (e.g. Lambe & Whiteman, 1969):

$E'=(1+\upsilon')(1-2\upsilon')/mv(1-\upsilon')$ where mv coefficient of volume compressibility.

Although the actual values given to the elastic parameters have a profound influence on the computed deformations prior to failure, they have little influence on the predicted factor of safety in slope stability analysis. Thus in the absence of meaningful data for E' and υ' they can be given nominal values (e.g $E'=10^5$ KN/m^2 and $\upsilon'=0.3$)

Factor of safety

FOS is computed by using factored shear strength parameters c_f' and ϕ_f' which is based on 'strength reduction technique'(e.g. Matsui & San, 1992)

$C_f' = C'/FOS$

$\Phi_f' = \arctan(\tan\phi'/FOS)$

Definition of Failure

When the algorithm cannot converge within a user-specified maximum number of iterations, the implication is that no stress distribution can be found that is simultaneously able to satisfy both the Mohr-Coulomb failure criterion and global equilibrium. If the algorithm is unable to satisfy these criteria, 'failure' is said to have occurred. Slope failure and numerical non-convergence occur simultaneously, and are accompanied by a dramatic increase in the nodal displacements within the mesh. Results can be represented in the form of a graph of FOS versus $E'\delta_{max}/\gamma H^2$ (a dimensionless displacement), where δ_{max} is the maximum nodal displacement at convergence and H is the height of the slope.

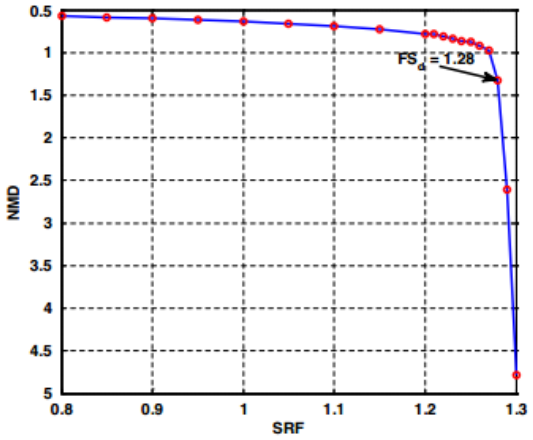

Figure 0.5 FOS versus dimensionless displacement. The rapid increase in displacement and the lack of convergence when FOS= 1.28 indicates slope failure.

3.2.2 RS^3

RS^3 is a brand new program for 3D analysis of geotechnical structures for civil and mining applications. Applicable for both rock and soil (*RS*^{3} = Rock and Soil 3-dimensional analysis program), *RS3* is a general purpose finite element analysis program for underground excavations, tunnel and support design, surface excavation, foundation design, embankments, consolidation, groundwater seepage and more.

3-dimensional model geometry is built up by creating a series of extruded 2-dimensional slices. Excavation and material boundaries can be defined independently for each slice, allowing you to easily create complex 3D models from a series of extruded 2D slices. The overall model orientation is defined by a primary axis, which can be horizontal, vertical or at any angle.

Finite element discretization and meshing

Meshing is automatic and 3-dimensional using uniform10-noded tetrahedral elements.

Boundary condition

Fixed boundary conditions are assumed along the base of the model, x restraint along the front and rear face, z restraint along lateral face and xz restrain along the four corner. The slope face was kept free.

Gravity loading

In the loading step, each finite element is given both an initial stress and a body force (self-weight). The initial vertical stress is estimated from the weight of the material above the element. RS3 automatically determines the ground surface above the element and the stress due to the material above the element. The horizontal to- vertical stress ratio σ_H/σ_V is kept as 1.0 (Pal et al. 2012).

Factor of safety

In RS3 SRF should be computed by using manual reduction of shear strength parameters.

Mesh convergence study

RS3 uses Newton-Raphson schemes for iteration. This iterative procedure is shown to be most robust and most economical in terms of computing time (Zdravkovic (2001a)). The force displacement relation spring can be written as

$P=KU$

P is the load applied, U the displacement and K is the non-linear stiffness of the spring which is held as a constant for each load step. The initial force is known, final force is also known from the load increment given, and current displacement is calculated with known stiffness and the difference between initial and final forces. This iterative procedure is continued until the difference between the forces are negligible and reduced to a set tolerance limit. The concept can be mathematically explained with following equations and Figure 3.6. The final displacement is cumulative displacement that occurred in all the iterations.

$K_O \Delta U_1 = P(n+1) - F_O$

$\Delta U_1 = K_O^{-1} (P_{(n+1)} - F_O)$

$U_{(n+1)} = U_n - \Delta U_{(1)}$

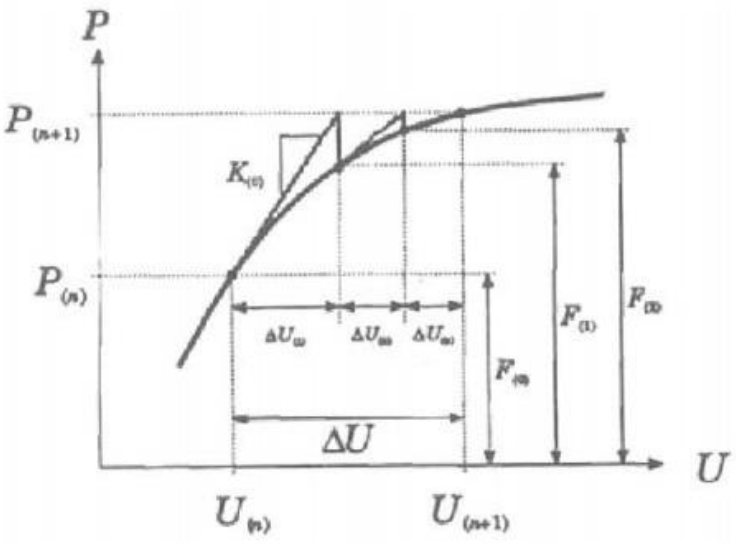

Figure 0.6 Iterative Scheme adopted in Newton Raphson method.

For plasticity analysis it tackles the problem by first obtaining an elastic solution, the stresses are checked against the yield criteria, if the yield criterion is violated plastic deformation takes place (Cai (2008)).

Input parameters and model considered

Different properties of the soil are determined from laboratory test are verified by using various literatures.

In the study author has used two types of model for the study. First type of model is used to determine optimum value of various parameters that influence the stability of pile slope system in case of sandy soil. This slope has been referred as General slope. Second type of slope is the actual slope at Ghurmi which has to be stabilized using pile reinforcement. This slope has been referred as Ghurmi Slope.

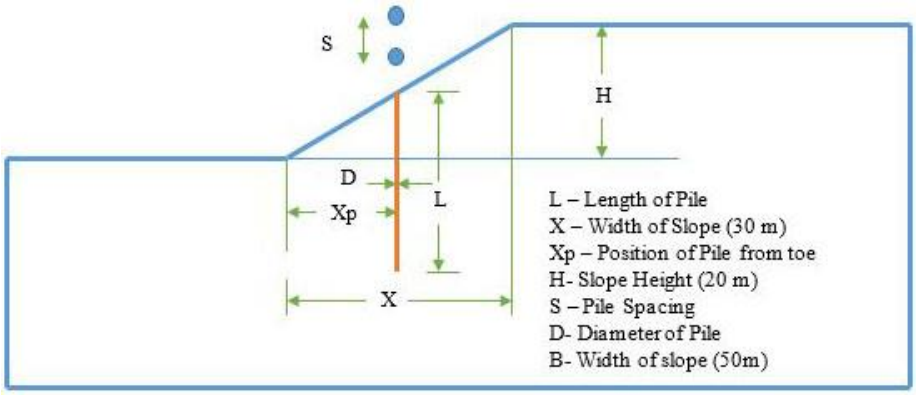

Figure 0.7 Geometry of the Pile Slope system for General Slope

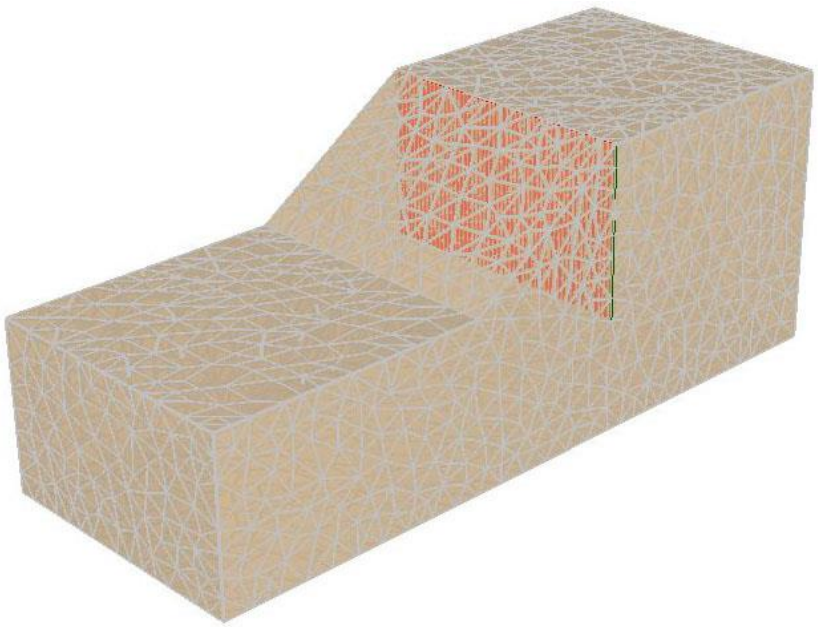

Figure 0.8 Model generated in RS3 for General Slope

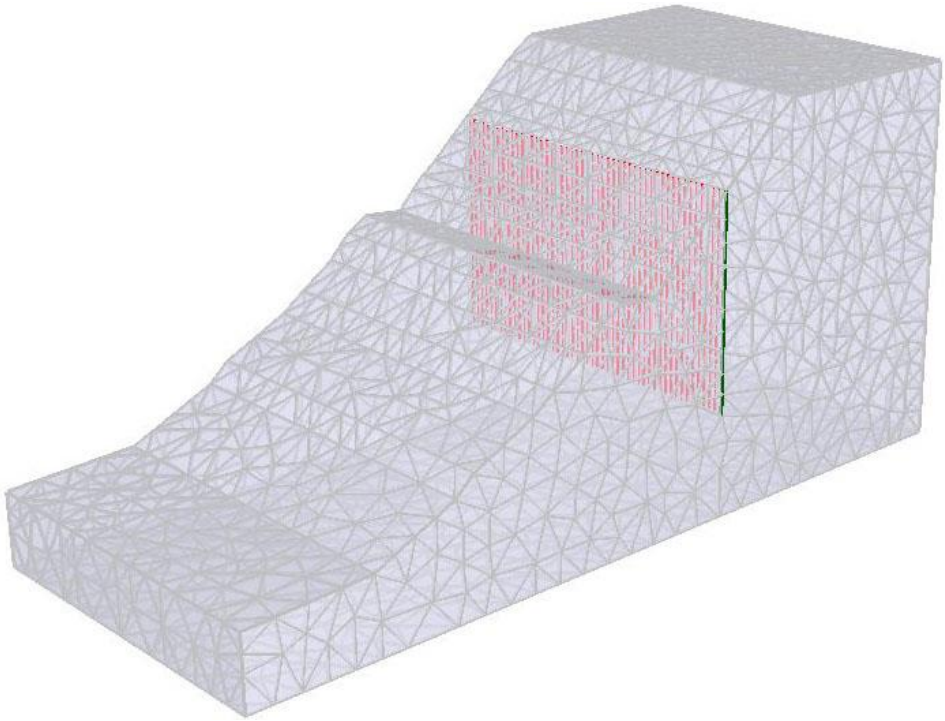

Figure 0.9 Geometry for pile soil system generated in RS3 for Ghurmi slope

Material model for soil:

Material: Clayey sand with gravel

Failure Criteria: Mohr-coulomb

Unit weight = 18 KN/m^3

Elastic Properties (Griffiths & Lane, 1999)

Modulus of elasticity = 10^5 Kpa

Poisson ratio = 0.3 (Griffiths & Lane, 1999)

Shear parameters (from laboratory test)

Cohesion (peak) = 2 Kpa

Angle of friction (peak) = 36°

Material model for Pile:

Material: Concrete

Element Formulation =Timoshenko

Unit weight = 25 KN/m^3

Modulus of elasticity = 35*10^6 Kpa

Poisson ratio = 0.2

Diameter of Pile =0.5 m

CHAPTER 4: RESULTS AND OUTCOMES

4.1 Parametric Analysis for Sandy Slope

4.1.1 Analysis using different Length of Piles

The factor of safety is computed by using manual shear Strength Reduction Technique. The length of pile is varied from 0 to 2 times of the height of the general slope. As the angle of internal friction of the Ghurmi site is about 36 degrees, so the same analysis procedure is repeated varying the value of ϕ for 30, 35 & 40 degrees. The sample calculation is shown in figure below and other calculations are attached in Annex.

Table 0.1 FOS computed for general slope having ϕ=40 degrees and L=1.5H using Manual shear Strength Reduction Technique.

FOS	ϕ(Degrees)	C (KN/m^2)	δ_{max}	NMD	Remarks
1.0000	40.0000	2.0000	0.0674	0.9356	
1.1000	36.3636	1.8182	0.0690	0.9583	
1.2000	33.3333	1.6667	0.0706	0.9803	
1.3000	30.7692	1.5385	0.0731	1.0153	
1.4000	28.5714	1.4286	0.0777	1.0789	
1.5000	26.6667	1.3333	0.2369	3.2899	
1.6000	25.0000	1.2500	0.7967	11.0650	
1.7000	23.5294	1.1765	1.5878	22.0529	
1.8000	22.2222	1.1111	1.4174	19.6867	
1.9000	21.0526	1.0526	1.8374	25.5190	
2.0000	20.0000	1.0000	1.6276	22.6058	
2.0400	19.6078	0.9804	3.3811	46.9599	
2.0500	19.5122	0.9756	3.4115	47.3825	
2.0700	19.3237	0.9662	2.6459	36.7483	
2.0900	19.1388	0.9569	2.9054	40.3529	
2.1000	19.0476	0.9524	5.7555	79.9372	Unstable

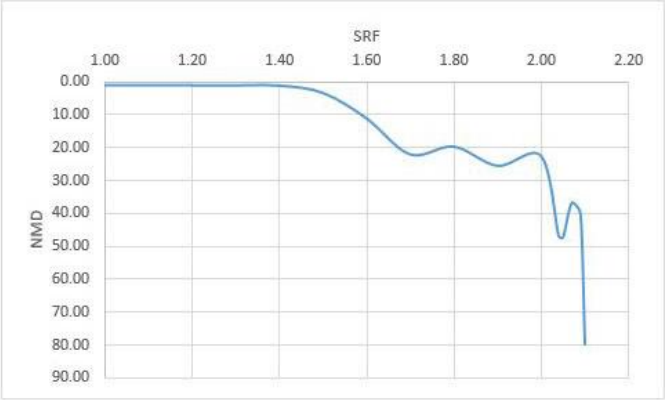

Figure 0.1 FOS plotted against Normalized Maximum Displacement (NMD) of general slope having ϕ=40 degrees and L=1.5H

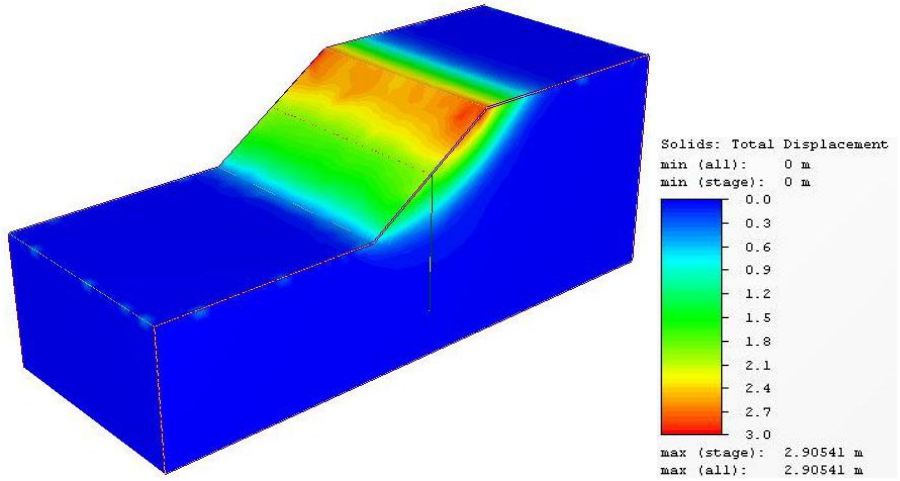

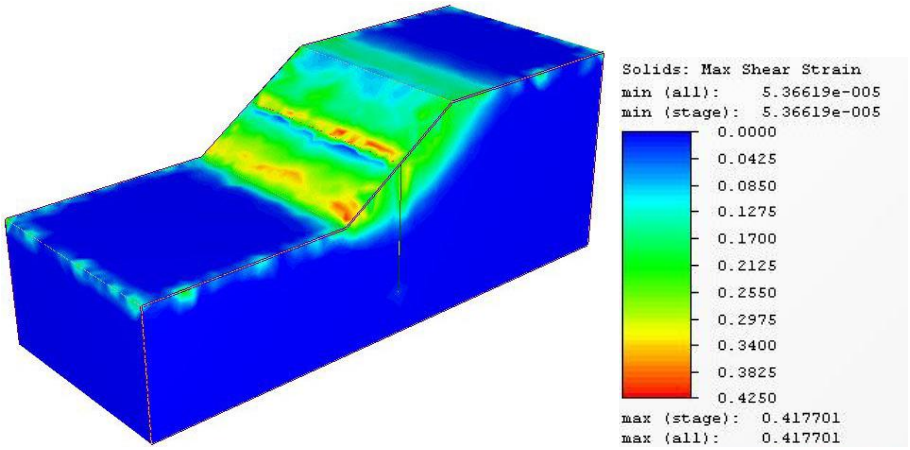

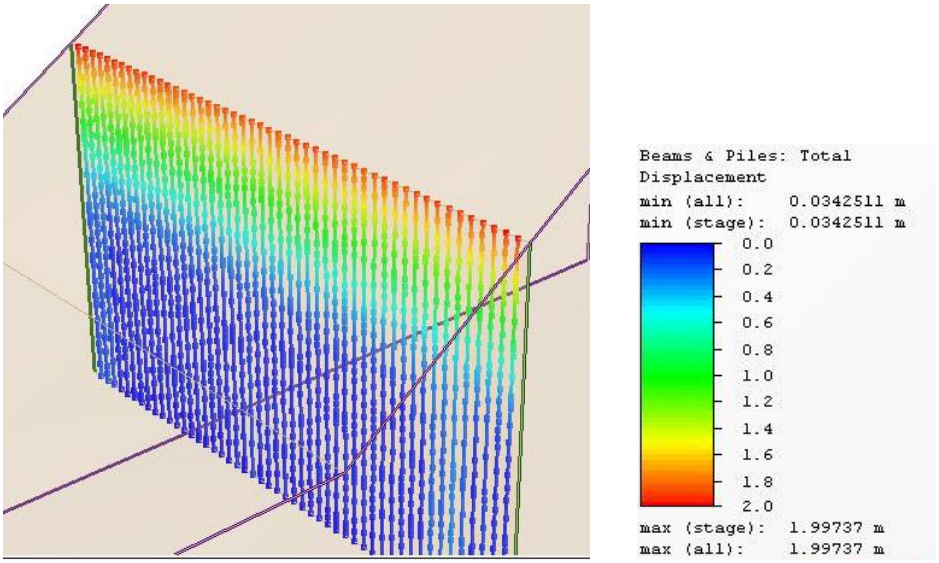

Figure 0.2 Slope displacement, Slope shear strain and pile displacement of general slope having ϕ=40 degrees and L=1.5H at critical FOS

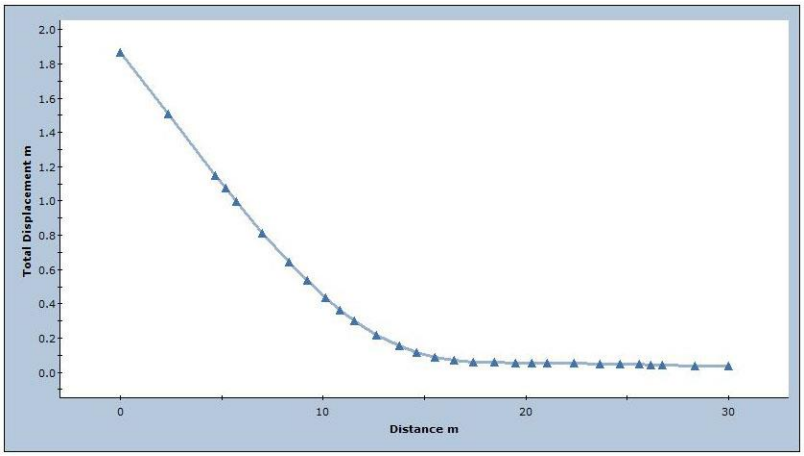

Figure 0.3 Total Displacement profile of a pile at center of general slope having ϕ=40 degrees and and L=1.5H at critical FOS

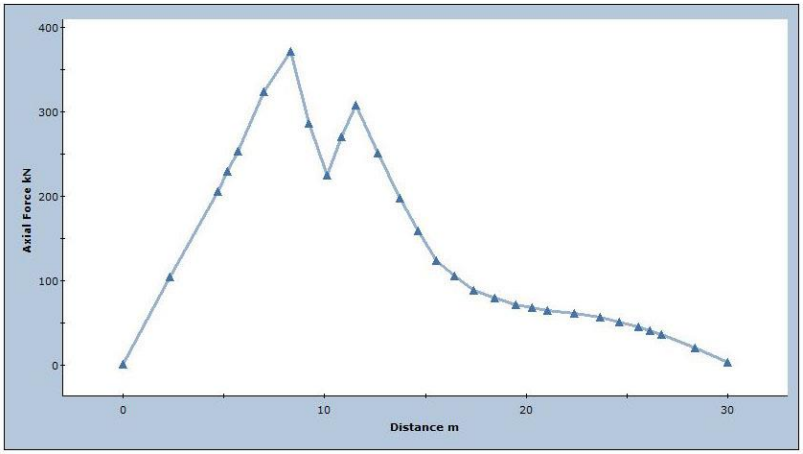

Figure 0.4 Axial Force profile of a pile at center of general slope having ϕ=40 degrees and and L=1.5H at critical FOS

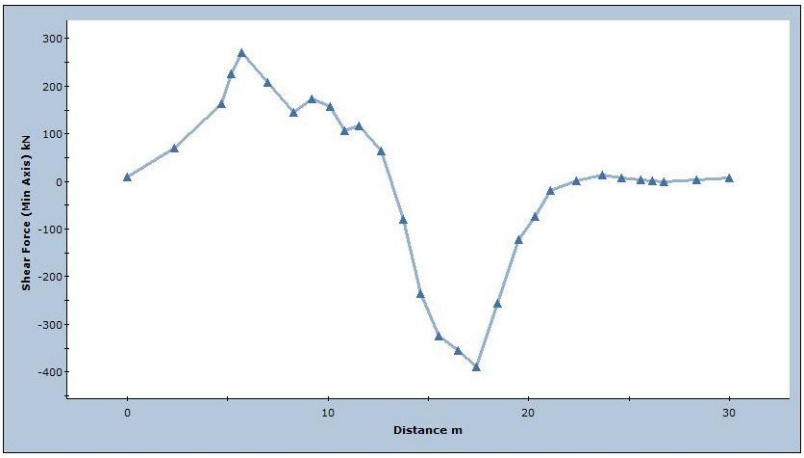

Figure 0.5 Shear Force profile of a pile at center of general slope having ϕ=40 degrees and L=1.5H at critical FOS

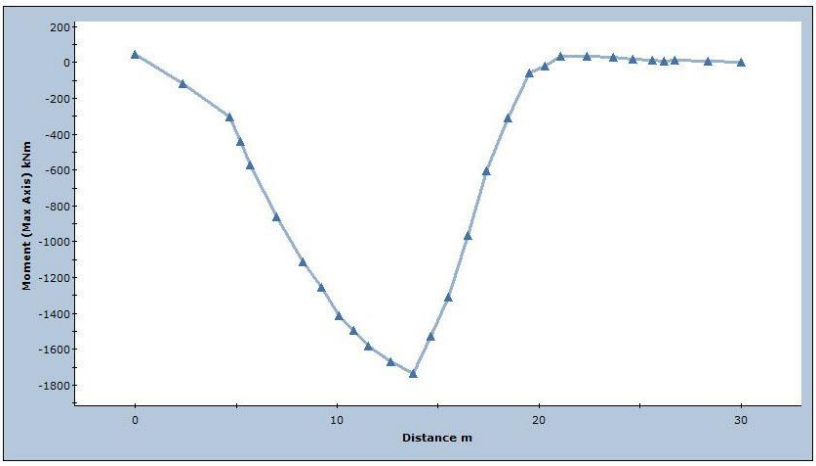

Figure 0.6 Bending Moment profile of a pile at center of general slope having ϕ=40 degrees and L=1.5H at critical FOS

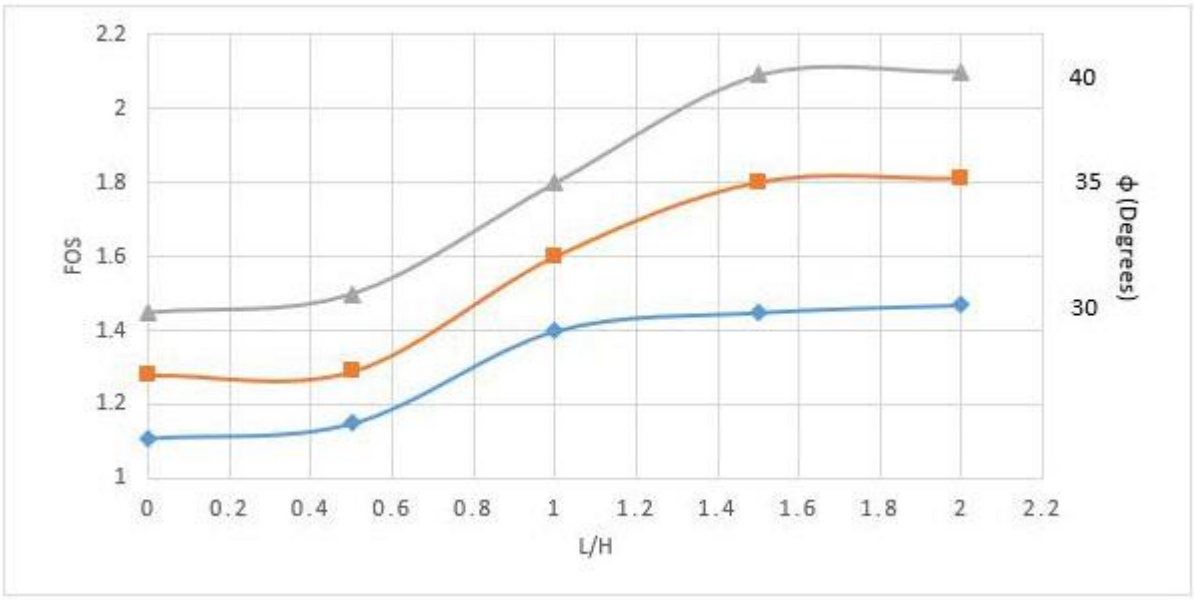

Figure 0.7 Variation of Safety factor with respect to length of the pile for sandy slope.

4.1.2 Analysis for different position of piles on slopes

Table 0.2 FOS computed for general slope having ϕ=35degrees and Xp/X=1 using Manual shear Strength Reduction Technique.

FOS	ϕ(Degrees)	C (KN/m^2)	δ_{max}	NMD	Remarks
1.0000	35.0000	2.0000	0.0688	0.9562	
1.1000	31.8182	1.8182	0.0703	0.9766	
1.2000	29.1667	1.6667	0.0732	1.0162	
1.2500	28.0000	1.6000	0.0763	1.0601	
1.2600	27.7778	1.5873	0.0769	1.0677	
1.2800	27.3438	1.5625	0.0837	1.1628	
1.2900	27.1318	1.5504	0.1025	1.4232	
1.3000	26.9231	1.5385	0.1478	2.0526	
1.3100	26.7176	1.5267	0.1762	2.4469	
1.3200	26.5152	1.5152	0.1606	2.2300	
1.3300	26.3158	1.5038	0.1673	2.3238	
1.3400	26.1194	1.4925	0.7464	10.3670	

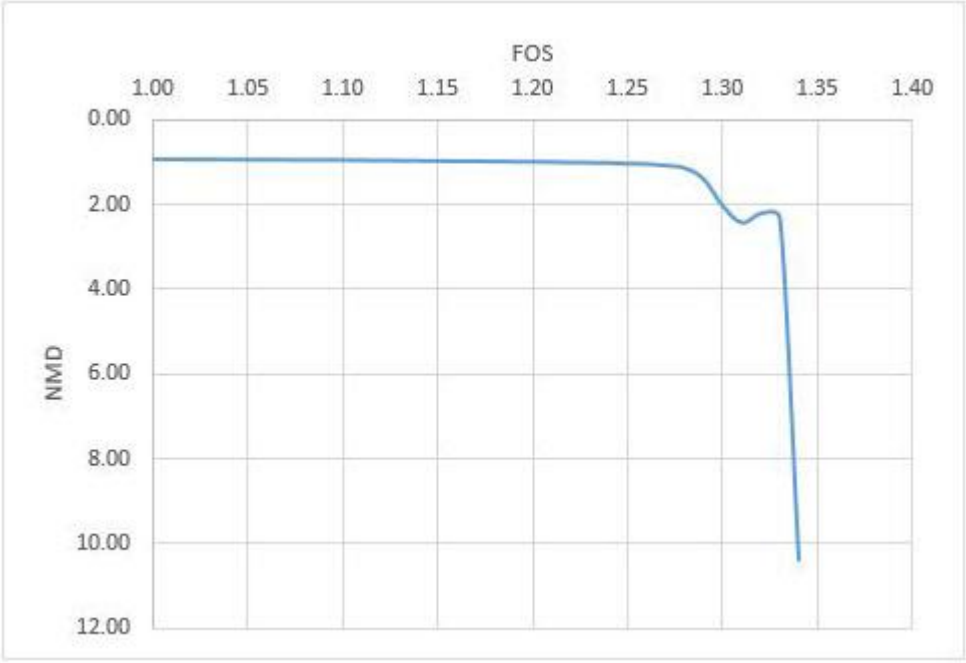

Figure 0.8 FOS plotted against Normalized Maximum Displacement (NMD) of general slope having ϕ=35 degrees and Xp/X=1

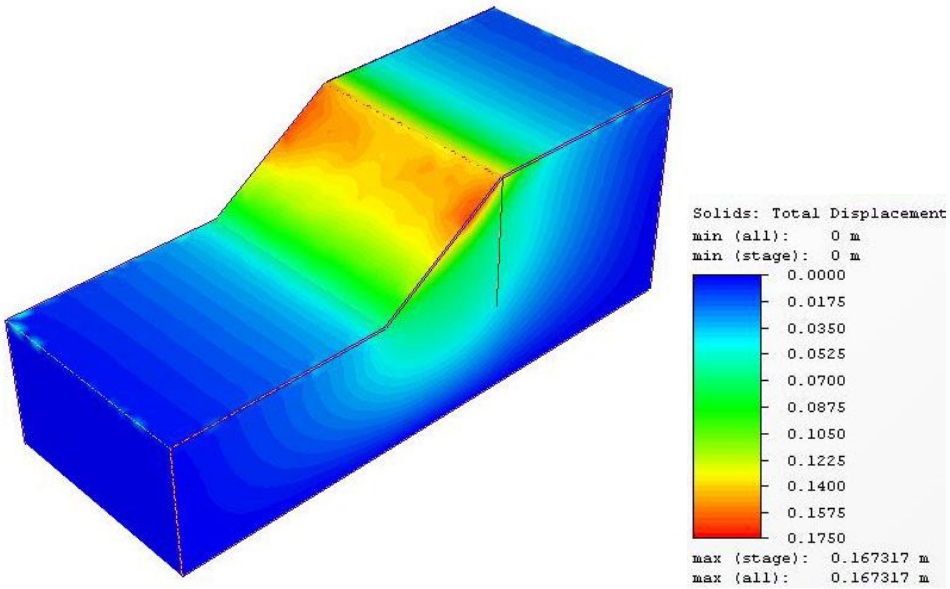

Figure 0.9 Displacement of slope having ϕ=35 with Pile having L=1.5H at the crest of the slope(ie Xp/X=1)

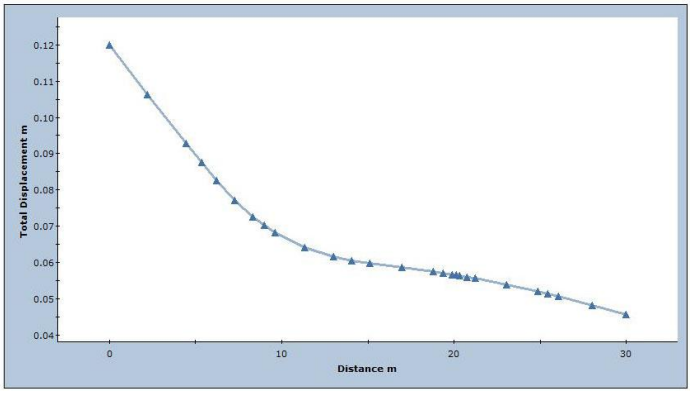

Figure 0.10 Total Displacement profile of a pile at crest (Xp/X=1) of general slope having ϕ=35 degrees and and L=1.5H at critical FOS

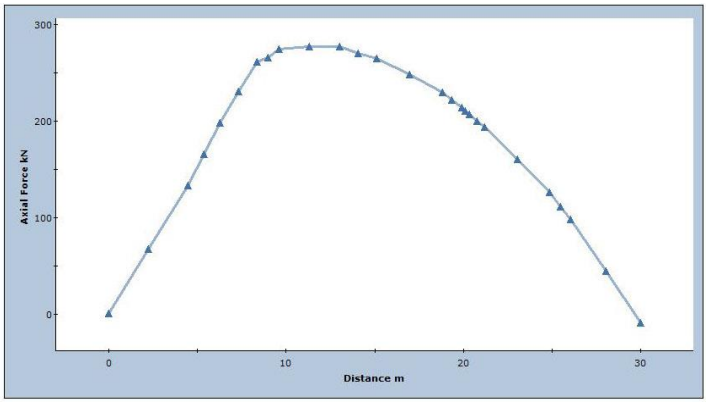

Figure 0.11 Axial Force profile of a pile at crest (Xp/X=1) of general slope having ϕ=35 degrees and L=1.5H at critical FOS

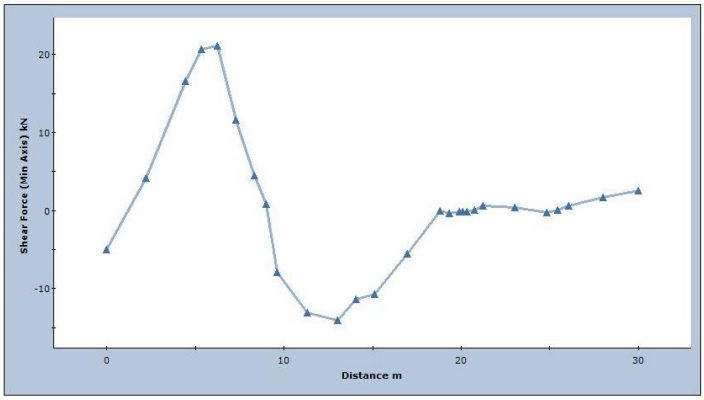

Figure 0.12 Shear Force profile of a pile at crest (Xp/X=1) of general slope having ϕ=35 degrees and L=1.5H at critical FOS

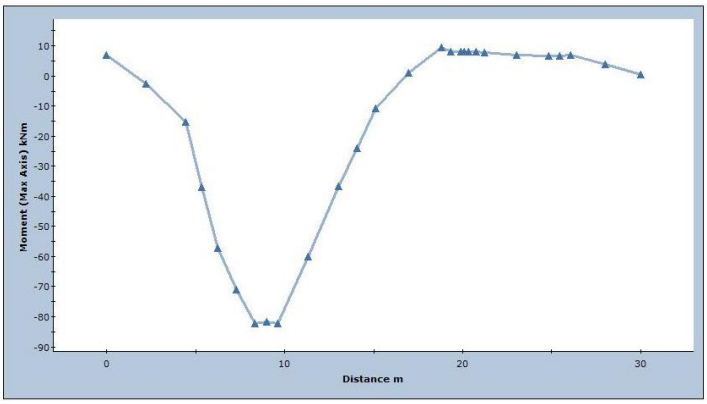

Figure 0.13 Bending Moment profile of a pile at crest (Xp/X=1) of general slope having ϕ=35 degrees and L=1.5H at critical FOS

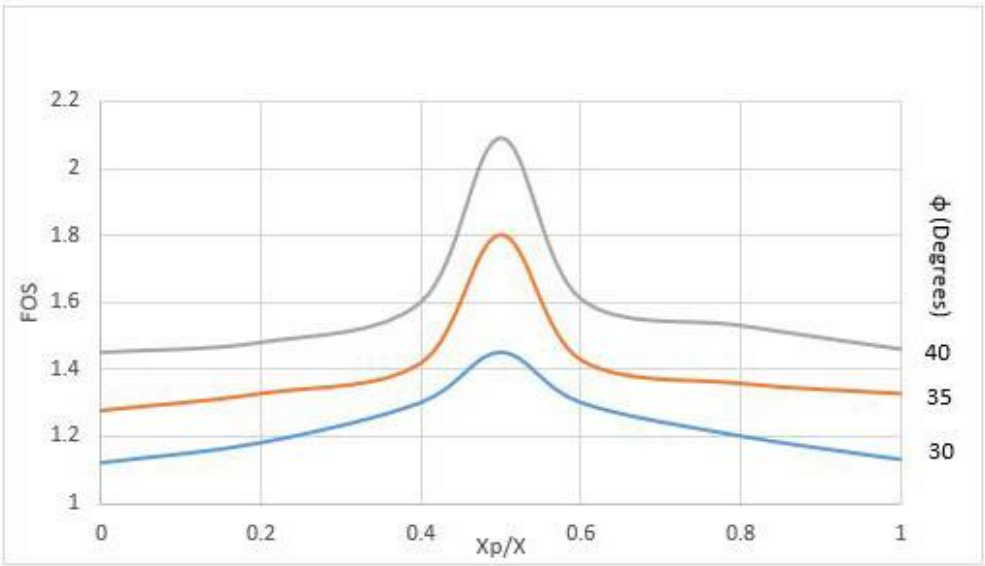

Figure 0.14 Variation of FOS with respect to position of the pile for the pile stabilized general slope.

4.2 Stability Analysis of Ghurmi Slope

Without Piles

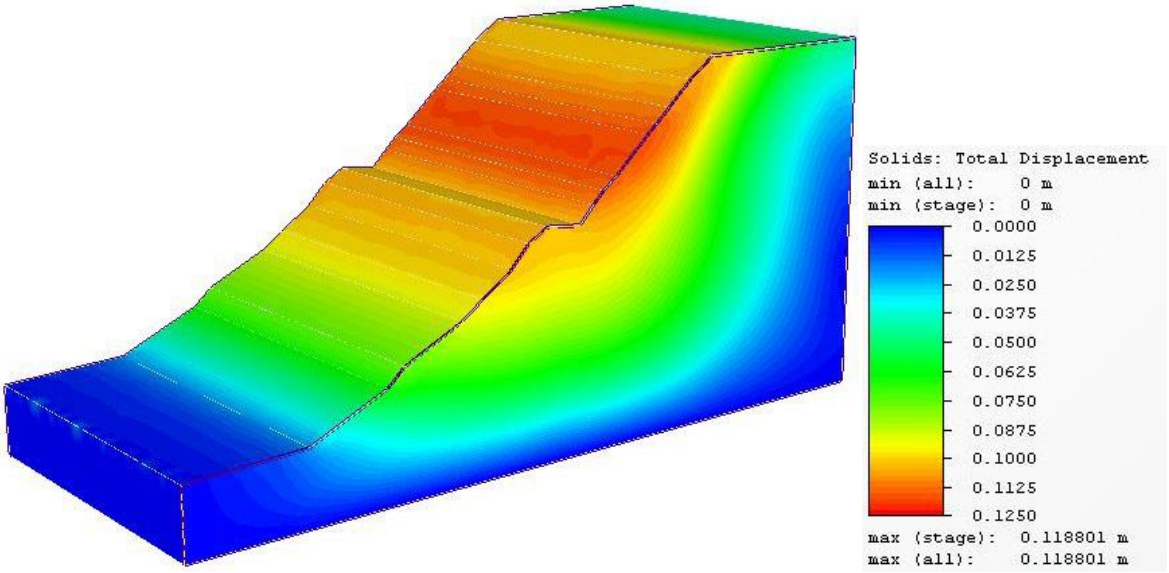

Figure 0.15 Displacement of Slope at Ghurmi at Critical FOS without piles

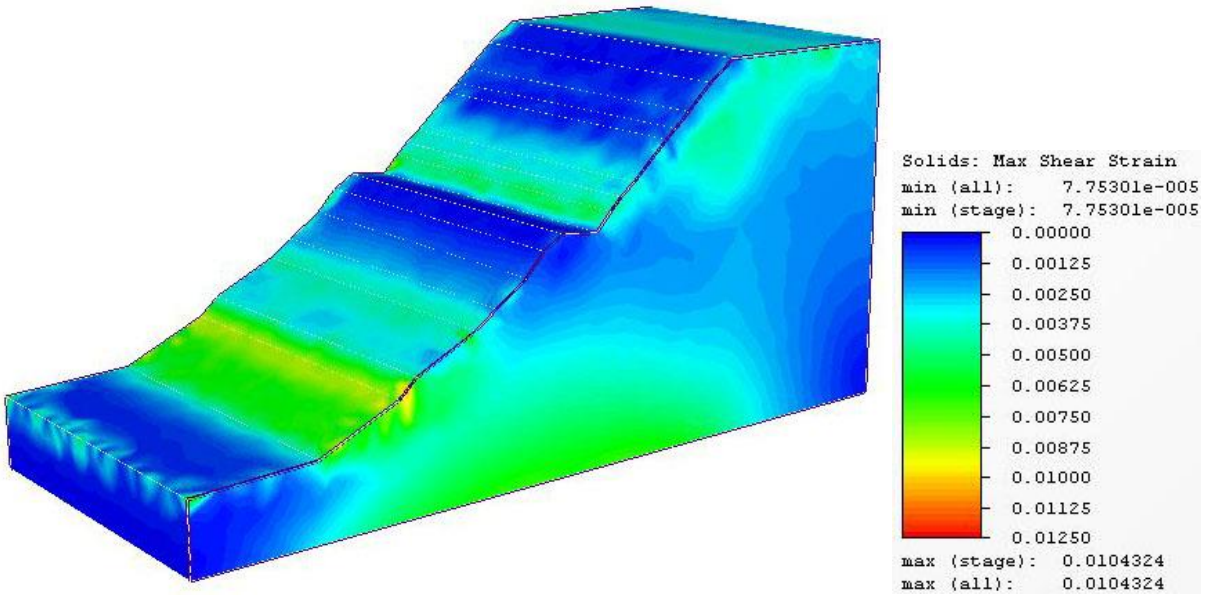

Figure 0.16 Shear strain of slope at Ghurmi at Critical FOS without piles

Table 0.3 FOS computed for Ghurmi slope without piles using Manual shear Strength Reduction Technique

FOS	ϕ(Degrees)	C (KN/m^2)	δ_{max}	Remarks
0.5000	72.0000	4.0000	0.0893	
0.6000	60.0000	3.3333	0.0900	
0.7000	51.4286	2.8571	0.0914	
0.8000	45.0000	2.5000	0.0937	
0.9000	40.0000	2.2222	0.0964	
1.0000	36.0000	2.0000	0.1013	
1.1000	32.7273	1.8182	0.1119	
1.1100	32.4324	1.8018	0.1133	
1.1200	32.1429	1.7857	0.1188	
1.1300	31.8584	1.7699	0.6338	
1.1500	31.3043	1.7391	1.7178	Unstable
1.2000	30.0000	1.6667	2.5338	Unstable

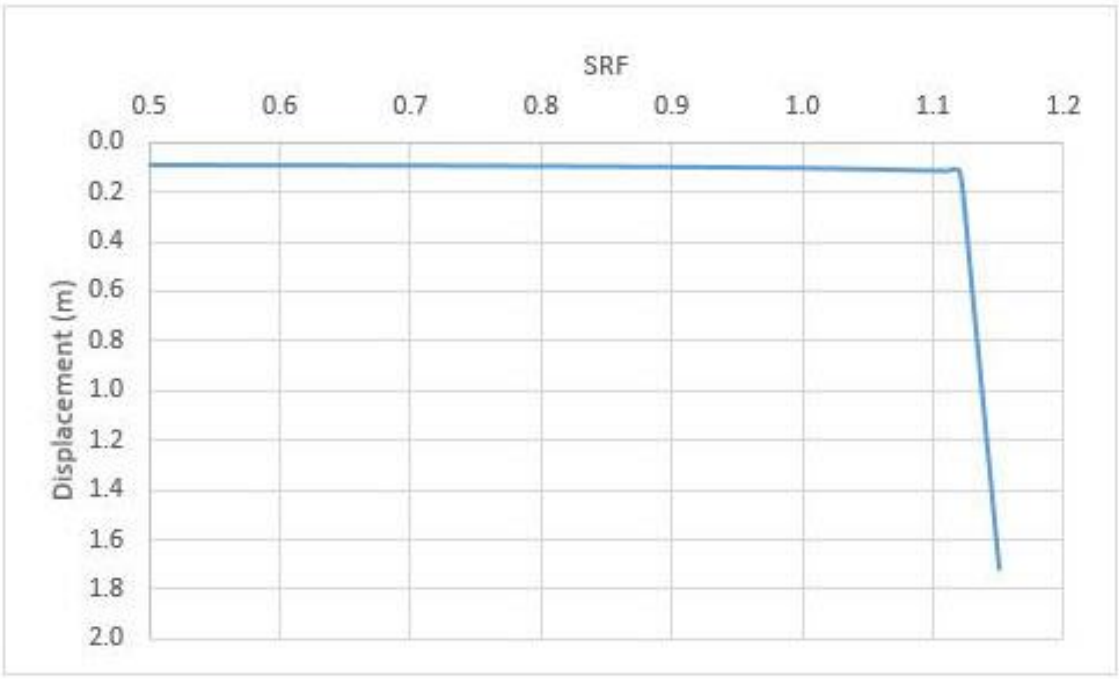

Figure 0.17 SRF plotted against Maximum Displacement of Ghurmi slope without piles

With Piles

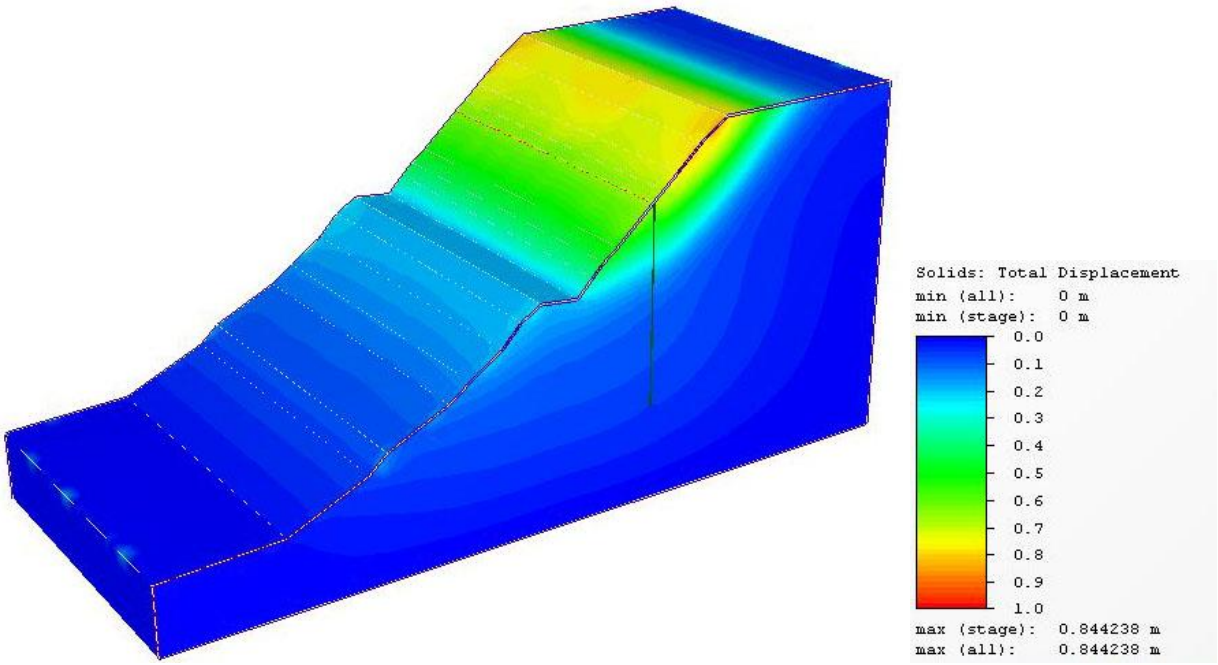

Figure 0.18 Displacement of Slope at Ghurmi at Critical FOS stabilized using piles (L=1.5H and Xp/X = 0.5)

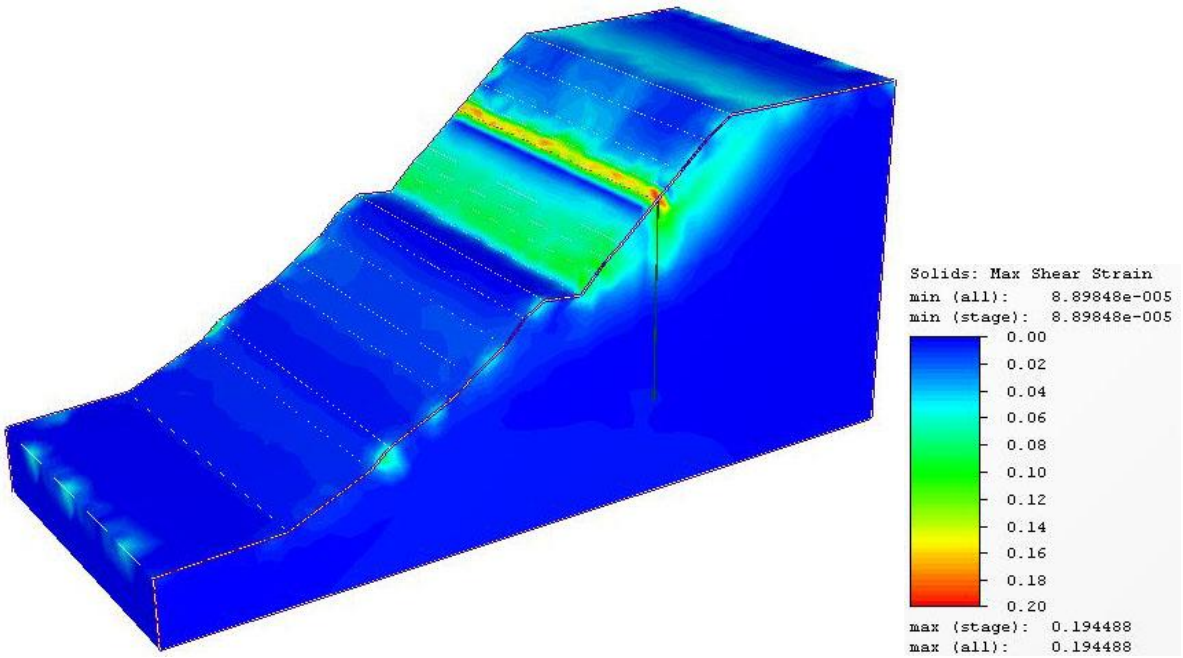

Figure 0.19 Shear strain of slope at Ghurmi at Critical FOS stabilized using piles (L=1.5H and Xp/X = 0.5)

Table 0.4 FOS computed for Ghurmi slope having with piles (L=1.5H and Xp/X = 0.5)using Manual shear Strength Reduction Technique

FOS	ϕ(Degrees)	C (KN/m^2)	δ_{max}	Remarks
0.5000	72.0000	4.0000	0.0889	
0.6000	60.0000	3.3333	0.0897	
0.7000	51.4286	2.8571	0.0910	
0.8000	45.0000	2.5000	0.0931	
0.9000	40.0000	2.2222	0.0959	
1.0000	36.0000	2.0000	0.1010	
1.1000	32.7273	1.8182	0.1229	
1.2000	30.0000	1.6667	0.6932	
1.2500	28.8000	1.6000	0.8442	
1.2600	28.5714	1.5873	2.4217	
1.2700	28.3465	1.5748	1.9489	
1.2800	28.1250	1.5625	2.6497	
1.2900	27.9070	1.5504	3.1826	
1.3000	27.6923	1.5385	4.0707	
1.3200	27.2727	1.5152	5.5840	Unstable

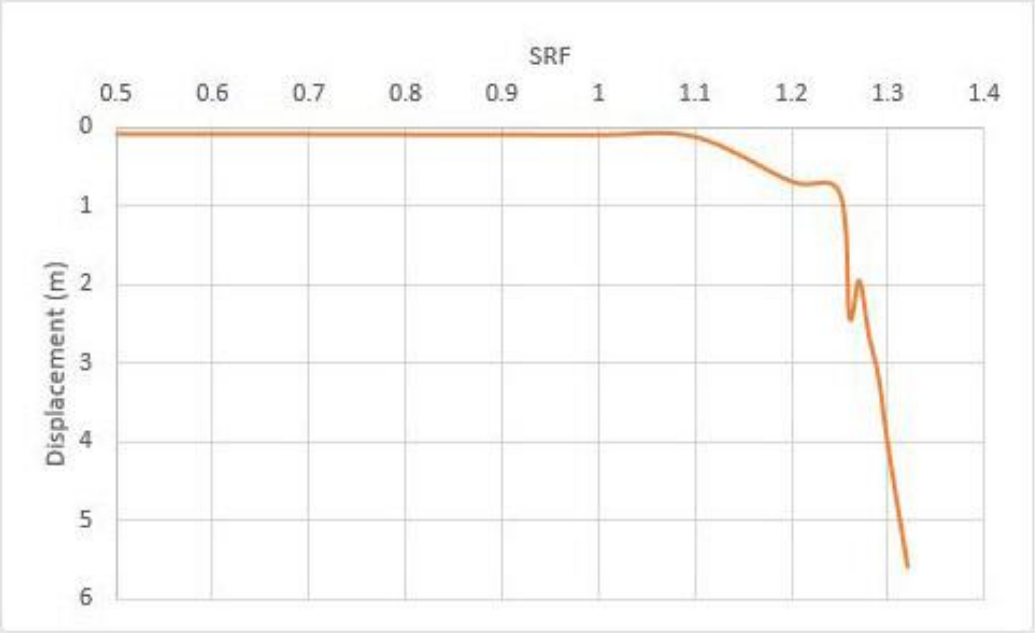

Figure 0.20 SRF plotted against Maximum Displacement of Ghurmi slope with piles

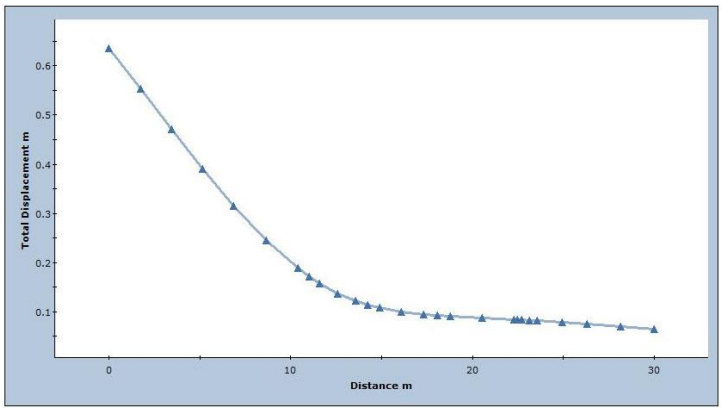

Figure 0.21 Total Displacement profile of a pile located at center at critical FOS

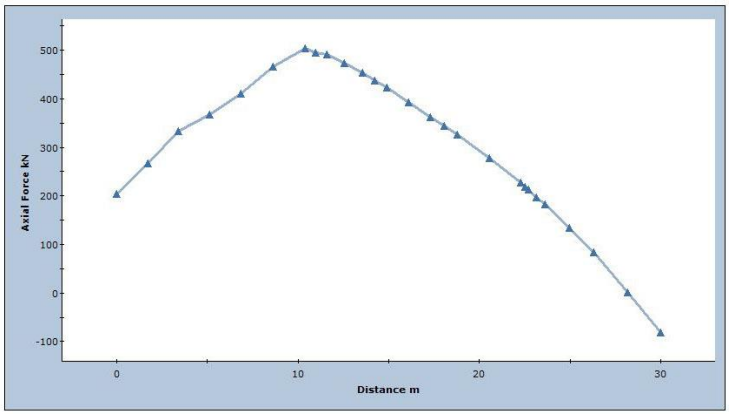

Figure 0.22 Axial Force profile of a pile located at center at critical FOS

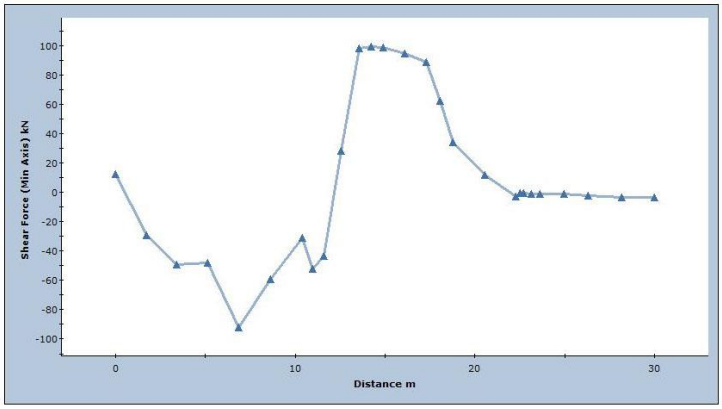

Figure 0.23 Shear Force profile of a pile located at center at critical FOS

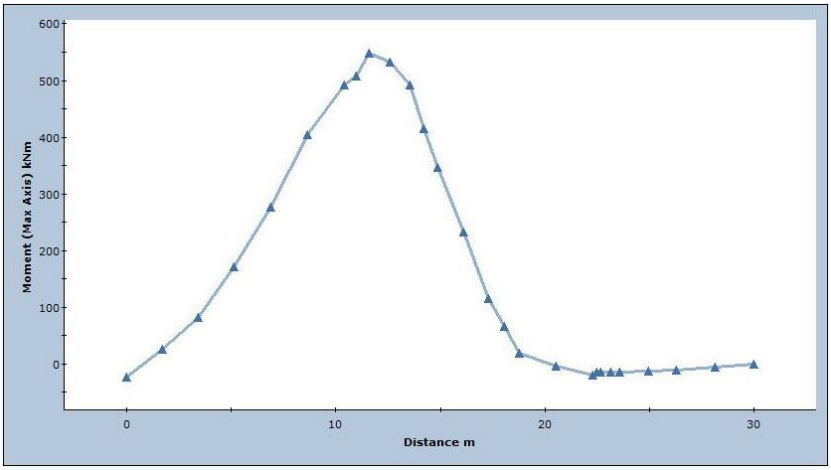

Figure 0.24 Bending Moment profile of a pile located at center at critical FOS

CHAPTER 5: VERIFICATION

5.1 Verification of lab test results

Computation of Unit weight (γ), Angle of internal Friction (φ), Cohesion (C), Bearing Capacity (σ)

- *Short Span Trail Bridge Standard (DoLIDAR)*

More than half of the materials are of individual grains visible to the naked eye (grain size bigger than 0.06 mm) - Coarse Grained soil

If more than half of the coarse fraction is smaller than 6 mm grain size - Sandy Soil

Bearing Capacity (σ)= 200-300 kN/m2

Angle of internal Friction (φ)= 31°-37°

Unit Weight (γ) = 18 kN/m3

- *Roadside Geotechnical Problems (DOR)*

For Clayey Sand (SC)with little Fines

Angle of internal Friction (φ)=32° ± 4°

Cohesion (C)= 0 KN/m2

Unit Weight (γ)= 1.96± 0.2 t/m2

5. 2 Verification of slope stability analysis results for General Slope

5.1.1 Without piles

PLAXIS-3D Foundation Version 1 (Brinkgreve and Broere,2007) is used for the verification. Basic soil elements are the 15-node wedge elements. For beams (i.e. pile), 3-node line elements are used, which are compatible with the 3-node sides of a soil element. Boreholes are used to define the soil stratigraphy and ground surface level. Soil mass is modeled using Mohr-Coulomb model.

Table 0.1 Comparison of FOS obtained from Plaxis-3D and RS3 for general slope without piles

Φ (Degrees)	RS^3 (Critical SRF)	PLAXIS-3D (Critical SRF)
30°	1.11	1.16
35°	1.28	1.33
40°	1.45	1.5

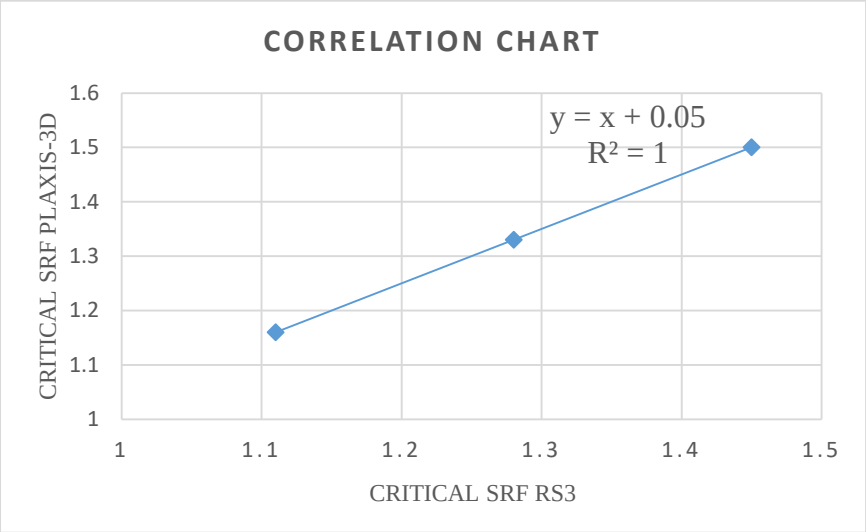

Figure 0.1 Correlation chart for the FOS obtained from RS3 and Plaxis 3D

General slope which has been used for parametric analysis is modeled in Plaxis-3D Foundation which is a commercial three dimensional finite element software. The slope stability analysis is performed for general slope without piles for three types of sandy slopes having different values of phi i.e 30, 35 and 40. The critical Factor of Safety obtained are compared with the critical Factor of Safety obtained from RS3. On plotting the value of critical FOS obtained against those obtained from Plaxis-3D Foundation, good correlation was found.

5.1.2 With Piles (Parametric Anayis)

The verification of results of parametric analysis is done using literature of Gandhi & Ilamparuthi, 2012. For the verification purpose, the results of the paper are analyzed using commercial software named Plot Digitizer.

Position of Piles

Parameters adopted by Author	Parameters adopted by Gandhi & Ilamparuthi, 2012
C = 2 Kpa	C = 5 Kpa
$\gamma = 18\ kN/m^3$	$\gamma = 18\ kN/m^3$
H =20m	H =10m
X =30m	X= 10 m
L=15m	L=15m
D = 0.5m	D = 0.5m
S/D = 2	S/D = 2
$\nu_{Soil} = 0.3$	$\nu_{soil} = 0.25$
$E_{soil} = 10^5$ Kpa	$E_{Soil} = 2 * 10^4$ Kpa
$E_{pile} = 35 * 10^6$ Kpa	$E_{pile} = 30 * 10^6$ Kpa
$\nu_{pile} = 0.2$	$\nu_{pile} = 0.2$

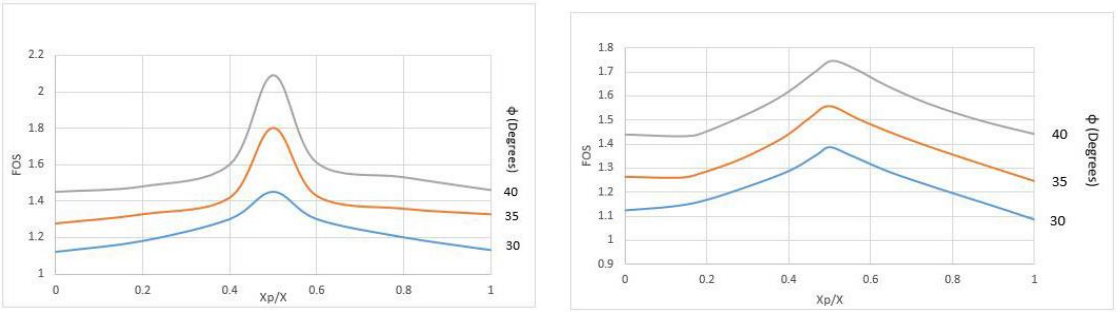

Figure 0.2 Comparison of results of pile position in sandy slope by author (Left) with Gandhi & Ilamparuthi, 2012 (Right)

In the curve generated by author the FOS is found to be maximum when pile is located at the center of sandy slope. Similar types of results are obtained when the results of Gandhi & Ilamparuthi, 2012 is plotted using commercial software named Plot Digitizer. Difference in nature of curve may be due to variation of few parameters of slope used by author against those used by Gandhi & Ilamparuthi, 2012.

Length of Piles

Parameters adopted by Author	Parameters adopted by Gandhi & Ilamparuthi, 2012
C = 2 Kpa	C = 5 Kpa
γ = 18 kN/m^3	γ = 18 kN/m^3
H =20m	H =10m
X= 30m	X = 10 m
L=15m	L=15m
D = 0.5m	D = 0.5m
S/D = 2	S/D = 2
ν_{Soil} = 0.3	ν_{soil}= 0.25
E_{soil} = 10^5 Kpa	E_{Soil} = 2* 10^4 Kpa
E_{pile} = 35* 10^6 Kpa	E_{pile} = 30* 10^6 Kpa
ν_{pile} = 0.2	ν_{pile} = 0.2
Xp/X = 0.5	Xp/X = 0.5

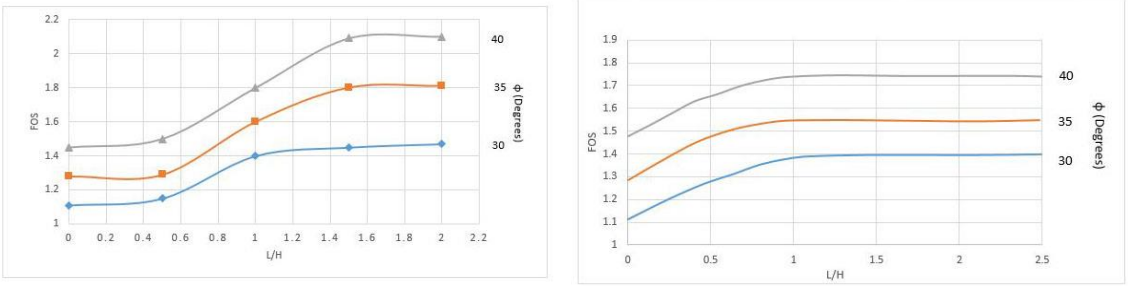

Figure 0.3 Comparison for Length of pile in sandy slopes with Gandhi & Ilamparuthi, 2012.

In the curve generated by author the FOS of sandy slope found to be increased with increase in length of pile upto L= 1.5H. When the L> 1.5H there is no significant increase in FOS with increase in length of pile. Similar types of results are obtained when the results of Gandhi & Ilamparuthi, 2012 is plotted using commercial software named Plot Digitizer. Difference in nature of curve may be due to variation of few parameters of slope used by author against those used by Gandhi & Ilamparuthi, 2012.

5.3 Verification of Ghurmi slope using Plaxis 3D Foundation

Table 0.2 FOS of Ghurmi slope obtained from RS3 and Plaxis 3D with and without using piles

	RS^3 (Critical SRF)	PLAXIS-3D (Critical SRF)	Tolerance
Without piles	1.12	1.05	6.25 %
With piles	1.25	1.11	11.2 %

The Ghurmi slope is modeled in Plaxis-3D Foundation for verification purpose. Factor of safety of the slope obtained without piles from Plaxis-3D Foundaiton is found within 6.25% tolerance with those results obtained from RS^3. Similarly the FOS obtained for the Ghurmi slope with piles are within 11.2 % tolerance with results obtained from RS^3.

CHAPTER 6: CONCLUSION AND RECOMMENDATION

6.1 Conclusion

When slope failures of highway-slopes are considered, the practical remedies are more limited as the slope crest is commonly the road grade, and the toe is typically at or near the right of- way boundary. In these cases, the crest cannot be modified without significant expense, additional mass cannot be added to the toe, the slope grade cannot be easily modified, and the shear strength of the ground typically cannot be improved without significant expense and traffic disruption. For such, ground pile reinforcement techniques appear to be the most realistic approach to achieving stability. The piles can be installed quickly and provide immediate strength improvements. The installation of the piles does not significantly disrupt traffic flow, and they can be installed from the shoulder of the road without completely closing the highway.

In addition, slope stabilizing piles have a cost similar to other low impact traditional landslide mitigation techniques.

But slope stabilizing piles is a very new technique and have not been thoroughly researched. Very few authors have attempted to study the behavior of pile slope system.

Stability of pile slope system is influenced by various factors such as Pile position on slope, Length of pile, Pile stiffness, Pile spacing, Slope angle, types of soil. It is extremely time-consuming to carry out a detailed 3D pile slope analysis considering all above factors. Among these pile positons on slope and Length of pile have significant role on the stability of pile slope system. The slope used by author for research purpose is sandy, so in this thesis parametric studies were performed to assess the influence of pile location and length on sandy slopes. A general sandy slope is considered and parametric studies is carried out using a commercial 3D software RS3. It is found that FOS is maximum when the pile is located at the center of slope. Similarly, the length of pile greater than 1.5H does not have significant role to increase FOS. These results obtained from parametric studies are applied to actual slope at Ghurmi which is aimed to stabilized using piles. Modeling in FEM has shown promising outcomes while using pile as a slope reinforcement technique, so as to make them engineered solution.

Finally, results obtained from RS3 for general slope is validated using commercial software Plaxis-3D Foundation. Results of parametric studies is verified using study of Gandhi & Ilamparuthi, 2012. Similarly, the slope stability analysis results obtained from

RS3 for Ghurmi slope is verified using Plaxis-3D Foundation. Thus results of this study is helpful to stabilize highway slopes in future.

6.2 Recommendations

This research work covers the analysis of the slope stability of the landslide area. Piles are chosen as the technique to reinforce the slopes over other practicing conventional methods. Improvement in stability of slopes after use of piles as stabilizing measure is analyzed by varying different parameters which influence the pile slope stability. But it is not possible to consider all factors because it is extremely time-consuming to carry out a detailed 3D pile slope analysis considering all the factors. Recommendations are made for future research in this subject area.

1. Pile spacing have significant role on the stability of pile slope system. When piles are at closer spacing they attract more force by resisting the movement of the soil. On increasing the spacing, the relative motion between the pile and soil develops arching of soil and this is effective till the spacing is 4D. Spacing more than 4D provide soil between the piles to move easily thus showing reduction in the factor of safety. The reduction in the factor of safety may be attributed to more loss in the arching effect due to increase in the spacing. Parametric studies can be carried out to study the effects of pile spacing as well.
2. This study has explored the influence of length of pile and position of pile for sandy slope stabilization. Similar types of study can be carried out for clayey slopes.
3. Slope angle and pile stiffness also plays significant role on the stability of pile slope system. Parametric studies can be carried out by using various slope angle and stiffness of the pile.
4. Author has used concrete pile for the stabilization of slope. Steel piles, wooden piles and composite piles can be used as alternative materials. This may be the another area of research.
5. Current study is done for dry slopes. But there is fluctuation of water table during monsoon. How the saturation affects the stability of pile slope system may be another subject of study.
6. Single piles may be inadequate for the stabilization of deep landslides. In such cases pile-groups may be the most efficient solution. Hence it is recommended to carry to stabilization of slopes using multiple rows of the piles.

REFERENCES

Ashour M, Ardalan H (2011) Analysis of pile stabilized slopes based on soil-pile interaction. Computers and Geotechnics, Vol. 39, pp. 85-97

Ashour M, Ardalan H (2010) Road embankments and slope stabilization. University Transportation Center for Alabama Report 09305

Ardalan H (2013) Analysis of Landslides and Slopes Stabilized using one row of piles. The University of Alabama in Huntsville, Ph.D. Thesis, Grant No. 27117

Ang EC (2005) Numerical Investigation of Load Transfer Mechanism in Slopes reinforced with Piles. University of Missouri-Columbia, Ph.D. Thesis.

Bateman RL, Walberg FC (1998) Pile design procedure for stabilizing channel slopes. International Conference on case histories in Geotechnical Engineering, paper 16

Department of Roads (2007) Roadside geotechnical problems: A practical guide to their solution. Road Maintenance and Development Project IDA Credit No. 3293-NEP

Department of Local Infrastructure Development and Agricultural Roads (2002) Short-Span Trail Bridge Standard.

Gandhi NR, Ilamparuthi K (2012) Studies on enhancing stability of slope using reinforcement. Proceedings of Indian Geotechnical Conference, Paper No. B201

Griffiths DV, Lane PA (1999) Slope stability analysis by finite element. Geotechnique 49(3):387-403

Jha SK (2013) Effect of Spatial Varaibility of Soil Properties on Slope Reliability Using Random Finite Element and First Order Second Moment Methods. Indian Geotech J, DOI 10.1007/s40098-014-0118-2

Kiousis P, Griffiths DV, Stewart JA (2010) Optimization of stabilization of highway embankments slopes using driven piles. Colorado Department of Transportation CDOT-2010-8

Kanungo DP, Pain A, Sharma S (2013) Finite element modelling approach to assess the stability of debris and rock slopes: a case study from the Indian Himalayas. Nat Hazards 69:1-24

Kourkoulis R, Gelagoti F, Anastasopoulos I, Gazetas G (2012) Slope Stabilizing Piles and Pile-Goups: Parametric Study and Design Insights. American Society of Civil Engineers 2011.137:663-667

Kondalamahanthy AK (2013) 2D and 3D Back Analysis of the Forest City Landslide (South Dakota). Iowa State University, paper 12992

Lee CY, Hull TS, Poulos HG (1995) Simplified pile-slope stability analysis. Computers and Geotechnics 17:1-16

Li X, Pei Xiangjun, Gutierrez M, He S (2012) Optimal location of piles in slope stabilization by limit analysis. Acta Geotechnica 7:253-259

Lirer S (2012) Landslide stabilizing piles: Experimental evidences and numerical interpretation. Engineering Geology149-150:70-77

Mujah D, Ahmad F, Hazarika H, Wantanabe N (2013) The design method of slope stabilizing piles: A review. International Journal of Current Engineering and Technology vol.3, No. 2

Popescu ME, Sasahara K (2008) Engineering measures for landslide disaster mitigation. IAEG Bulletin 60,1:69-74

Poulos HG (1999) Design of slope stabilizing piles. University of Sydney, N.S.W., Australia ISBN 9058090795

Rocscience (2016) A 3D finite element program for calculating stresses and strains. Geomechanics software and Research, Rocscience INC, Toraonto,Canada.

Sun SW, Zhu BZ, Wang JC (2013) Design method for stabilization of earth slopes with micropiles. The Japanese Geotechnical society 53:487-497

Upreti BN, Dhital MR (1996) Landslide Studies and Management in Nepal. ICIMOD ISBN 92-9115-502-0

Washington State Department of Transportation (1998) Development of P-Y curves for analysis of laterally loaded piles in western Washington. WA-RD 153.1

Wei WB, Cheng YM (2009) Strength reduction analysis for slope reinforced with one row of piles. Computers and Geotechnics 36:1176-1185

ANNEX A

Lab Test Results

Sieve Analysis Results

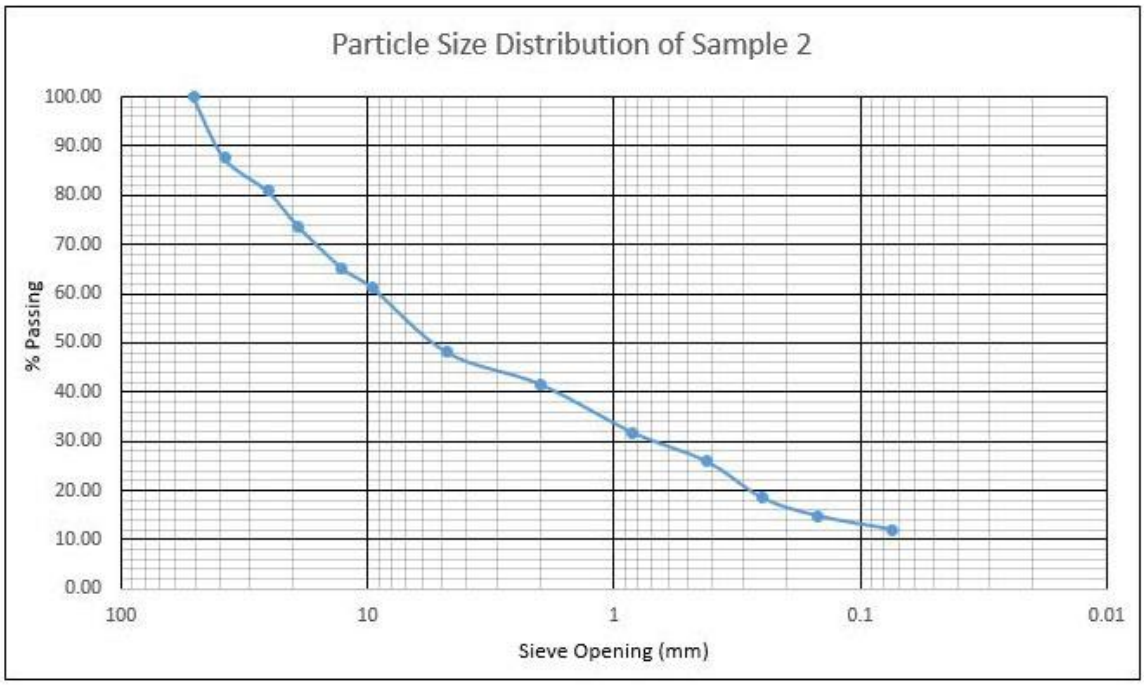

Figure A.1 Particle Size distribution of sample 2

% Passing 75μ Sieve = 12.03 % (Coarse Grained Soils)

% Passing 4.75 mm Sieve = 48.06 % (Sands)

% Fines = 12.03 % (Sand with Fines)

PI= 0.73 (LL-20) = 0.73(20-20)=0 { PI=20-0=20} Plots above A-Line (SC)

% Gravel = 51.94 % (Clayey Sand with Gravel)

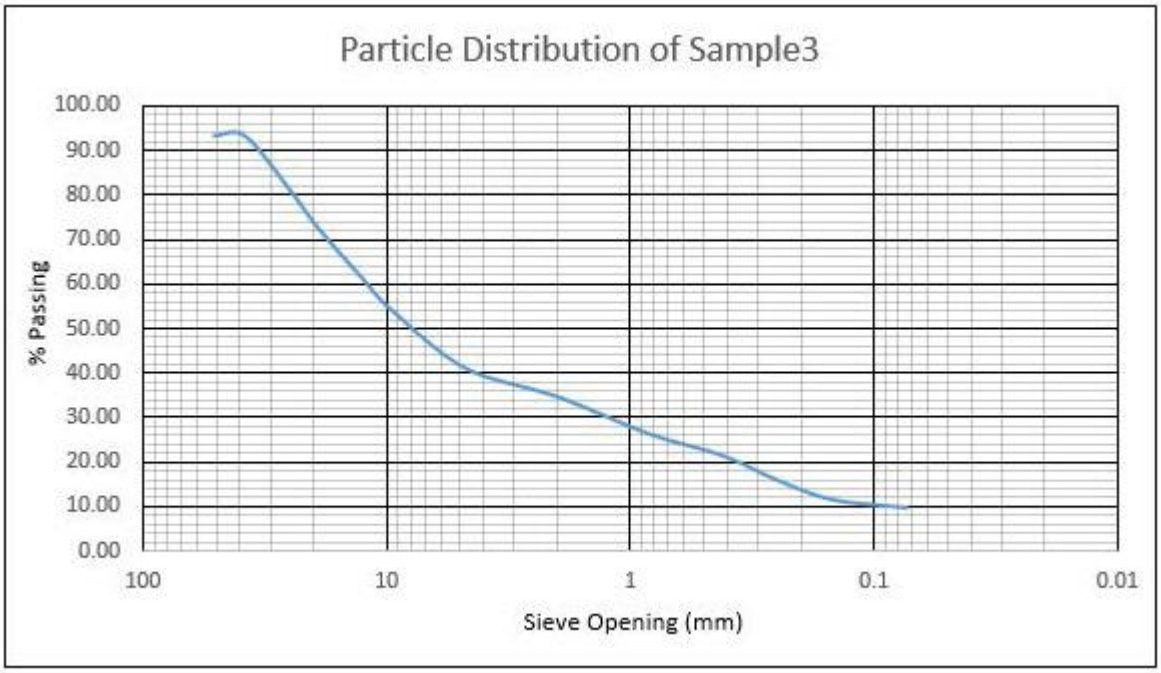

Figure A.2 Particle size distribution of sample 3

% Passing 75 μ Sieve = 9.74 % (Coarse Grained Soils)

% Passing 4.75 mm Sieve= 41.06 % (Sands)

% Fines= 9.74% (5%-12%)

$Cu=(D_{60}/D_{10}) = (10.5/0.1) =105$

$C_C=(D_{30}^2/D_{10}*D_{60}) = (1.22/0.1*10.5) =1.37$

% Sand= 31.32%

Poorly Graded Gravel with Clay and Sand

Direct ShearTest Results

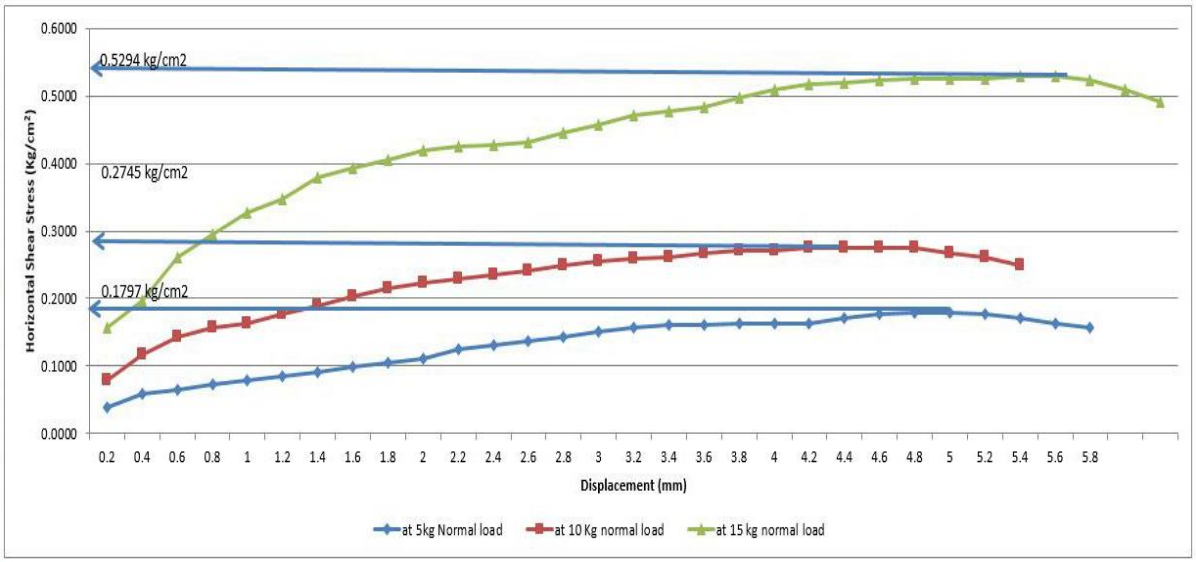

Figure A.3 Horizontal shear stress vs displacement of sample 2

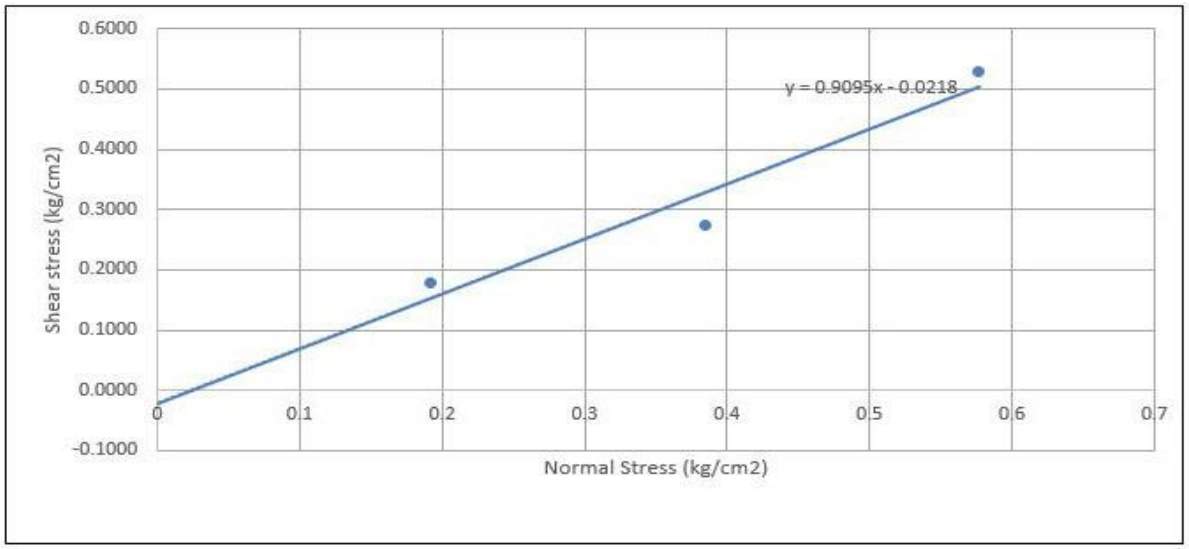

Figure A.4 Normal Stress vs Horizontal Shear stress of sample 2

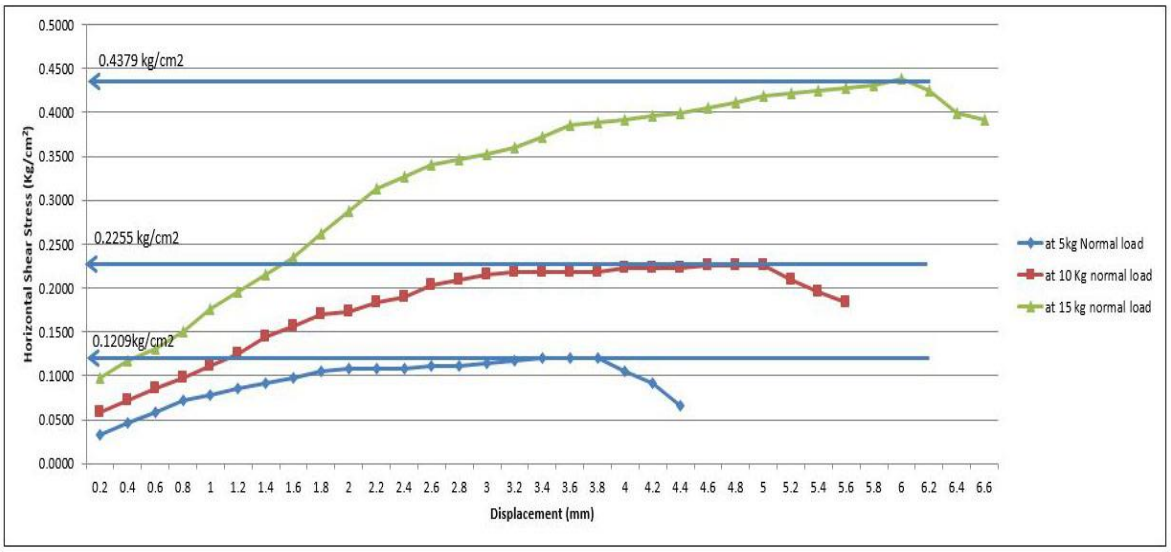

Figure A.5 Horizontal shear stress vs displacement of sample 3

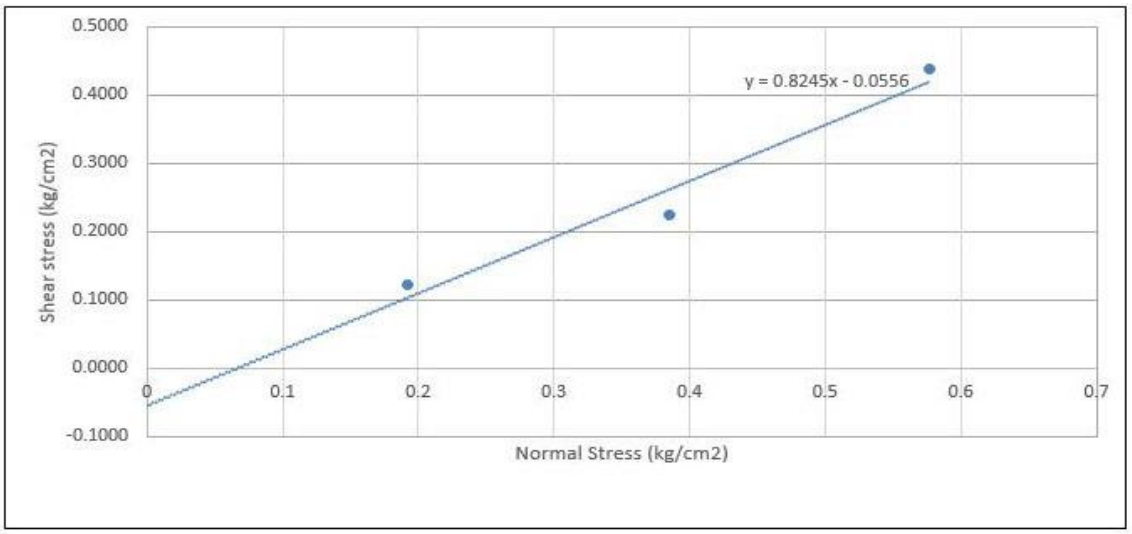

Figure A.6 Normal stress vs Horizontal shear stress of sample 3

ANNEX B

Results of Parametric Analysis

Effect of Pile Length

For ϕ=30 degree

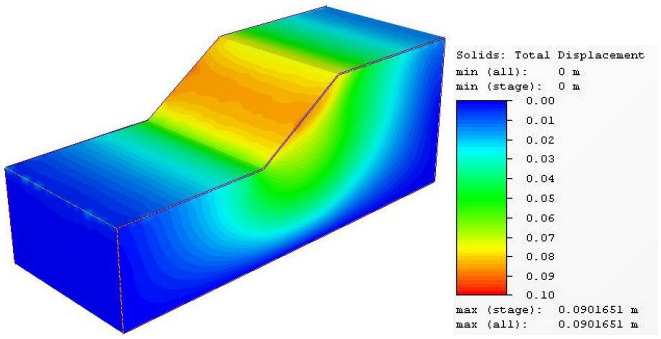

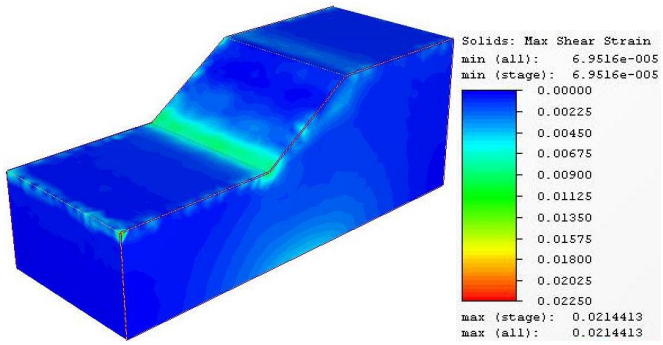

L=0 (Without piles)

FOS	ϕ(Degrees)	C (KN/m^2)	δ_{max}	NMD	Remarks
1.0000	30.0000	2.0000	0.0740	1.0274	
1.0500	28.5714	1.9048	0.0760	1.0557	
1.0700	28.0374	1.8692	0.0778	1.0801	
1.0800	27.7778	1.8519	0.0784	1.0895	
1.0900	27.5229	1.8349	0.0806	1.1196	
1.1000	27.2727	1.8182	0.0831	1.1535	
1.1100	27.0270	1.8018	0.0901	1.2515	
1.1200	26.7857	1.7857	0.3312	4.6006	
1.1300	26.5487	1.7699	0.7841	10.8898	
1.1400	26.3158	1.7544	1.3915	19.3267	Unstable

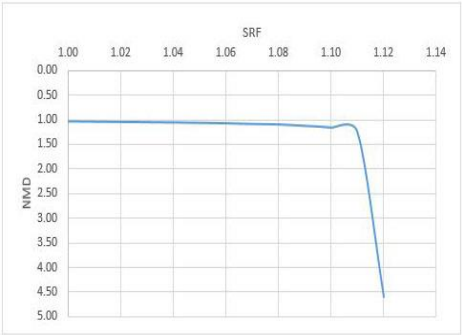

Figure B.1 FOS computed for general slope without piles for ϕ=30 degrees

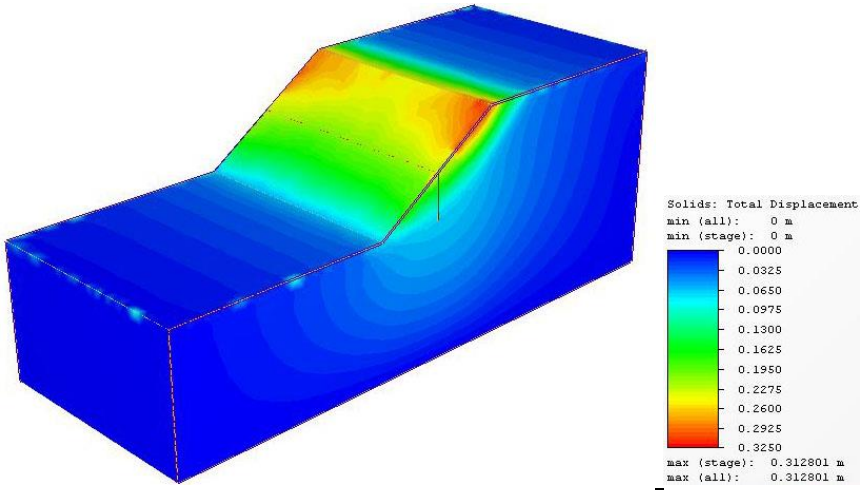

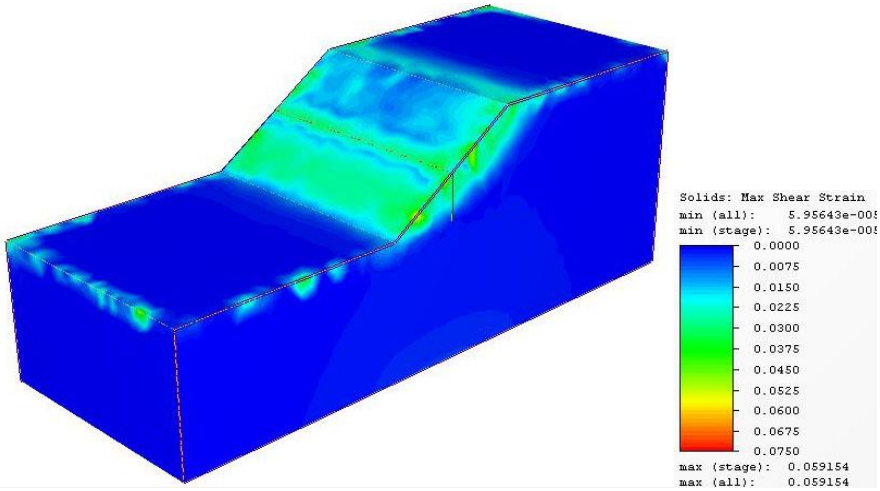

L=10m

FOS	ϕ(Degrees)	C (KN/m^2)	δ_{max}	NMD	Remarks
1.0000	30.0000	2.0000	0.0739	1.0271	
1.1000	27.2727	1.8182	0.0830	1.1523	
1.1100	27.0270	1.8018	0.0902	1.2523	
1.1200	26.7857	1.7857	0.1116	1.5506	
1.1300	26.5487	1.7699	0.2412	3.3494	
1.1400	26.3158	1.7544	0.2849	3.9575	
1.1500	26.0870	1.7391	0.3128	4.3445	
1.1700	25.6410	1.7094	0.8909	12.3742	
1.1800	25.4237	1.6949	1.5269	21.2064	Unstable
1.2000	25.0000	1.6667	2.0866	28.9799	Unstable

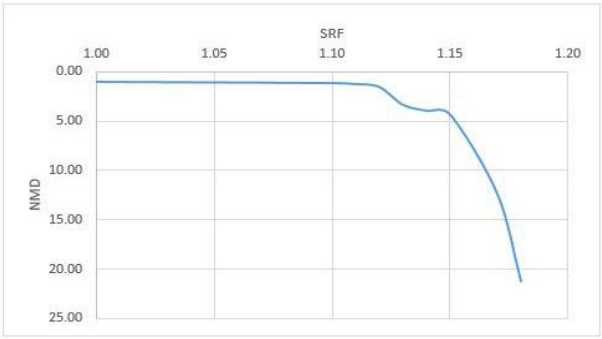

Figure B.2 FOS for general for L=0.5 H & ϕ=30 degrees

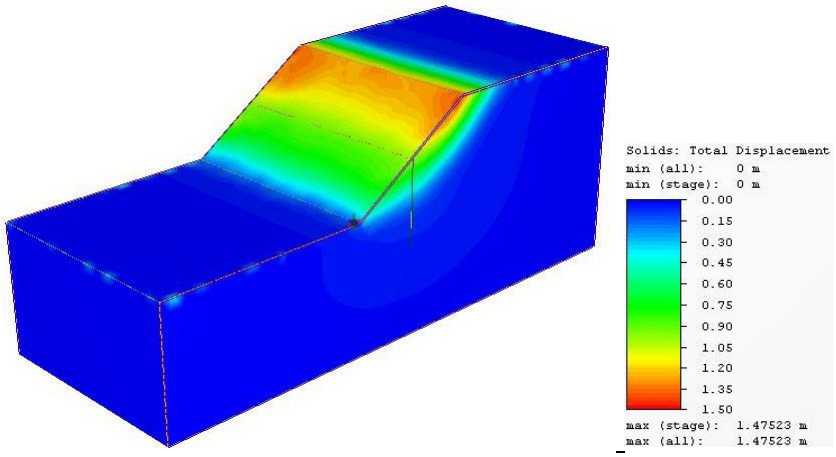

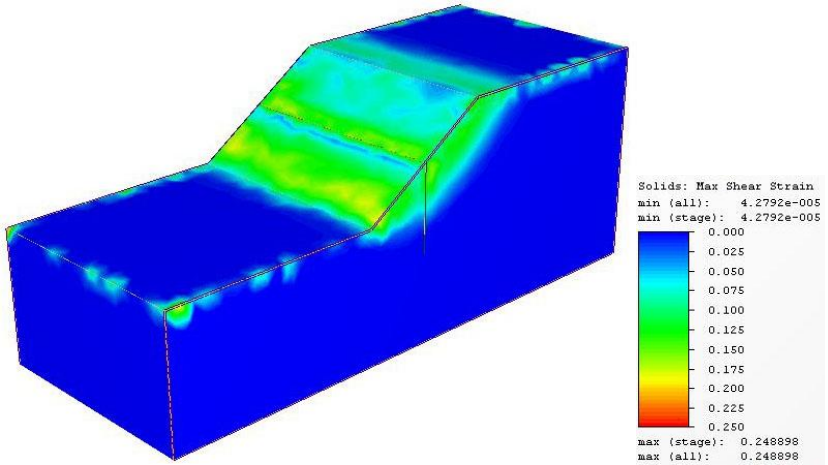

L=20m

FOS	ϕ(Degrees)	C (KN/m^2)	δ_{max}	NMD	Remarks
1.0000	30.0000	2.0000	0.0740	1.0276	
1.1000	27.2727	1.8182	0.0842	1.1690	
1.1100	27.0270	1.8018	0.0927	1.2880	
1.1200	26.7857	1.7857	0.1159	1.6101	
1.1250	26.6667	1.7778	0.1350	1.8746	
1.1300	26.5487	1.7699	0.2471	3.4323	
1.1400	26.3158	1.7544	0.2393	3.3231	
1.2000	25.0000	1.6667	0.4758	6.6089	
1.3000	23.0769	1.5385	1.3069	18.1508	
1.4000	21.4286	1.4286	1.4752	20.4893	
1.5000	20.0000	1.3333	5.0323	69.8925	
1.6000	18.7500	1.2500	3.6390	50.5419	
1.6500	18.1818	1.2121	4.8812	67.7944	
1.6600	18.0723	1.2048	5.0804	70.5617	
1.6700	17.9641	1.1976	5.4823	76.1426	
1.6800	17.8571	1.1905	5.7333	79.6297	
1.6900	17.7515	1.1834	5.5665	77.3129	Unstable
1.7000	17.6471	1.1765	6.3290	87.9024	Unstable

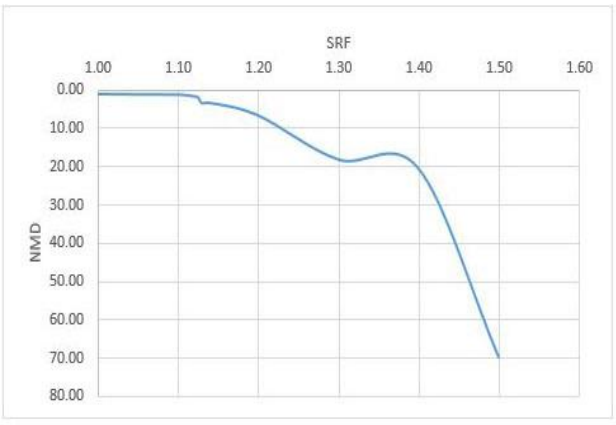

Figure B.3 FOS for general slope for L=1.0 H & ϕ=30 degrees

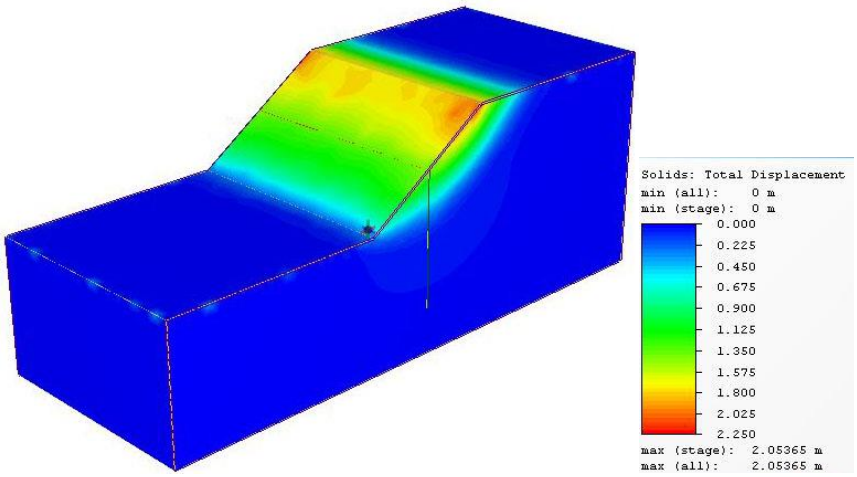

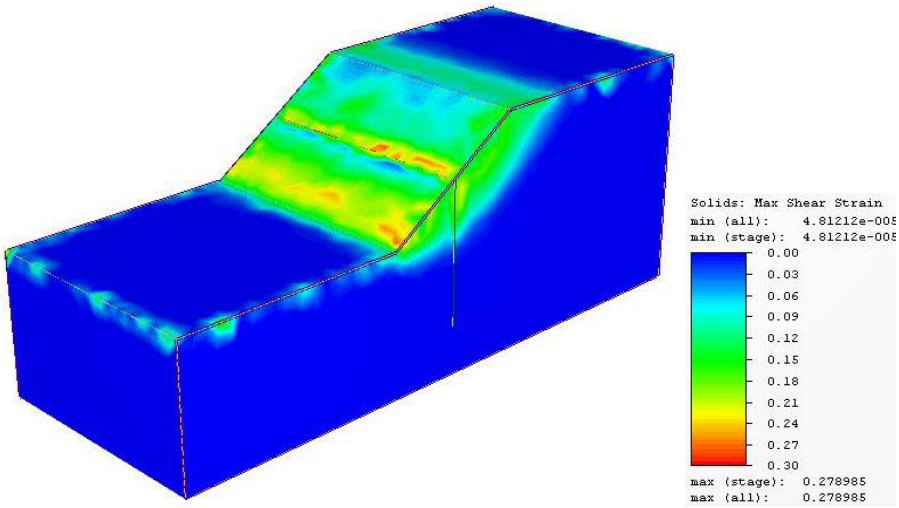

L=30m

FOS	ϕ(Degrees)	C (KN/m^2)	δ_{max}	NMD	Remarks
1.0000	30.0000	2.0000	0.0732	1.0164	
1.1000	27.2727	1.8182	0.0825	1.1458	
1.2000	25.0000	1.6667	0.5292	7.3493	
1.3000	23.0769	1.5385	1.4858	20.6360	
1.4000	21.4286	1.4286	2.0537	28.5229	
1.4500	20.6897	1.3793	2.6086	36.2307	
1.4700	20.4082	1.3605	3.7060	51.4728	Unstable

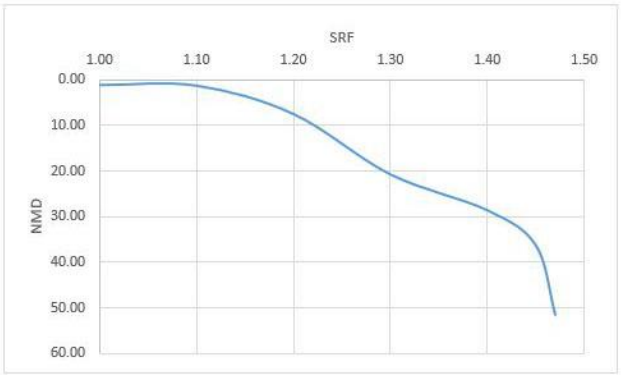

Figure B.4 FOS for general slope for L=1.5 H & ϕ=30 degrees

For ϕ=35

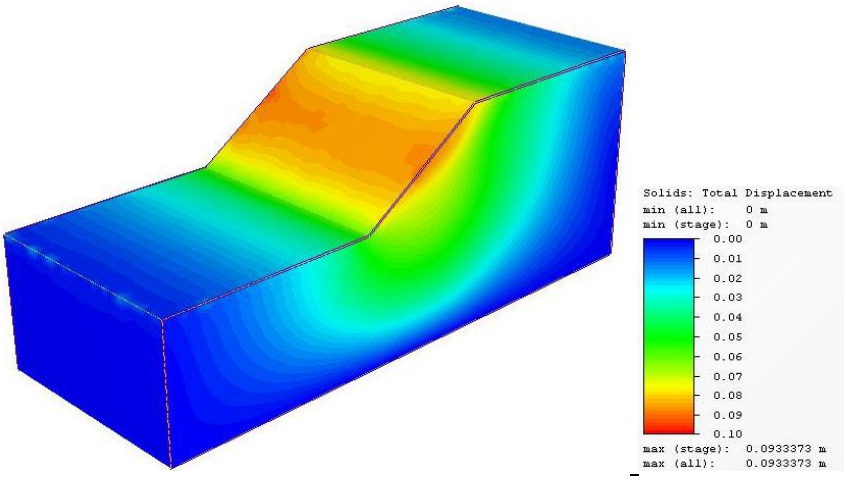

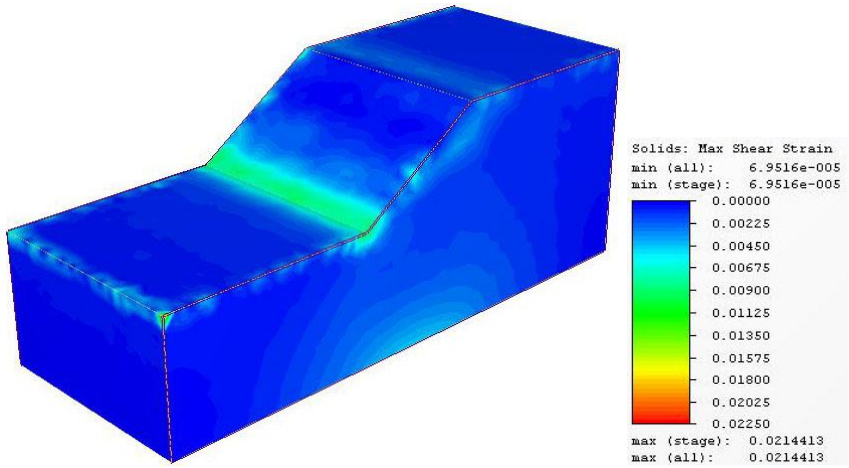

L=0 (Without piles)

FOS	ϕ(Degrees)	C (KN/m^2)	δ_{max}	NMD	Remarks
1.0000	35.0000	2.0000	0.0701	0.9733	
1.1000	31.8182	1.8182	0.0721	1.0017	
1.2000	29.1667	1.6667	0.0756	1.0506	
1.2100	28.9256	1.6529	0.0760	1.0550	
1.2500	28.0000	1.6000	0.0789	1.0956	
1.2700	27.5591	1.5748	0.0833	1.1566	
1.2800	27.3438	1.5625	0.0933	1.2964	
1.2900	27.1318	1.5504	0.3047	4.2322	
1.3000	26.9231	1.5385	0.5828	8.0948	
1.3100	26.7176	1.5267	1.2473	17.3236	
1.3200	26.5152	1.5152	1.4326	19.8968	Unstable

Figure B.5 FOS for general slope for without piles for ϕ=35 degrees

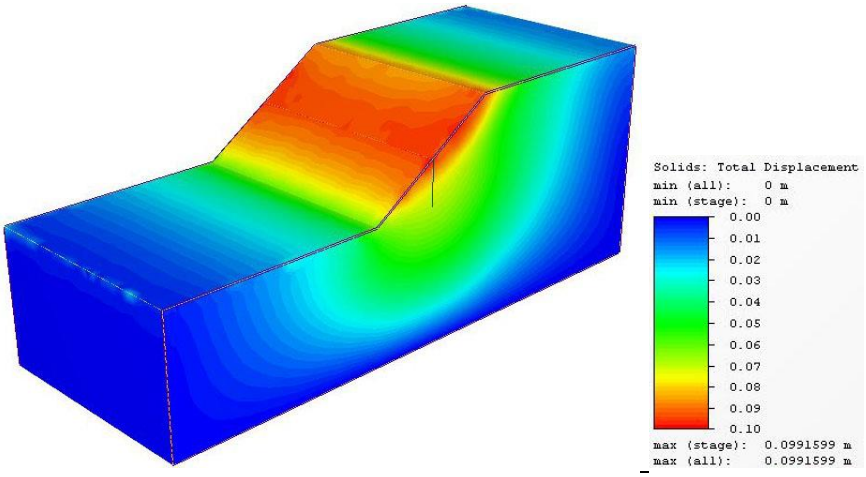

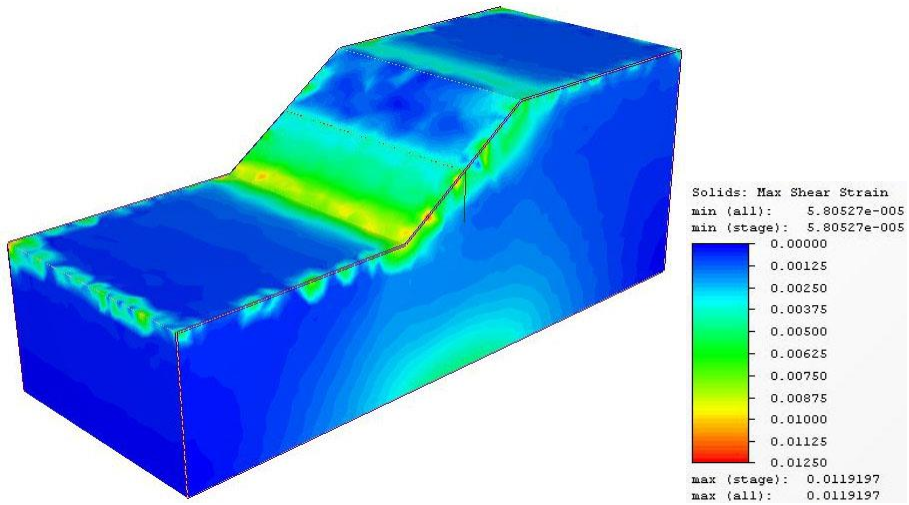

L=10 m

FOS	ϕ(Degrees)	C (KN/m^2)	δ_{max}	NMD	Remarks
1.0000	35.0000	2.0000	0.0698	0.9700	
1.1000	31.8182	1.8182	0.0721	1.0019	
1.2000	29.1667	1.6667	0.0755	1.0480	
1.2100	28.9256	1.6529	0.0758	1.0529	
1.2200	28.6885	1.6393	0.0764	1.0608	
1.2300	28.4553	1.6260	0.0769	1.0678	
1.2400	28.2258	1.6129	0.0784	1.0890	
1.2500	28.0000	1.6000	0.0791	1.0979	
1.2600	27.7778	1.5873	0.0809	1.1231	
1.2700	27.5591	1.5748	0.0830	1.1525	
1.2800	27.3438	1.5625	0.0883	1.2259	
1.2900	27.1318	1.5504	0.0992	1.3772	
1.3000	26.9231	1.5385	0.2420	3.3613	
1.3500	25.9259	1.4815	0.8642	12.0032	
1.3600	25.7353	1.4706	1.4617	20.3015	Unstable

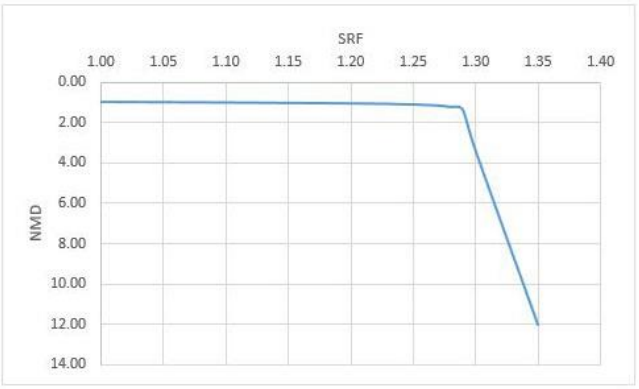

Figure B.6 FOS for general slope for L=0.5 H & ϕ=35 degrees

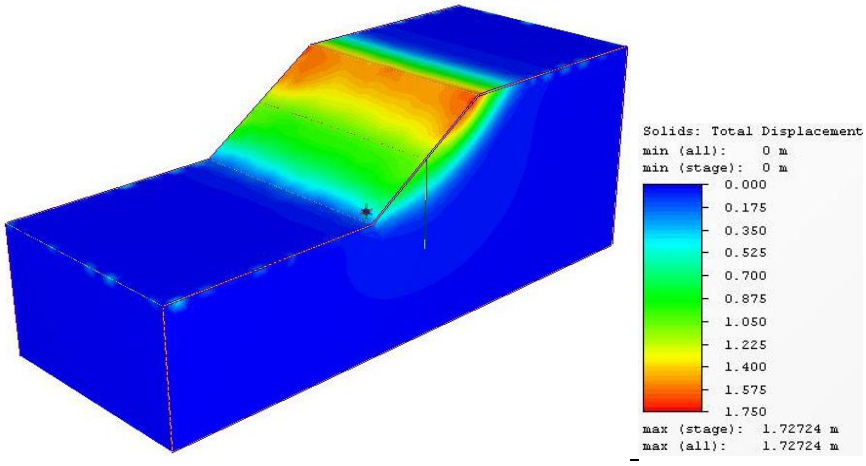

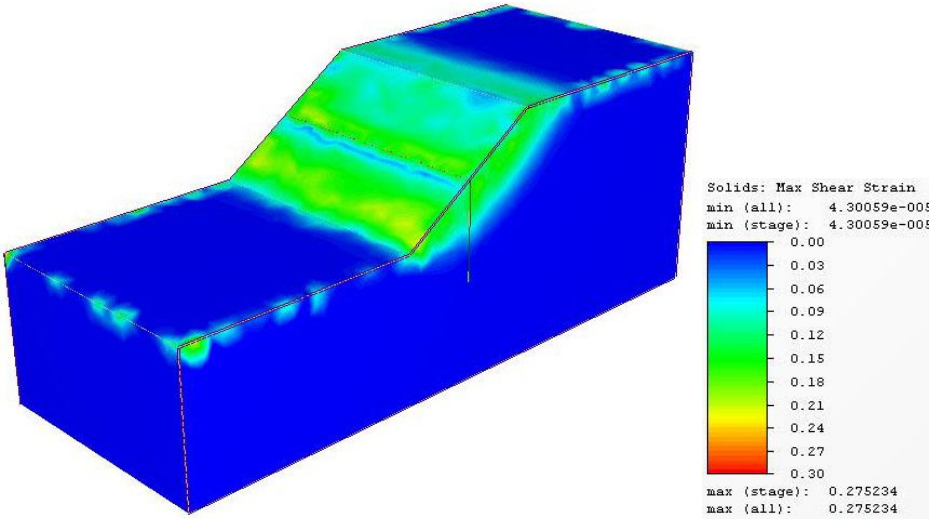

L=20 m

FOS	ϕ(Degrees	C (KN/m^2)	δ_{max}	NMD	Remarks
1.0000	35.0000	2.0000	0.0702	0.9750	
1.1000	31.8182	1.8182	0.0722	1.0033	
1.2000	29.1667	1.6667	0.0758	1.0525	
1.2100	28.9256	1.6529	0.0761	1.0576	
1.2200	28.6885	1.6393	0.0765	1.0628	
1.2300	28.4553	1.6260	0.0779	1.0820	
1.2400	28.2258	1.6129	0.0783	1.0869	
1.2500	28.0000	1.6000	0.0805	1.1186	
1.2600	27.7778	1.5873	0.0816	1.1335	
1.2700	27.5591	1.5748	0.0843	1.1711	
1.2800	27.3438	1.5625	0.0911	1.2650	
1.2900	27.1318	1.5504	0.1105	1.5347	
1.3000	26.9231	1.5385	0.1409	1.9569	
1.4000	25.0000	1.4286	0.6203	8.6154	
1.5000	23.3333	1.3333	1.3546	18.8140	
1.6000	21.8750	1.2500	1.7272	23.9894	
1.7000	20.5882	1.1765	4.2508	59.0389	
1.8000	19.4444	1.1111	2.7341	37.9732	
1.8500	18.9189	1.0811	3.6240	50.3339	
1.8700	18.7166	1.0695	3.5976	49.9668	
1.8900	18.5185	1.0582	4.2768	59.4001	
1.9000	18.4211	1.0526	4.1662	57.8632	
1.9100	18.3246	1.0471	4.8760	67.7217	
1.9400	18.0412	1.0309	5.5572	77.1835	
1.9500	17.9487	1.0256	4.7524	66.0058	Unstable

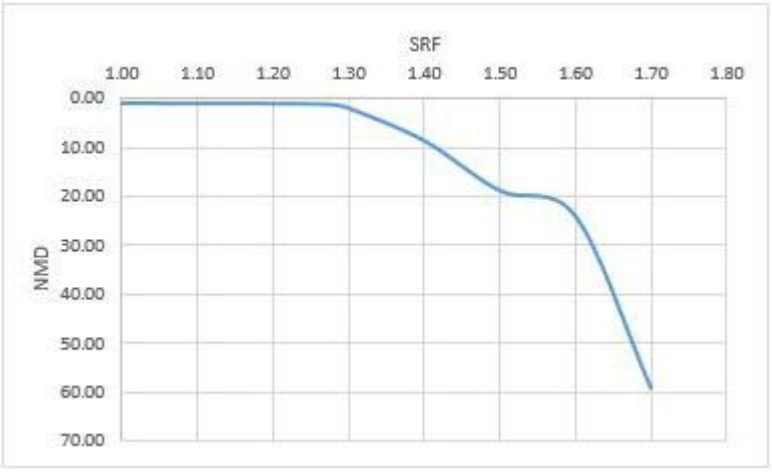

Figure B.7 FOS for general slope for L=1.0 H & ϕ=35 degrees

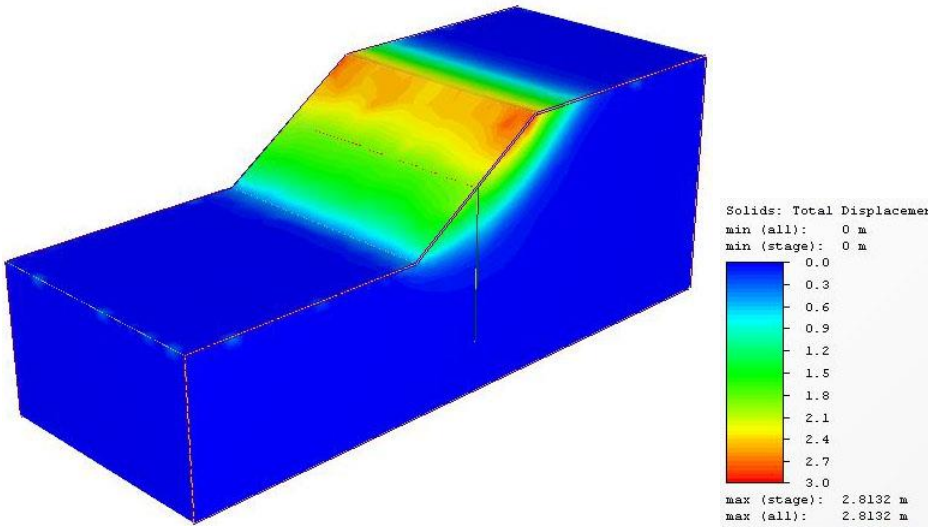

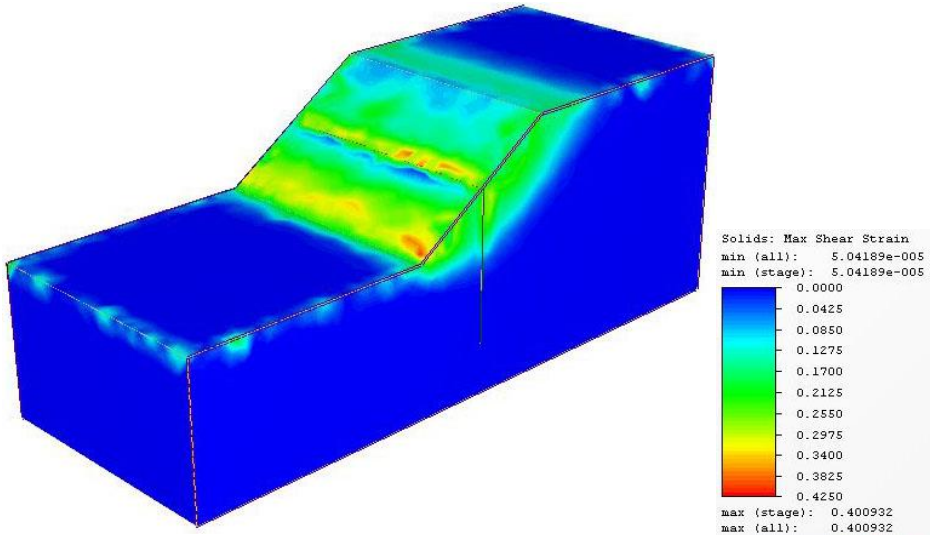

L=30m

FOS	ϕ(Degrees)	C (KN/m^2)	δ_{max}	NMD	Remarks
1.0000	35.0000	2.0000	0.0695	0.9656	
1.1000	31.8182	1.8182	0.0714	0.9912	
1.2000	29.1667	1.6667	0.0750	1.0421	
1.3000	26.9231	1.5385	0.1388	1.9282	
1.4000	25.0000	1.4286	0.5810	8.0695	
1.5000	23.3333	1.3333	1.3938	19.3588	
1.6000	21.8750	1.2500	1.9743	27.4203	
1.6500	21.2121	1.2121	2.0000	27.7778	
1.7000	20.5882	1.1765	2.2947	31.8711	
1.7500	20.0000	1.1429	2.8132	39.0719	
1.7900	19.5531	1.1173	3.7273	51.7675	
1.8000	19.4444	1.1111	2.8132	39.0722	
1.8100	19.3370	1.1050	4.9840	69.2219	
1.8200	19.2308	1.0989	2.9488	40.9558	Unstable

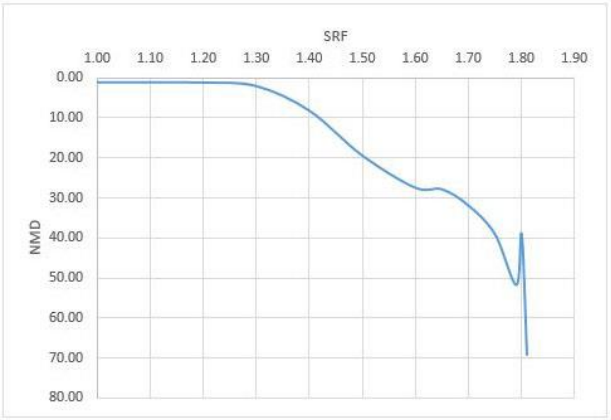

Figure B.8 FOS for general slope for L=1.5 H & ϕ=35 degrees

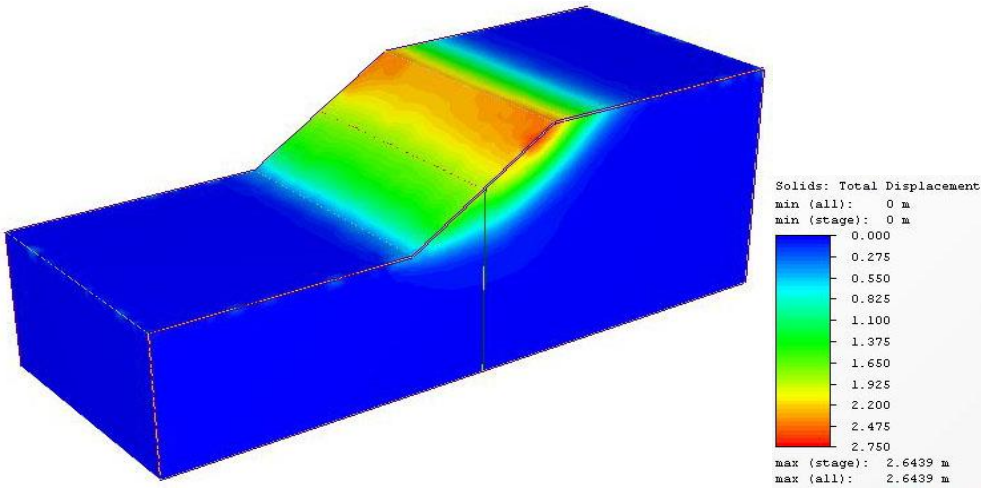

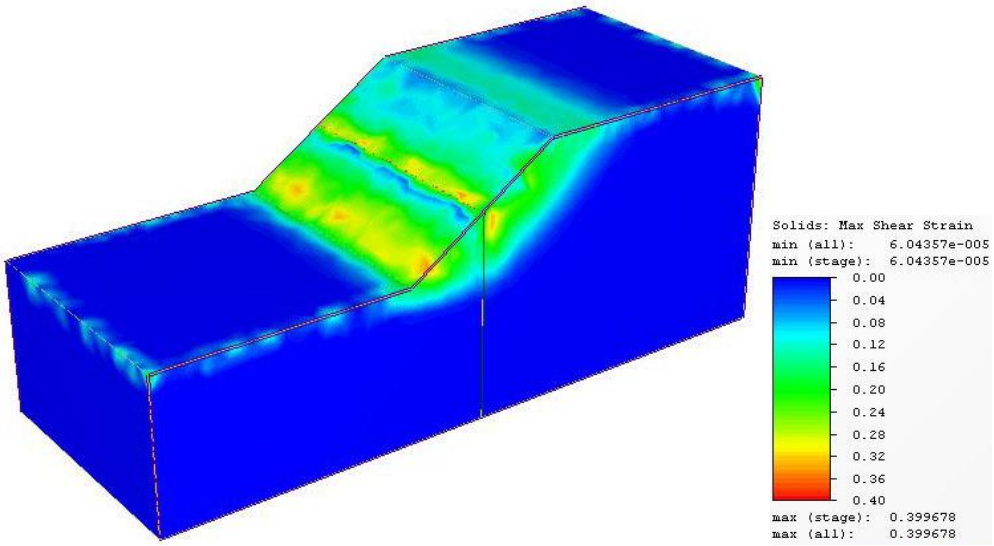

L=40m

FOS	ϕ(Degrees)	C (KN/m^2)	δ_{max}	NMD	Remarks
1.0000	35.0000	2.0000	0.0695	0.9658	
1.1000	31.8182	1.8182	0.0716	0.9942	
1.2000	29.1667	1.6667	0.0755	1.0480	
1.3000	26.9231	1.5385	0.1214	1.6860	
1.4000	25.0000	1.4286	0.4887	6.7873	
1.5000	23.3333	1.3333	1.0432	14.4893	
1.6000	21.8750	1.2500	1.5275	21.2149	
1.7000	20.5882	1.1765	3.2588	45.2610	
1.8000	19.4444	1.1111	3.0819	42.8042	
1.8100	19.3370	1.1050	2.6439	36.7208	
1.8200	19.2308	1.0989	3.6500	50.6944	
1.8300	19.1257	1.0929	3.0900	42.9167	us

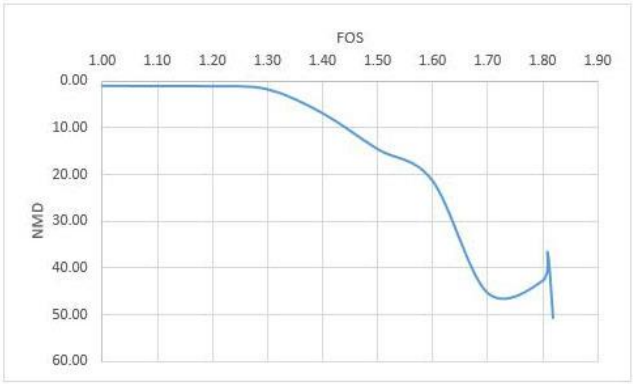

Figure B.9 FOS for general slope for L=2 H & ϕ=35 degrees

For ϕ=40 degrees

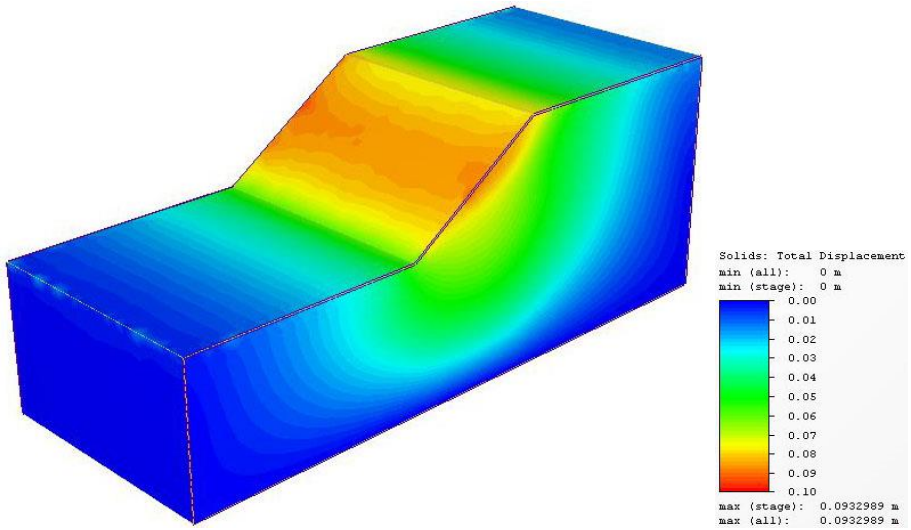

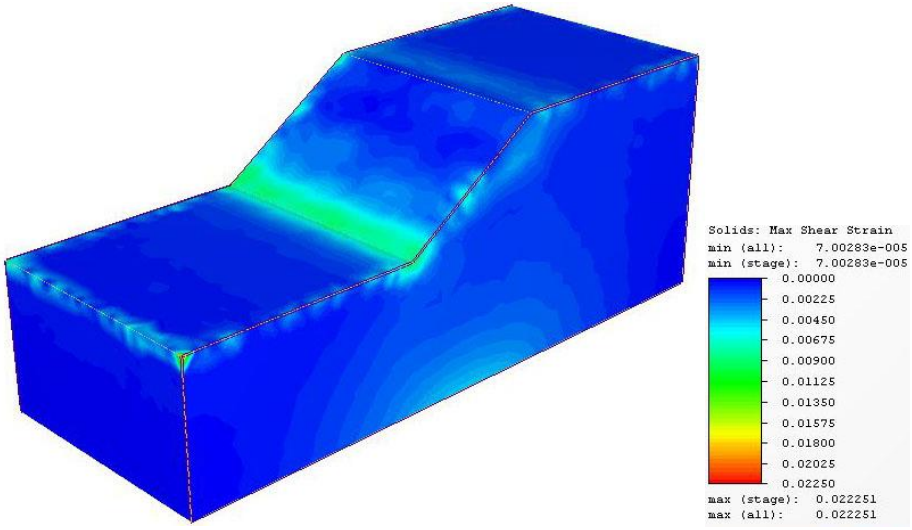

L=0(Without piles)

FOS	ϕ(Degrees)	C (KN/m^2)	δ_{max}	NMD	Remarks
1	40.000	2.000	0.06758	0.938607	
1.1	36.364	1.818	0.069562	0.966133	
1.2	33.333	1.667	0.071283	0.990046	
1.3	30.769	1.538	0.07372	1.023885	
1.4	28.571	1.429	0.077922	1.082243	
1.45	27.586	1.379	0.093299	1.295818	
1.46	27.397	1.370	0.495391	6.880431	
1.47	27.211	1.361	0.540606	7.508417	
1.48	27.027	1.351	1.20224	16.69778	
1.49	26.846	1.342	1.381	19.18056	Unstable
1.5	26.667	1.333	1.47868	20.53722	Unstable

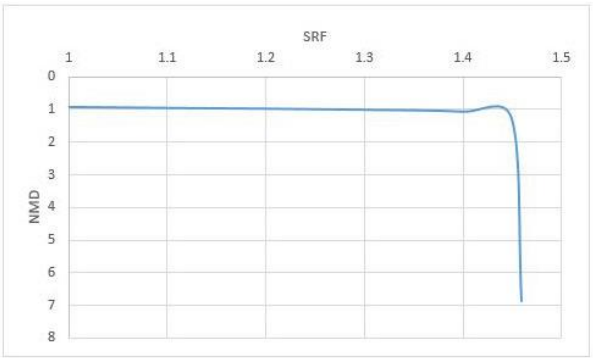

Figure B.10 FOS for general slope for without piles for ϕ=40 degrees

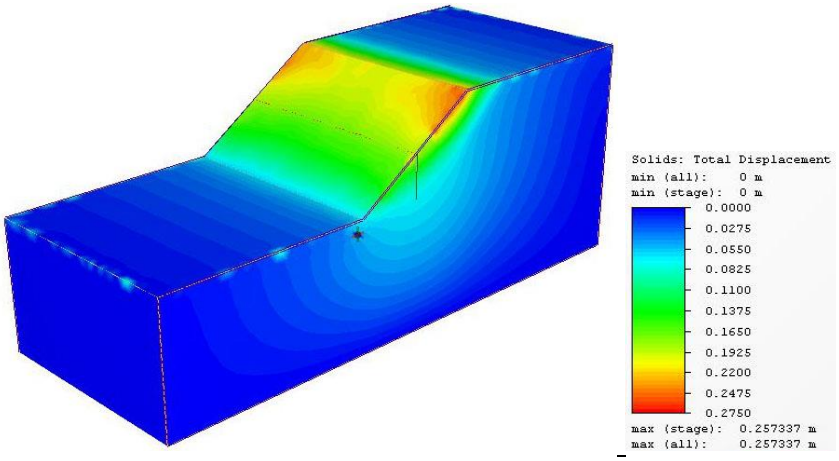

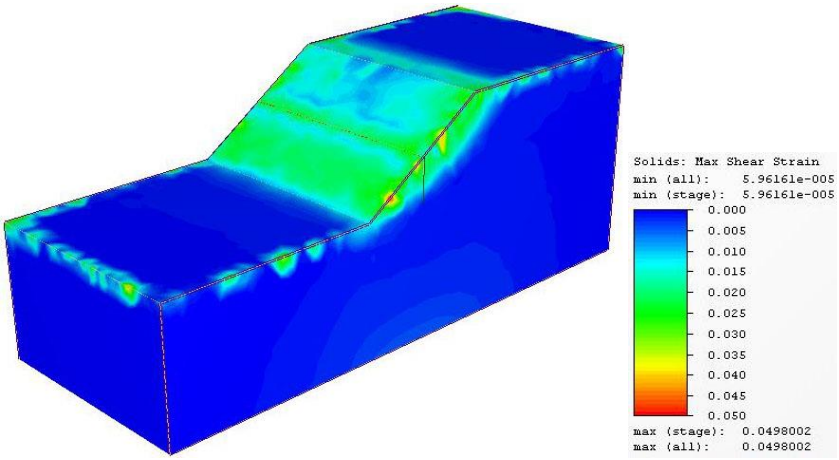

L= 10m

FOS	ϕ(Degrees)	C (KN/m^2)	δ_{max}	NMD	Remarks
1.0000	40.0000	2.0000	0.0677	0.9403	
1.1000	36.3636	1.8182	0.0694	0.9641	
1.2000	33.3333	1.6667	0.0713	0.9901	
1.3000	30.7692	1.5385	0.0740	1.0276	
1.4000	28.5714	1.4286	0.0782	1.0864	
1.4100	28.3688	1.4184	0.0787	1.0933	
1.4200	28.1690	1.4085	0.0803	1.1159	
1.4300	27.9720	1.3986	0.0809	1.1240	
1.4400	27.7778	1.3889	0.0829	1.1518	
1.4500	27.5862	1.3793	0.0881	1.2241	
1.4600	27.3973	1.3699	0.1012	1.4050	
1.4700	27.2109	1.3605	0.1352	1.8783	
1.4800	27.0270	1.3514	0.2457	3.4128	
1.4900	26.8456	1.3423	0.2819	3.9156	
1.5000	26.6667	1.3333	0.2573	3.5741	
1.5300	26.1438	1.3072	0.8285	11.5069	
1.5400	25.9740	1.2987	1.1467	15.9268	
1.5500	25.8065	1.2903	1.5559	21.6099	Unstable
1.6000	25.0000	1.2500	2.4960	34.6668	Unstable

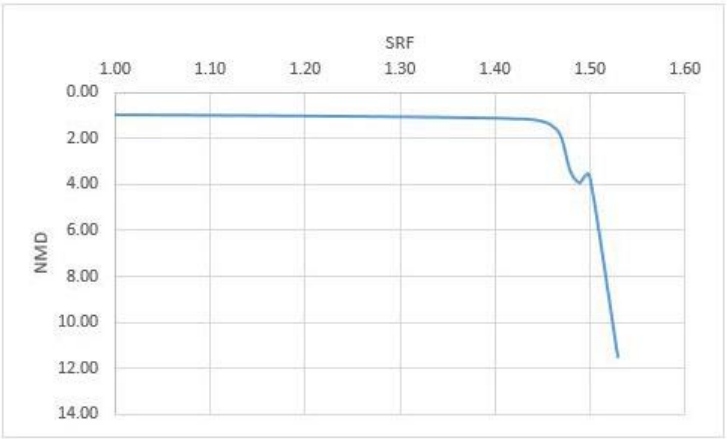

Figure B.11 FOS for general slope for L=0.5 H & ϕ=40 degrees

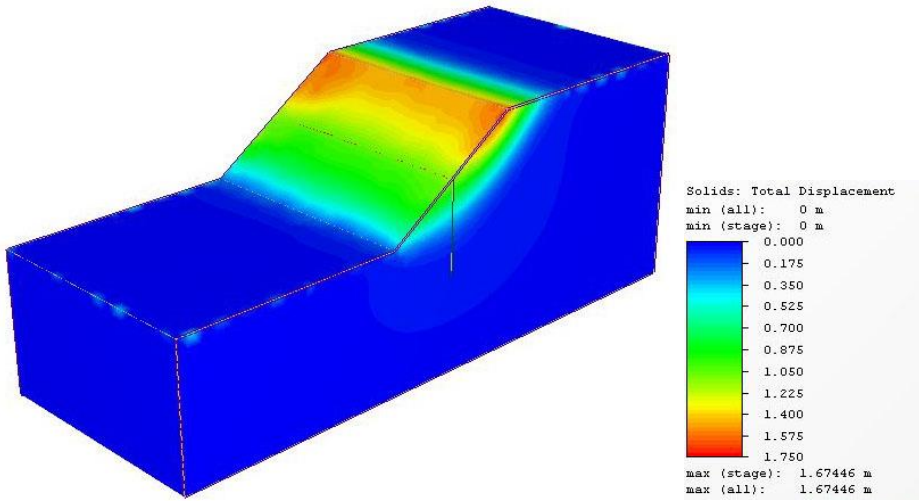

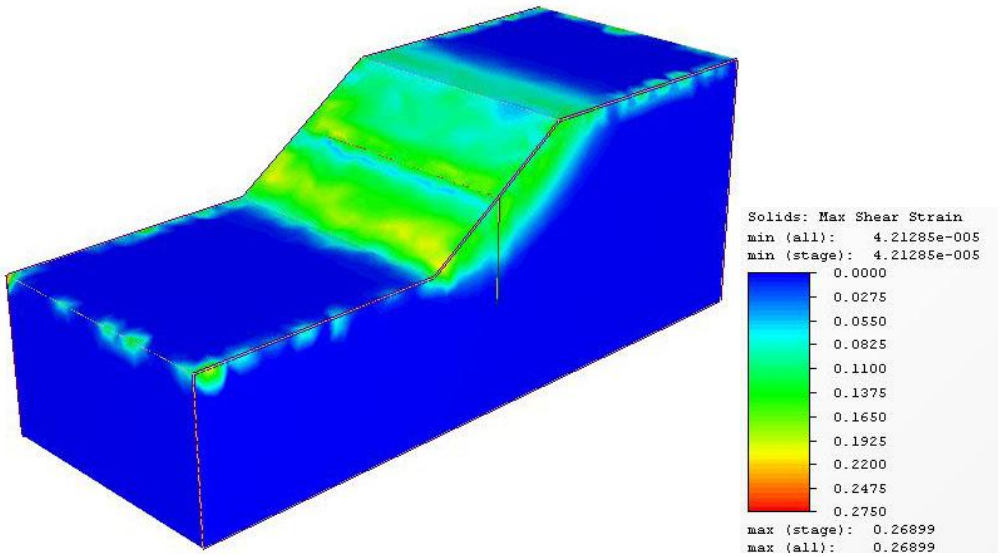

L=20 m

FOS	ϕ(Degrees)	C (KN/m^2)	δ_{max}	NMD	Remarks
1.0000	40.0000	2.0000	0.0676	0.9385	
1.1000	36.3636	1.8182	0.0694	0.9640	
1.2000	33.3333	1.6667	0.0713	0.9900	
1.3000	30.7692	1.5385	0.0741	1.0285	
1.4000	28.5714	1.4286	0.0784	1.0887	
1.4500	27.5862	1.3793	0.0911	1.2647	
1.4600	27.3973	1.3699	0.1053	1.4627	
1.4700	27.2109	1.3605	0.1324	1.8393	
1.4800	27.0270	1.3514	0.2318	3.2197	
1.4900	26.8456	1.3423	0.2460	3.4169	
1.5000	26.6667	1.3333	0.3486	4.8415	
1.6000	25.0000	1.2500	1.1424	15.8660	
1.7000	23.5294	1.1765	1.1931	16.5703	
1.8000	22.2222	1.1111	1.6745	23.2564	
1.9000	21.0526	1.0526	3.6602	50.8364	
2.0000	20.0000	1.0000	5.2241	72.5564	
2.1000	19.0476	0.9524	3.5416	49.1885	
2.2000	18.1818	0.9091	4.8917	67.9404	
2.2100	18.0995	0.9050	5.0482	70.1135	
2.2200	18.0180	0.9009	5.3854	74.7967	Unstable

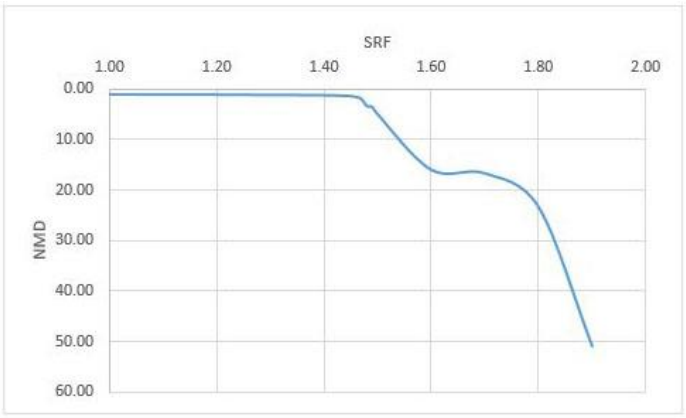

Figure B.12 FOS for general slope for L=1.0 H & ϕ=40 degrees

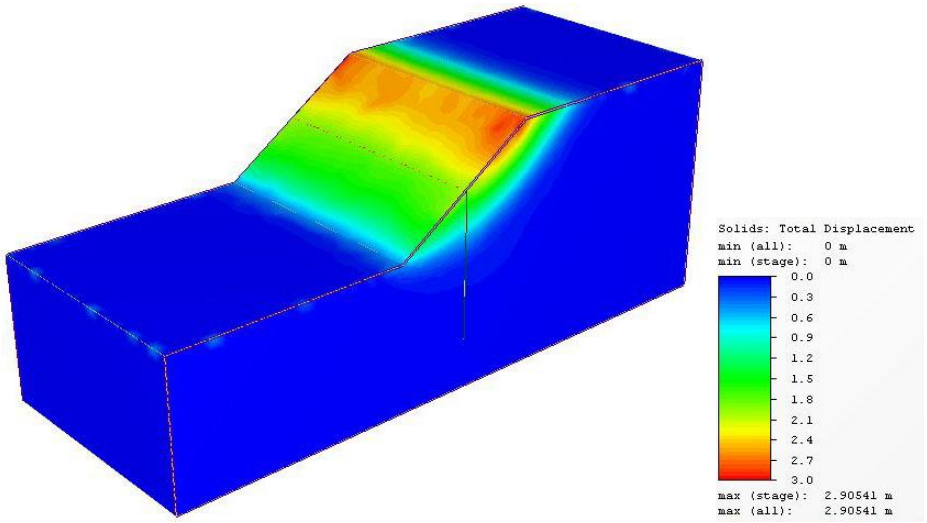

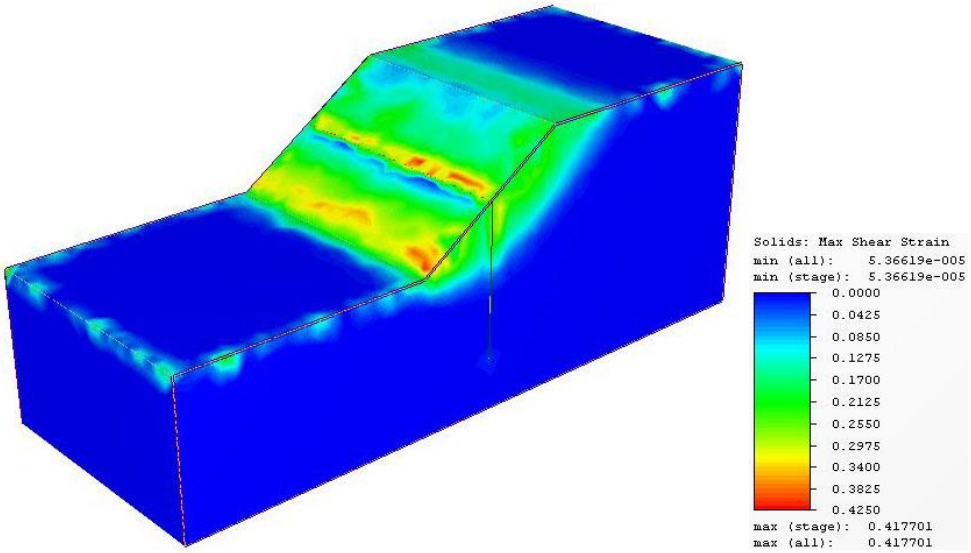

L=30 m

FOS	ϕ(Degrees)	C (KN/m^2)	δ_{max}	NMD	Remarks
1.0000	40.0000	2.0000	0.0674	0.9356	
1.1000	36.3636	1.8182	0.0690	0.9583	
1.2000	33.3333	1.6667	0.0706	0.9803	
1.3000	30.7692	1.5385	0.0731	1.0153	
1.4000	28.5714	1.4286	0.0777	1.0789	
1.5000	26.6667	1.3333	0.2369	3.2899	
1.6000	25.0000	1.2500	0.7967	11.0650	
1.7000	23.5294	1.1765	1.5878	22.0529	
1.8000	22.2222	1.1111	1.4174	19.6867	
1.9000	21.0526	1.0526	1.8374	25.5190	
2.0000	20.0000	1.0000	1.6276	22.6058	
2.0400	19.6078	0.9804	3.3811	46.9599	
2.0500	19.5122	0.9756	3.4115	47.3825	
2.0700	19.3237	0.9662	2.6459	36.7483	
2.0900	19.1388	0.9569	2.9054	40.3529	
2.1000	19.0476	0.9524	5.7555	79.9372	Unstable

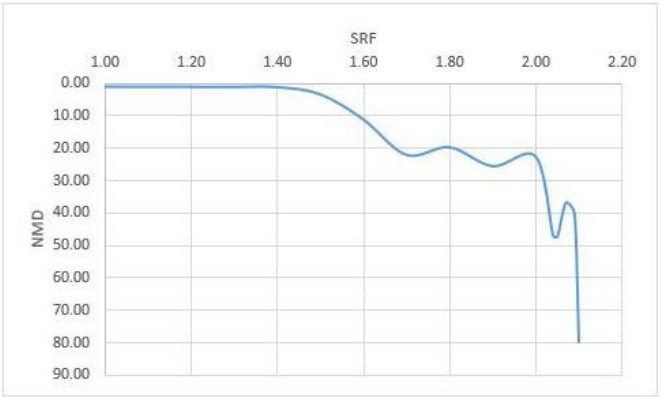

Figure B.13 FOS for general slope for L=1.5 H & ϕ=40 degrees

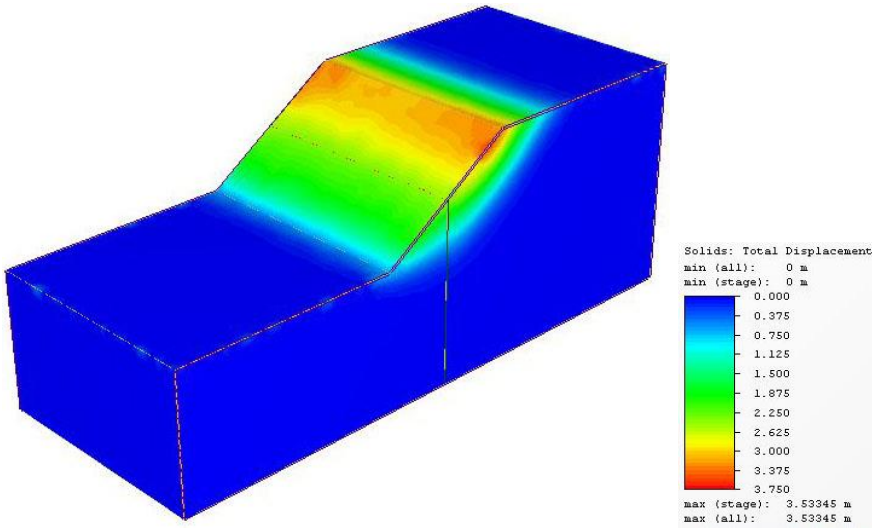

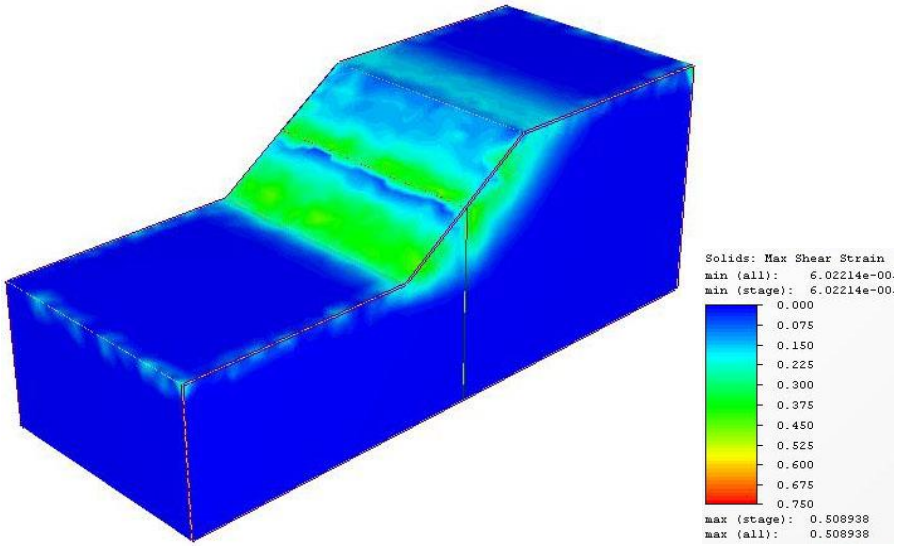

L=40 m

FOS	ϕ(Degrees)	C (KN/m^2)	δ_{max}	NMD	Remarks
1.0000	40.0000	2.0000	0.0673	0.9347	
1.1000	36.3636	1.8182	0.0690	0.9580	
1.2000	33.3333	1.6667	0.0707	0.9825	
1.3000	30.7692	1.5385	0.0728	1.0114	
1.4000	28.5714	1.4286	0.0780	1.0828	
1.5000	26.6667	1.3333	0.2448	3.3999	
1.6000	25.0000	1.2500	0.7199	9.9981	
1.7000	23.5294	1.1765	1.3962	19.3914	
1.8000	22.2222	1.1111	1.6324	22.6721	
1.9000	21.0526	1.0526	1.9986	27.7583	
2.0000	20.0000	1.0000	2.4192	33.6000	
2.1000	19.0476	0.9524	3.5335	49.0757	
2.2000	18.1818	0.9091	5.0895	70.6871	
2.3000	17.3913	0.8696	8.5011	118.0701	
2.3100	17.3160	0.8658	6.7167	93.2869	
2.3200	17.2414	0.8621	4.3816	60.8561	
2.3300	17.1674	0.8584	4.2647	59.2315	
2.3400	17.0940	0.8547	5.3927	74.8985	Unstable

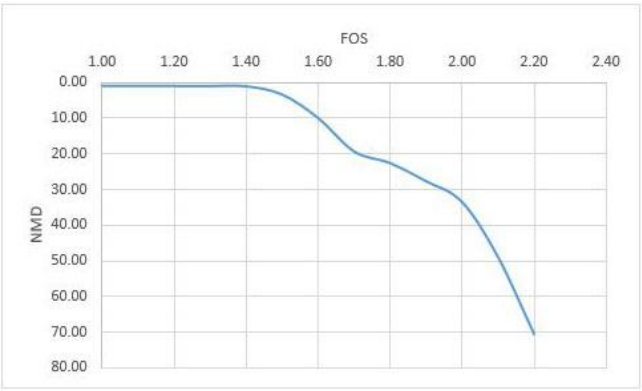

Figure B.14 FOS for general slope for L=2 H & ϕ=40 degrees

Effect of Pile Position

For ϕ=30 degrees

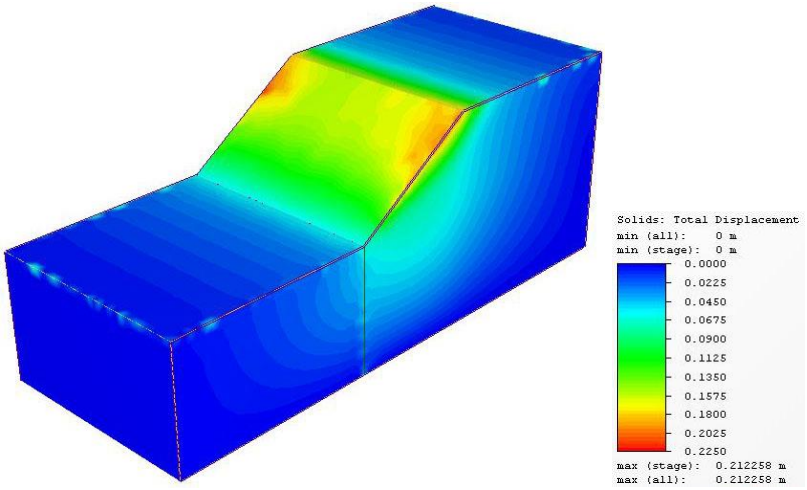

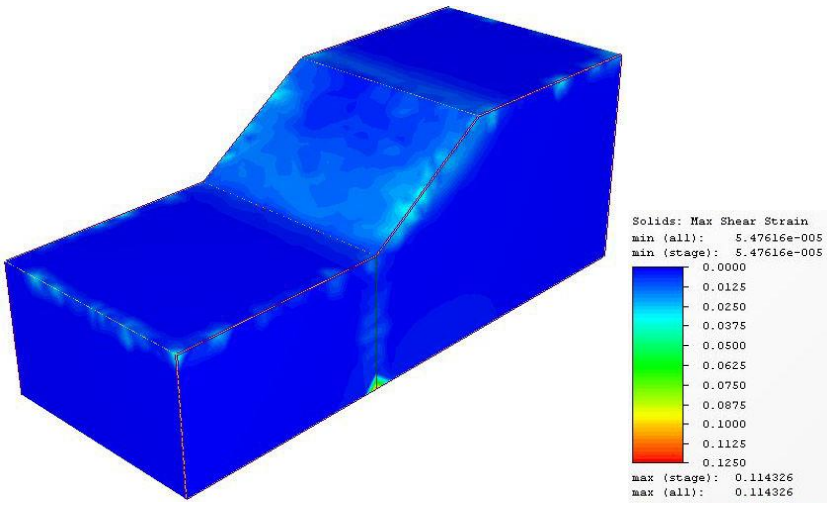

Xp=0

FOS	ϕ(Degrees)	C (KN/m^2)	δ_{max}	NMD	Remarks
1.0000	30.0000	2.0000	0.0737	1.0239	
1.1000	27.2727	1.8182	0.0820	1.1392	
1.1100	27.0270	1.8018	0.0950	1.3199	
1.1200	26.7857	1.7857	0.2123	2.9480	
1.1300	26.5487	1.7699	0.8812	12.2388	
1.1400	26.3158	1.7544	1.0630	14.7644	
1.1500	26.0870	1.7391	0.8363	11.6153	
1.2000	25.0000	1.6667	1.6754	23.2690	
1.2600	23.8095	1.5873	1.2126	16.8422	
1.2700	23.6220	1.5748	1.7914	24.8806	Unstable
1.3000	23.0769	1.5385	4.2123	58.5044	Unstable

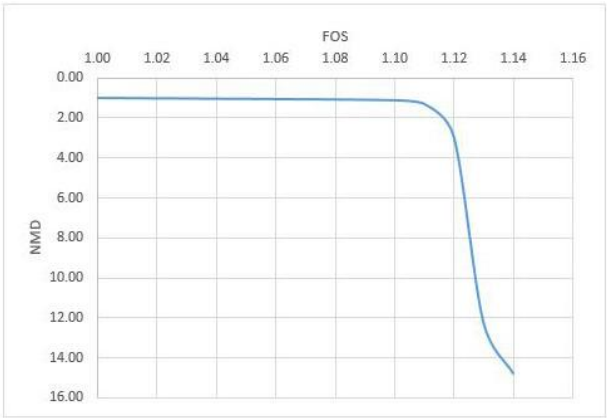

Figure B.15 FOS for general slope for Xp/X=0 & ϕ=30 degrees

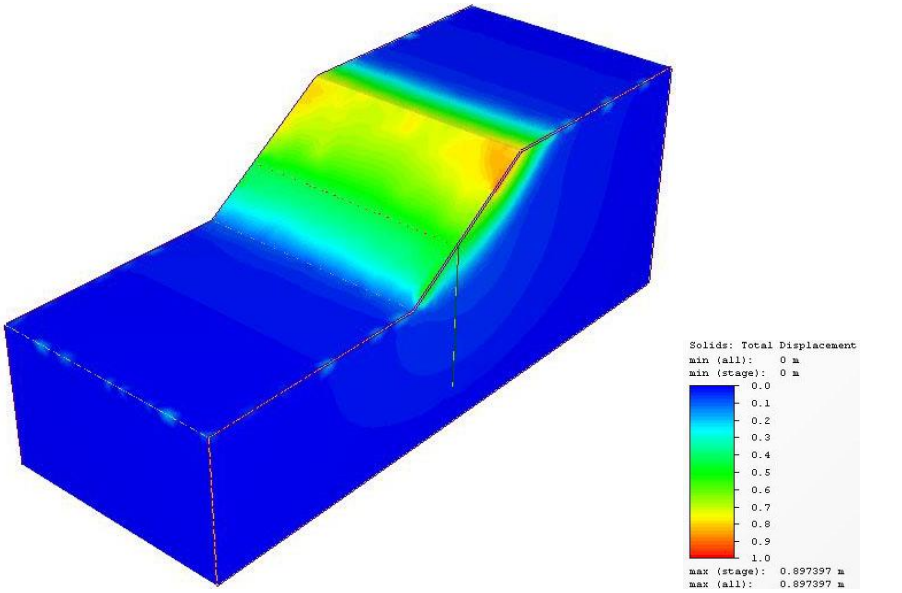

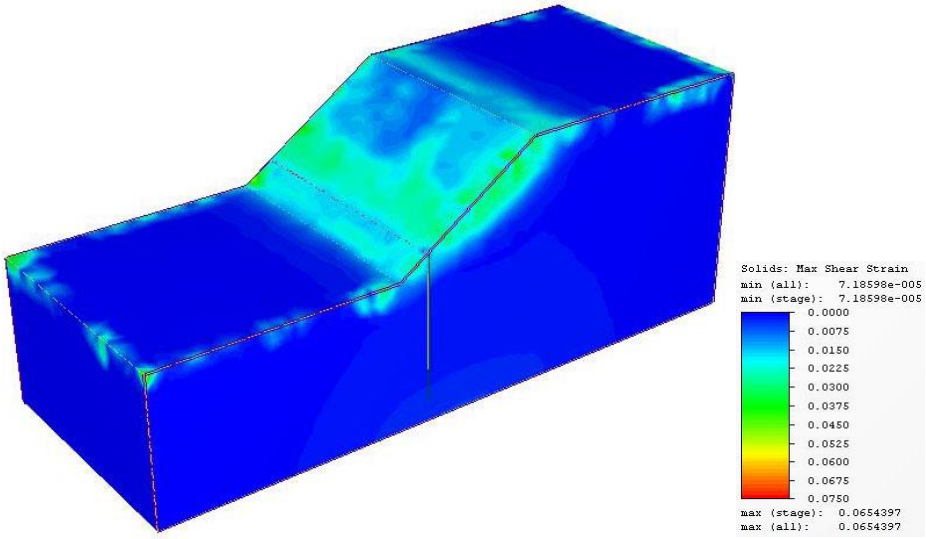

Xp=0.2

FOS	ϕ(Degrees)	C (KN/m^2)	δ_{max}	NMD	Remarks
1.0000	30.0000	2.0000	0.0735	1.0207	
1.1000	27.2727	1.8182	0.0824	1.1440	
1.1200	26.7857	1.7857	0.0992	1.3782	
1.1300	26.5487	1.7699	0.1221	1.6957	
1.1400	26.3158	1.7544	0.2262	3.1416	
1.1500	26.0870	1.7391	0.2725	3.7853	
1.1600	25.8621	1.7241	0.2435	3.3814	
1.1700	25.6410	1.7094	0.2610	3.6256	
1.1800	25.4237	1.6949	0.2916	4.0504	
1.1900	25.2101	1.6807	1.0331	14.3485	
1.2000	25.0000	1.6667	0.7910	10.9861	
1.3000	23.0769	1.5385	1.4364	19.9503	
1.3500	22.2222	1.4815	1.9283	26.7815	
1.3800	21.7391	1.4493	2.6436	36.7172	
1.3900	21.5827	1.4388	2.4646	34.2307	
1.4000	21.4286	1.4286	3.4467	47.8701	Unstable

Figure B.16 FOS for general slope for Xp/X=0.2 & ϕ=30 degrees

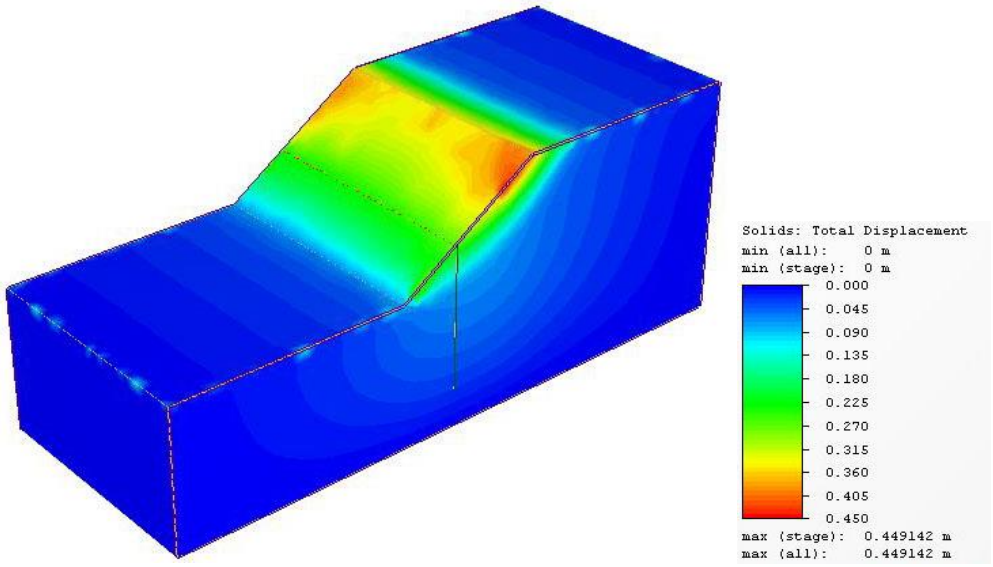

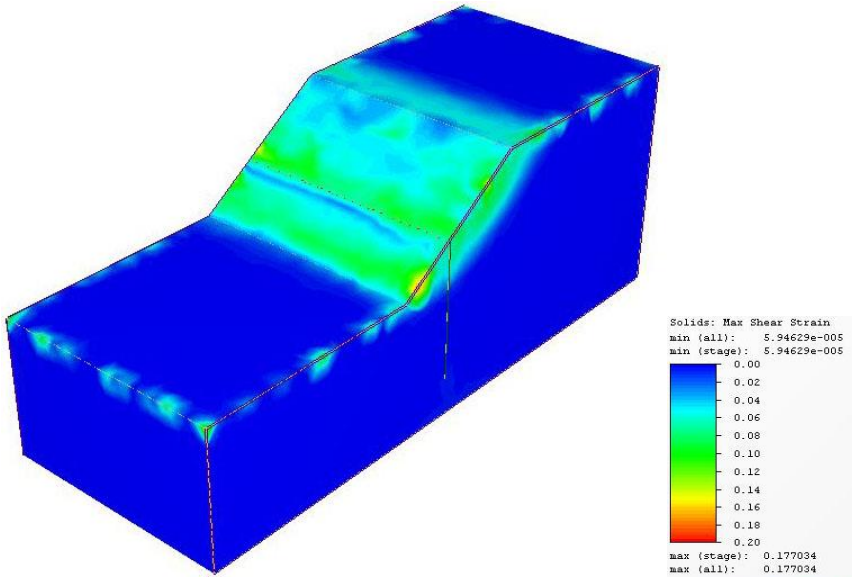

Xp=0.4

FOS	ϕ(Degrees)	C (KN/m^2)	δ_{max}	NMD	Remarks
1.0000	30.0000	2.0000	0.0759	1.0540	
1.1000	27.2727	1.8182	0.0867	1.2037	
1.1100	27.0270	1.8018	0.0986	1.3697	
1.1200	26.7857	1.7857	0.1495	2.0768	
1.1300	26.5487	1.7699	0.2517	3.4957	
1.1400	26.3158	1.7544	0.3186	4.4252	
1.1500	26.0870	1.7391	0.2485	3.4511	
1.2000	25.0000	1.6667	0.6331	8.7929	
1.3000	23.0769	1.5385	0.8974	12.4638	
1.3100	22.9008	1.5267	1.4465	20.0908	
1.3200	22.7273	1.5152	1.2121	16.8353	
1.3300	22.5564	1.5038	1.3970	19.4025	
1.3500	22.2222	1.4815	1.5719	21.8315	
1.4000	21.4286	1.4286	2.2622	31.4194	
1.5000	20.0000	1.3333	2.3252	32.2946	
1.6000	18.7500	1.2500	3.4403	47.7824	
1.6400	18.2927	1.2195	2.3216	32.2444	
1.6500	18.1818	1.2121	4.0675	56.4924	
1.6600	18.0723	1.2048	4.5784	63.5894	
1.6700	17.9641	1.1976	2.4767	34.3988	Unstable
1.7000	17.6471	1.1765	8.3045	115.3408	Unstable

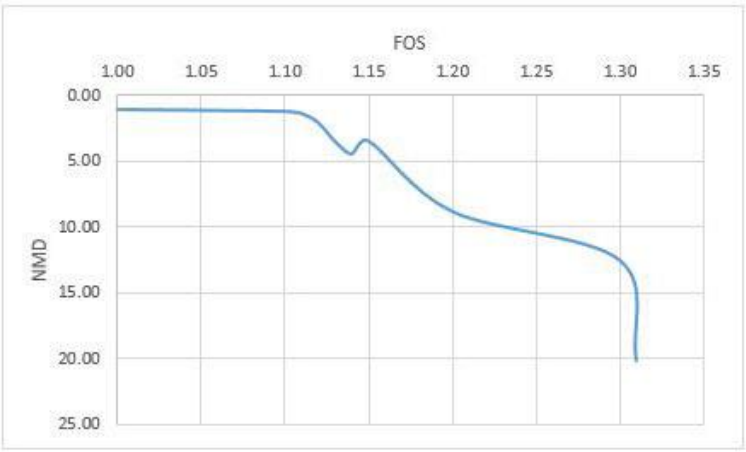

Figure B.17 FOS for general slope for Xp/X=0.4 & ϕ=30 degrees

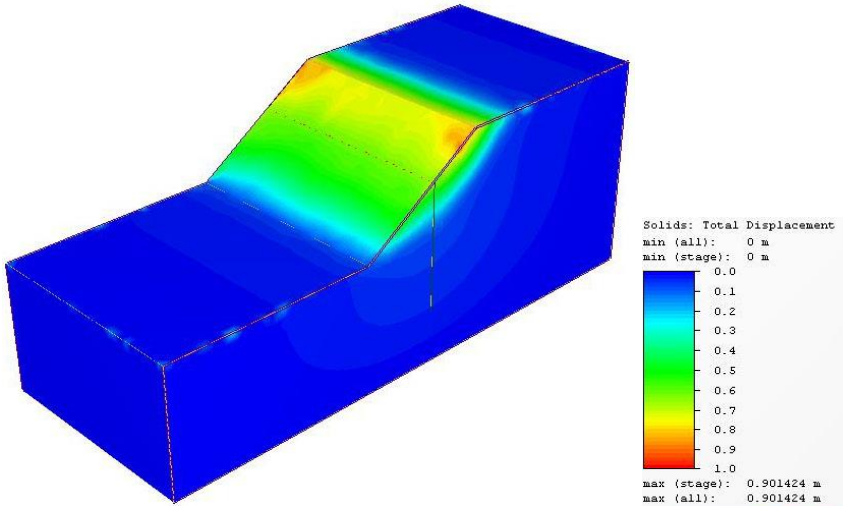

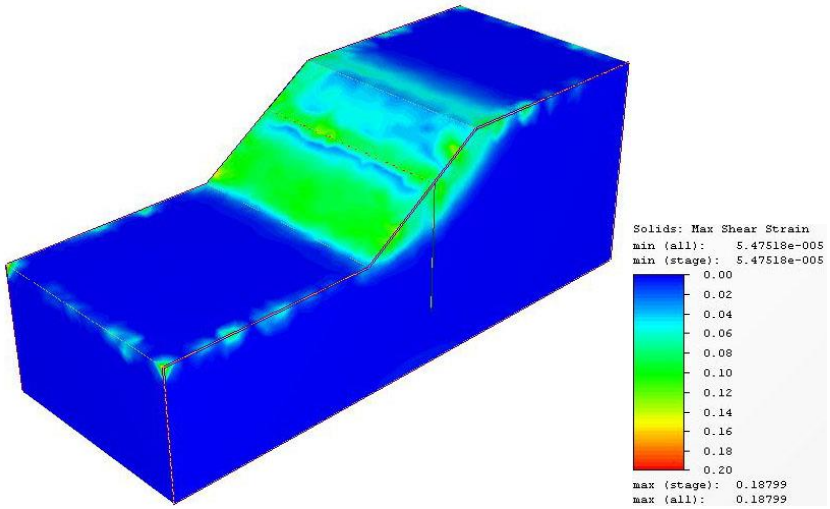

Xp=0.6

FOS	ϕ(Degrees)	C (KN/m^2)	δ_{max}	NMD	Remarks
1.0000	30.0000	2.0000	0.0733	1.0180	
1.1000	27.2727	1.8182	0.0835	1.1596	
1.1100	27.0270	1.8018	0.0926	1.2860	
1.1200	26.7857	1.7857	0.1246	1.7311	
1.1300	26.5487	1.7699	0.2023	2.8092	
1.1400	26.3158	1.7544	0.2513	3.4908	
1.1500	26.0870	1.7391	0.2705	3.7568	
1.1600	25.8621	1.7241	0.3717	5.1631	
1.1700	25.6410	1.7094	0.2824	3.9229	
1.1800	25.4237	1.6949	0.2940	4.0827	
1.1900	25.2101	1.6807	0.5009	6.9572	
1.2000	25.0000	1.6667	0.6467	8.9818	
1.3000	23.0769	1.5385	0.9014	12.5198	
1.3100	22.9008	1.5267	1.1187	15.5374	
1.3500	22.2222	1.4815	1.2651	17.5714	
1.4000	21.4286	1.4286	2.0112	27.9335	
1.5000	20.0000	1.3333	4.3747	60.7592	

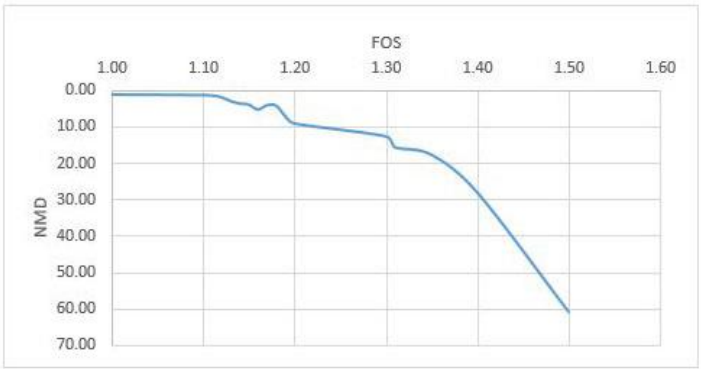

Figure B.18 FOS for general slope for Xp/X=0.6 & ϕ=30 degrees

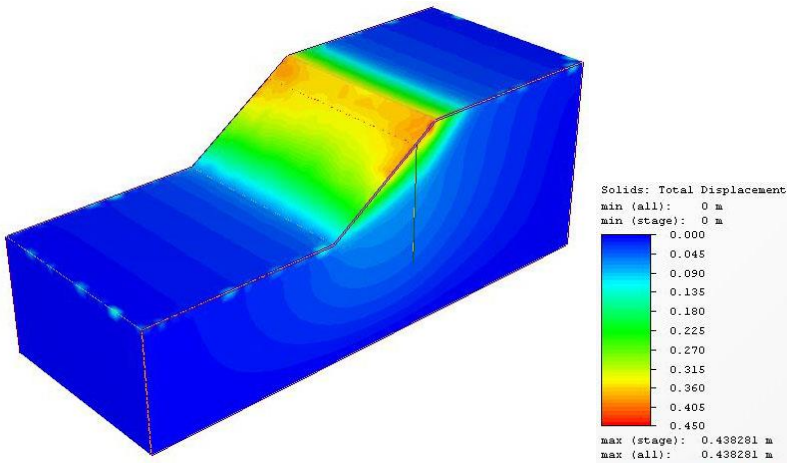

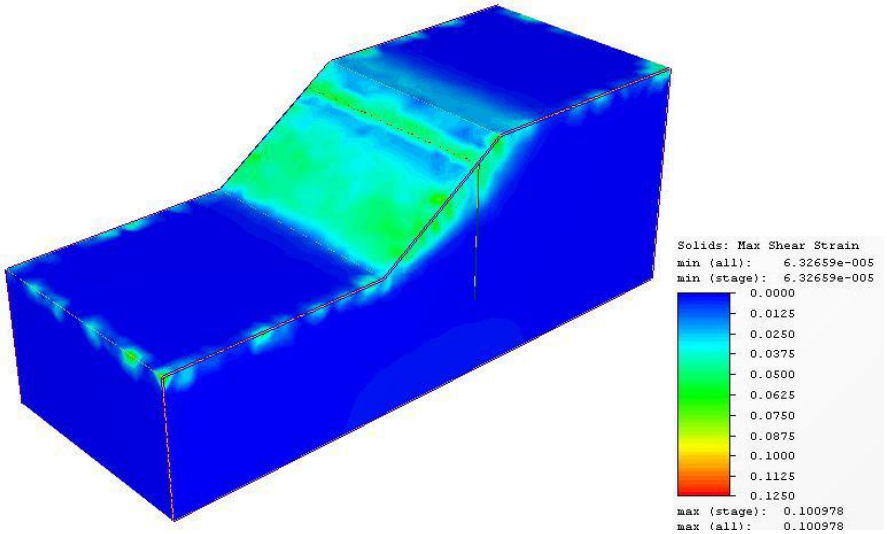

Xp=0.8

FOS	ϕ(Degrees)	C (KN/m^2)	δ_{max}	NMD	Remarks
1.0000	30.0000	2.0000	0.0724	1.0060	
1.0500	28.5714	1.9048	0.0746	1.0368	
1.0700	28.0374	1.8692	0.0757	1.0509	
1.0800	27.7778	1.8519	0.0770	1.0698	
1.0900	27.5229	1.8349	0.0783	1.0881	
1.1000	27.2727	1.8182	0.0803	1.1147	
1.1100	27.0270	1.8018	0.0867	1.2047	
1.1200	26.7857	1.7857	0.0967	1.3437	
1.1300	26.5487	1.7699	0.2061	2.8630	
1.1400	26.3158	1.7544	0.2326	3.2299	
1.1500	26.0870	1.7391	0.3064	4.2559	
1.2000	25.0000	1.6667	0.4383	6.0872	
1.2100	24.7934	1.6529	0.7123	9.8936	
1.2200	24.5902	1.6393	0.8839	12.2764	
1.2300	24.3902	1.6260	0.9871	13.7094	
1.2500	24.0000	1.6000	1.0909	15.1517	

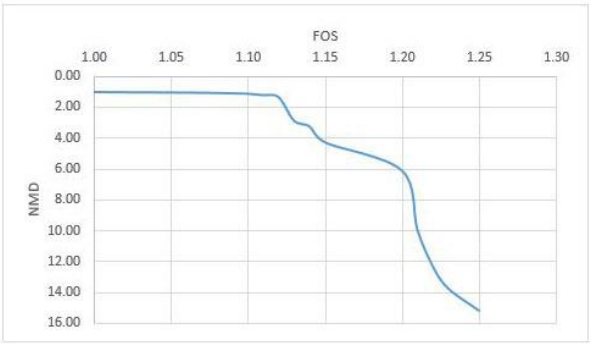

Figure B.19 FOS for general slope for Xp/X=0.8 & ϕ=30 degrees

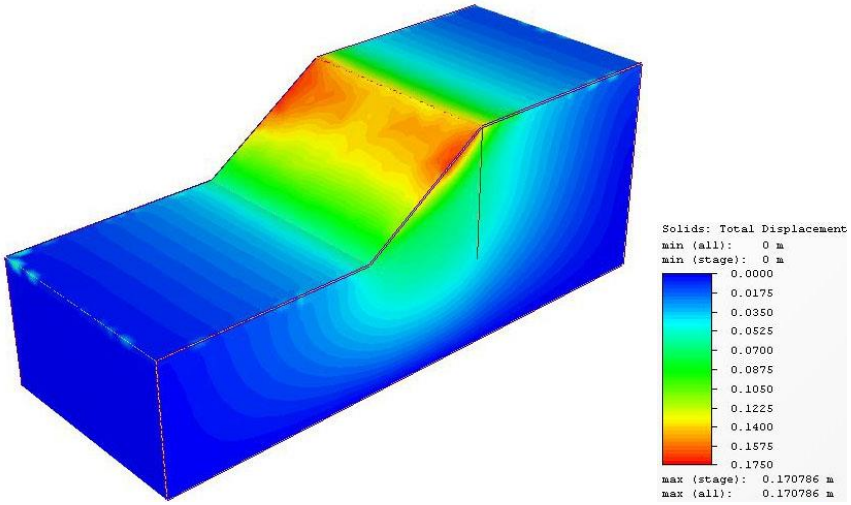

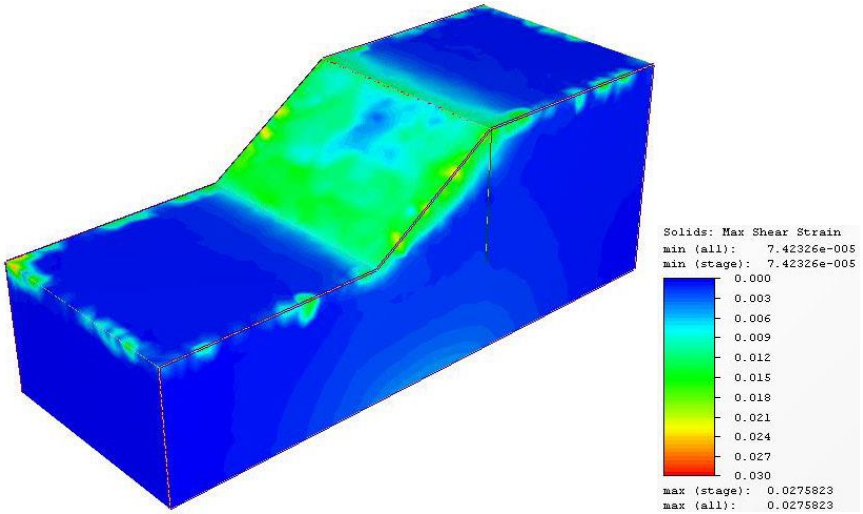

Xp=1

FOS	ϕ(Degrees)	C (KN/m^2)	δ_{max}	NMD	Remarks
1.0000	30.0000	2.0000	0.0717	0.9957	
1.1000	27.2727	1.8182	0.0783	1.0882	
1.1100	27.0270	1.8018	0.0833	1.1576	
1.1200	26.7857	1.7857	0.0981	1.3621	
1.1300	26.5487	1.7699	0.1708	2.3720	
1.1400	26.3158	1.7544	0.2642	3.6691	
1.1500	26.0870	1.7391	0.5279	7.3324	
1.1700	25.6410	1.7094	0.7620	10.5836	
1.2000	25.0000	1.6667	0.4229	5.8740	
1.2500	24.0000	1.6000	0.9931	13.7932	
1.2600	23.8095	1.5873	0.7669	10.6521	
1.2700	23.6220	1.5748	1.2657	17.5789	Unstable
1.3000	23.0769	1.5385	1.5059	20.9154	Unstable

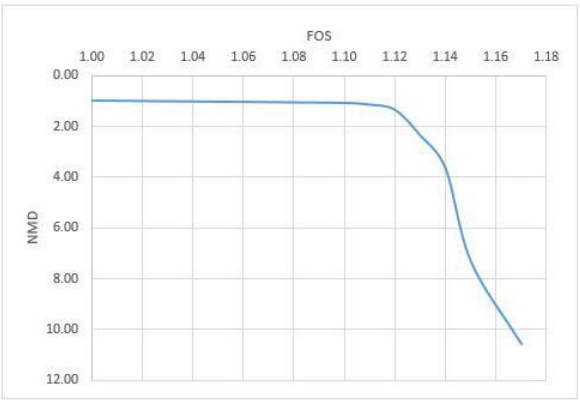

Figure B.20 FOS for general slope for Xp/X=1 & ϕ=30 degrees

For ϕ=35 Degrees

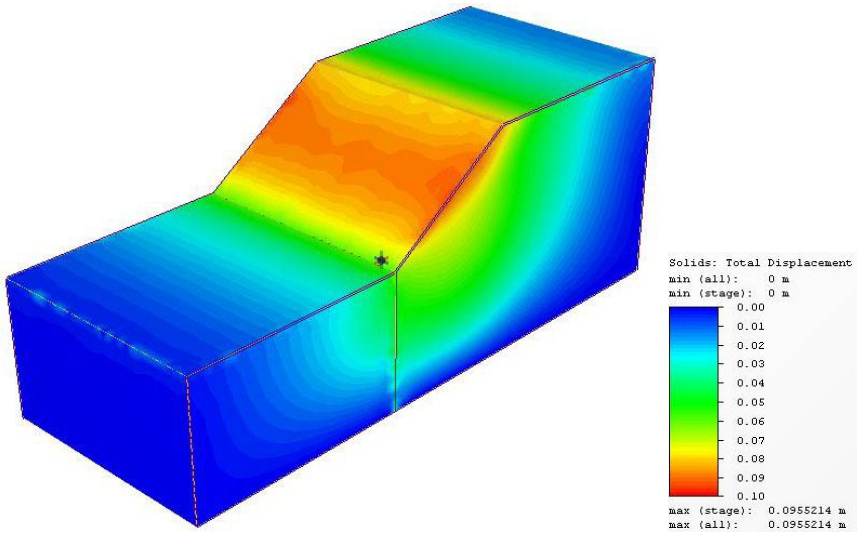

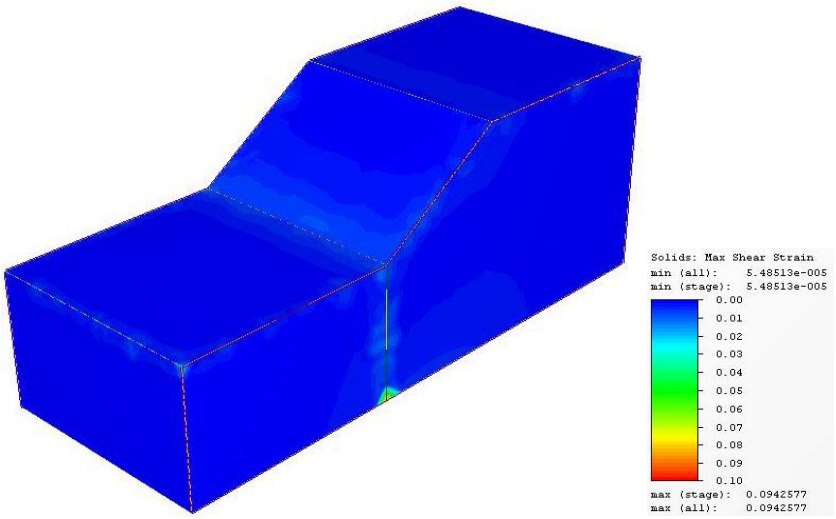

Xp=0

FOS	ϕ(Degrees)	C (KN/m^2)	δ_{max}	NMD	Remarks
1.0000	35.0000	2.0000	0.0697	0.9677	
1.1000	31.8182	1.8182	0.0717	0.9965	
1.2000	29.1667	1.6667	0.0755	1.0486	
1.2500	28.0000	1.6000	0.0797	1.1071	
1.2700	27.5591	1.5748	0.0840	1.1672	
1.2800	27.3438	1.5625	0.0955	1.3267	
1.2900	27.1318	1.5504	0.4039	5.6092	
1.3000	26.9231	1.5385	0.3288	4.5664	
1.4000	25.0000	1.4286	0.6929	9.6234	
1.4300	24.4755	1.3986	0.8209	11.4017	
1.4400	24.3056	1.3889	1.5777	21.9125	Unstable
1.4500	24.1379	1.3793	1.5538	21.5801	Unstable

Figure B.21 FOS for general slope for Xp/X=0 & ϕ=35 degrees

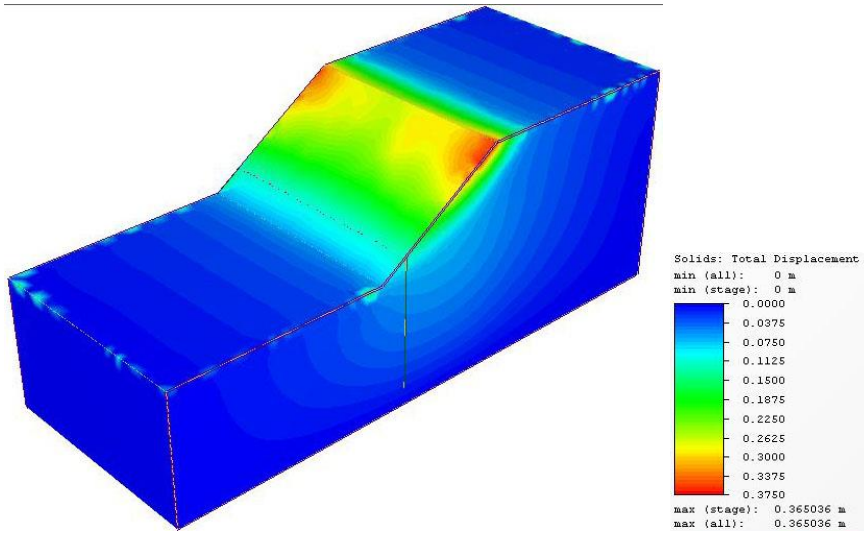

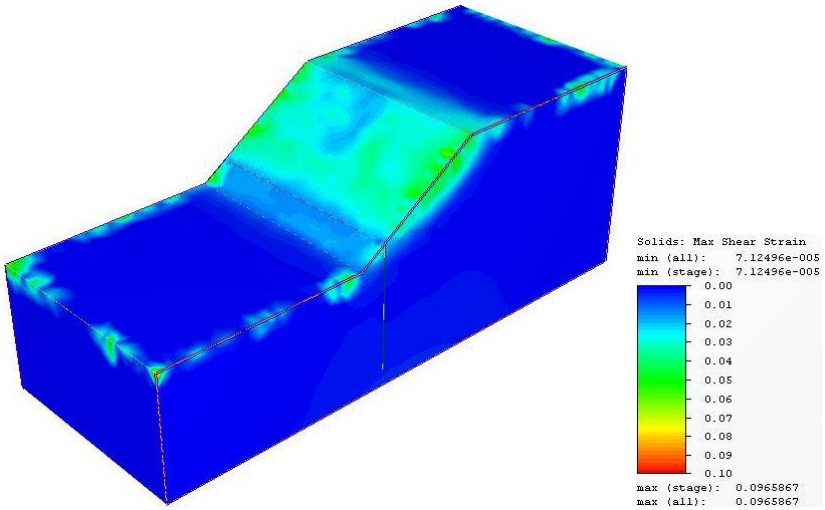

Xp=0.2

FOS	ϕ(Degrees)	C (KN/m^2)	δ_{max}	NMD	Remarks
1.00000	35.00000	2.00000	0.07014	0.97420	
1.10000	31.81818	1.81818	0.07187	0.99820	
1.20000	29.16667	1.66667	0.07515	1.04371	
1.25000	28.00000	1.60000	0.07966	1.10642	
1.27000	27.55906	1.57480	0.08235	1.14368	
1.28000	27.34375	1.56250	0.08641	1.20008	
1.29000	27.13178	1.55039	0.09499	1.31935	
1.30000	26.92308	1.53846	0.11874	1.64913	
1.31000	26.71756	1.52672	0.21412	2.97392	
1.32000	26.51515	1.51515	0.24149	3.35399	
1.33000	26.31579	1.50376	0.36504	5.06994	
1.34000	26.11940	1.49254	0.63375	8.80211	
1.35000	25.92593	1.48148	0.46319	6.43317	
1.40000	25.00000	1.42857	0.74715	10.37704	

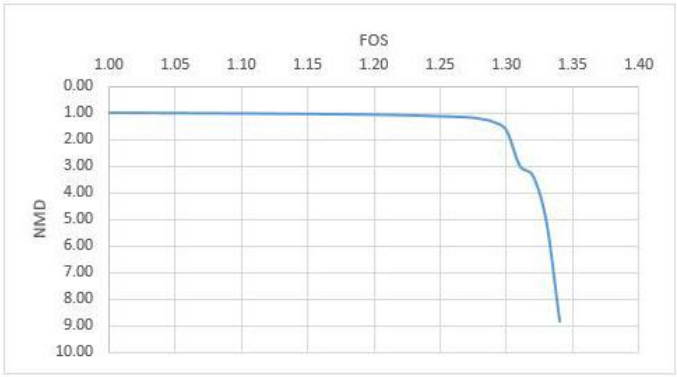

Figure B.22 FOS for general slope for Xp/X=0.2 & ϕ=35 degrees

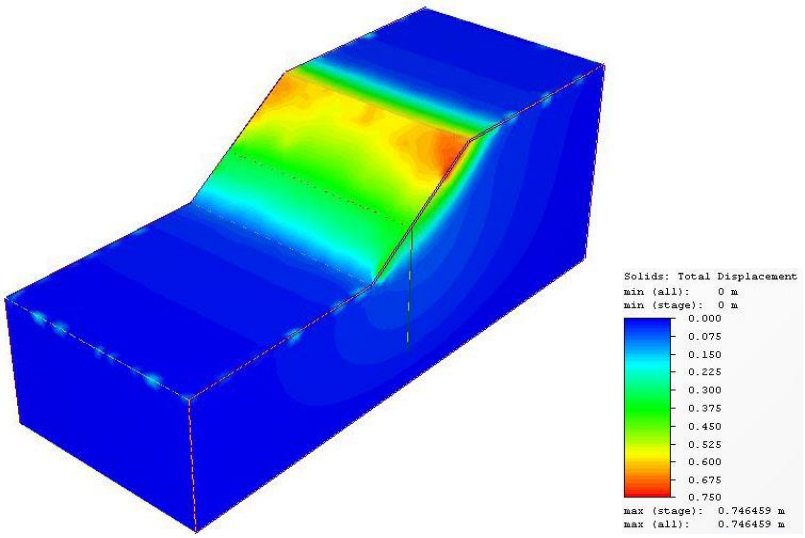

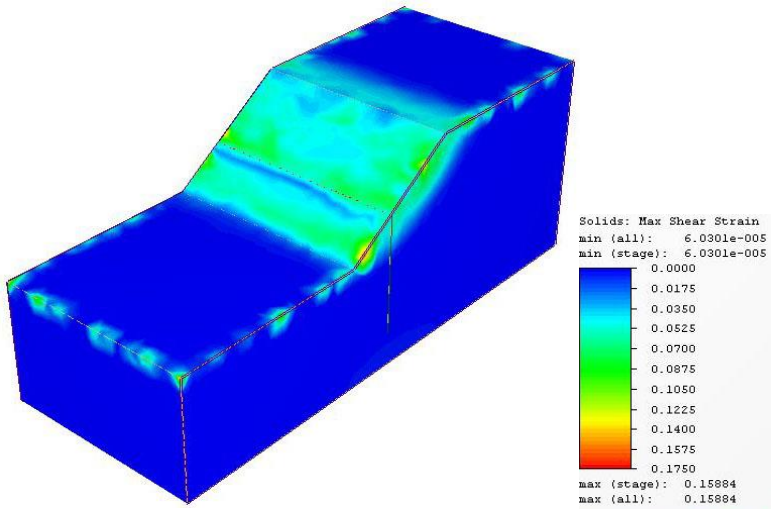

Xp=0.4

FOS	ϕ(Degrees)	C (KN/m^2)	δ_{max}	NMD	Remarks
1.0000	35.0000	2.0000	0.0714	0.9910	
1.1000	31.8182	1.8182	0.0738	1.0244	
1.2000	29.1667	1.6667	0.0773	1.0739	
1.2500	28.0000	1.6000	0.0823	1.1434	
1.2700	27.5591	1.5748	0.0873	1.2131	
1.2800	27.3438	1.5625	0.0995	1.3817	
1.2900	27.1318	1.5504	0.1278	1.7749	
1.3000	26.9231	1.5385	0.2388	3.3166	
1.3100	26.7176	1.5267	0.2490	3.4582	
1.3200	26.5152	1.5152	0.2473	3.4348	
1.3300	26.3158	1.5038	0.4116	5.7161	
1.4000	25.0000	1.4286	0.6117	8.4965	
1.4100	24.8227	1.4184	0.6568	9.1224	
1.4200	24.6479	1.4085	0.7465	10.3675	
1.4300	24.4755	1.3986	1.0492	14.5724	
1.4700	23.8095	1.3605	1.2473	17.3229	

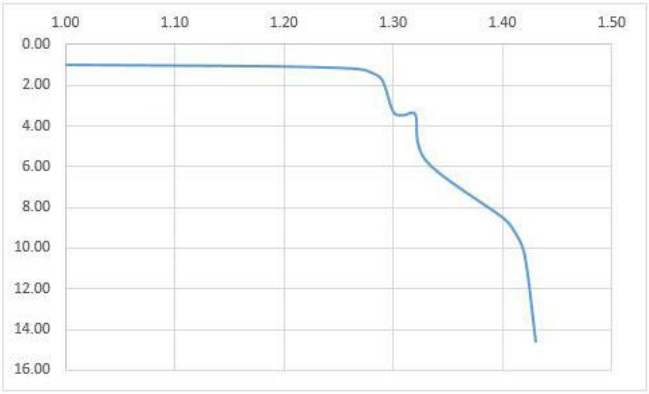

Figure B.23 FOS for general slope for Xp/X=0.4 & ϕ=35 degrees

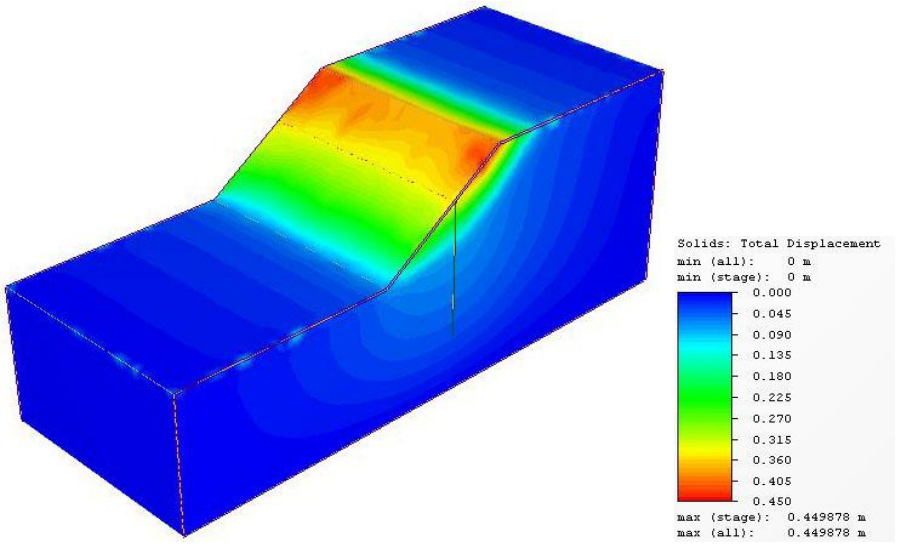

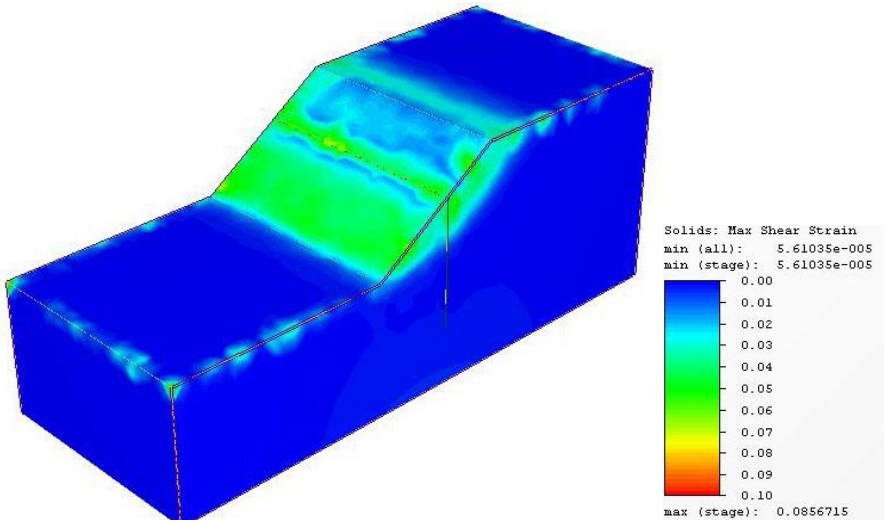

Xp=0.6

FOS	ϕ(Degrees)	C (KN/m^2)	δ_{max}	NMD	Remarks
1.0000	35.0000	2.0000	0.0693	0.9622	
1.1000	31.8182	1.8182	0.0714	0.9915	
1.2000	29.1667	1.6667	0.0749	1.0400	
1.2500	28.0000	1.6000	0.0793	1.1015	
1.2700	27.5591	1.5748	0.0849	1.1790	
1.2800	27.3438	1.5625	0.0952	1.3229	
1.2900	27.1318	1.5504	0.1173	1.6291	
1.3000	26.9231	1.5385	0.1269	1.7632	
1.4000	25.0000	1.4286	0.5678	7.8861	
1.4300	24.4755	1.3986	0.4499	6.2483	
1.4400	24.3056	1.3889	1.4199	19.7208	
1.4500	24.1379	1.3793	0.8255	11.4658	
1.4700	23.8095	1.3605	0.8334	11.5754	
1.4800	23.6486	1.3514	1.0793	14.9906	
1.5000	23.3333	1.3333	1.4939	20.7488	

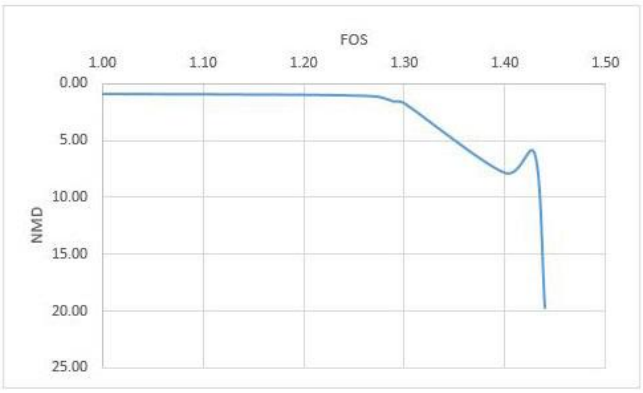

Figure B.24 FOS for general slope for Xp/X=0.6 & ϕ=35 degrees

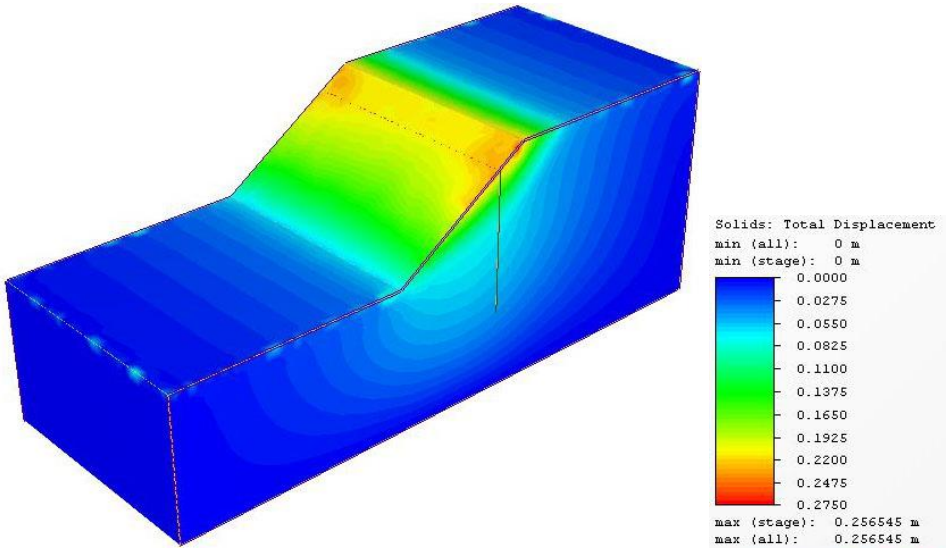

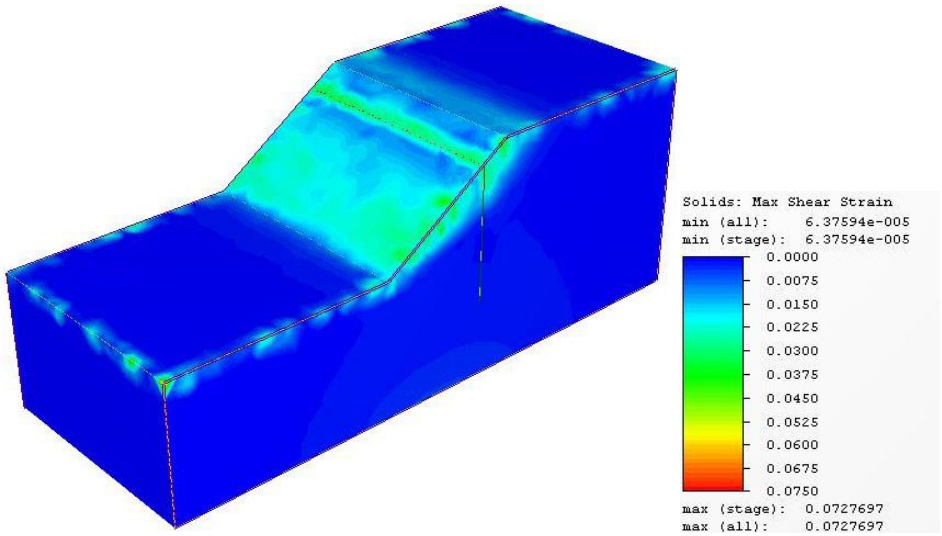

Xp=0.8

FOS	ϕ(Degrees)	C (KN/m^2)	δ_{max}	NMD	Remarks
1.0000	35.0000	2.0000	0.0692	0.9605	
1.1000	31.8182	1.8182	0.0708	0.9835	
1.2000	29.1667	1.6667	0.0739	1.0262	
1.2500	28.0000	1.6000	0.0775	1.0760	
1.3000	26.9231	1.5385	0.1920	2.6664	
1.3200	26.5152	1.5152	0.2095	2.9093	
1.3300	26.3158	1.5038	0.2864	3.9777	
1.3400	26.1194	1.4925	0.3334	4.6303	
1.3500	25.9259	1.4815	0.3797	5.2736	
1.3600	25.7353	1.4706	0.2565	3.5631	
1.3700	25.5474	1.4599	0.5809	8.0683	
1.4000	25.0000	1.4286	0.7821	10.8624	
1.5000	23.3333	1.3333	0.9753	13.5460	
1.6000	21.8750	1.2500	2.1424	29.7553	Unstable

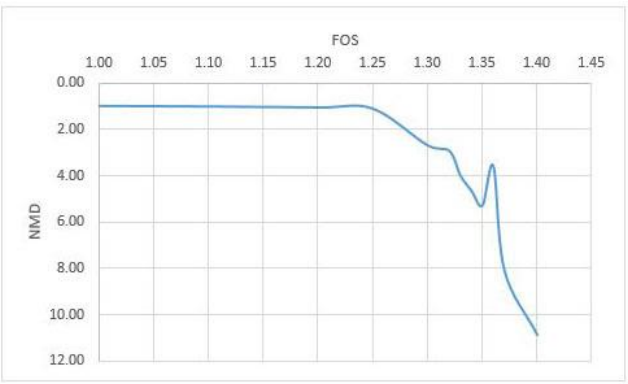

Figure B.25 FOS for general slope for Xp/X=0.8 & ϕ=35 degrees

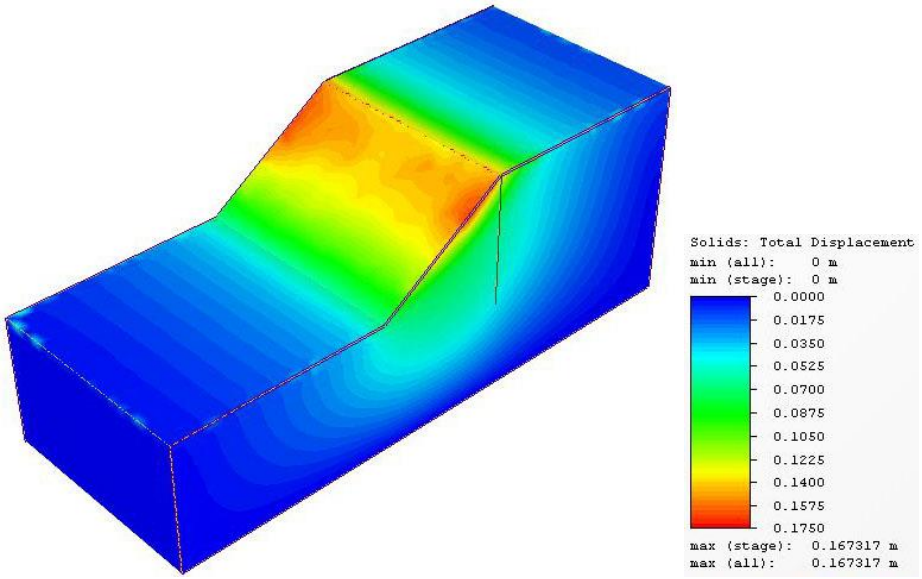

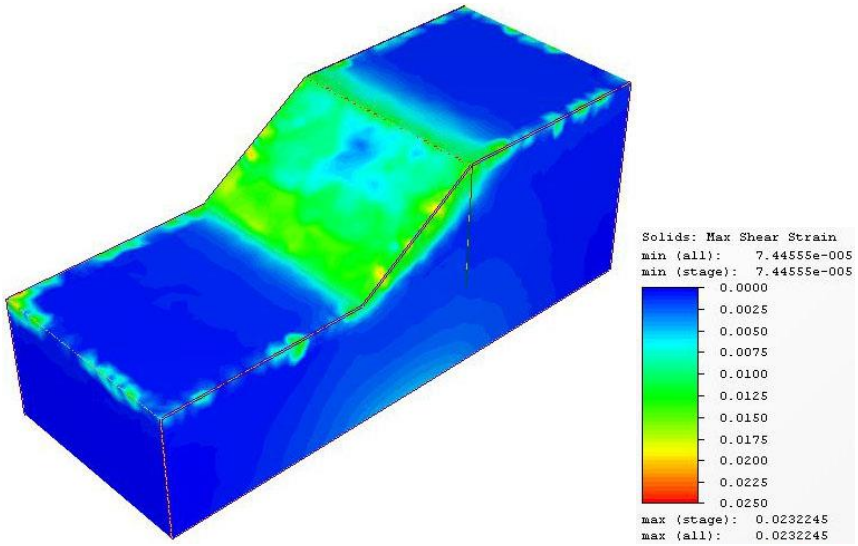

Xp=1

FOS	ϕ(Degrees)	C (KN/m^2)	δ_{max}	NMD	Remarks
1.0000	35.0000	2.0000	0.0688	0.9562	
1.1000	31.8182	1.8182	0.0703	0.9766	
1.2000	29.1667	1.6667	0.0732	1.0162	
1.2500	28.0000	1.6000	0.0763	1.0601	
1.2600	27.7778	1.5873	0.0769	1.0677	
1.2800	27.3438	1.5625	0.0837	1.1628	
1.2900	27.1318	1.5504	0.1025	1.4232	
1.3000	26.9231	1.5385	0.1478	2.0526	
1.3100	26.7176	1.5267	0.1762	2.4469	
1.3200	26.5152	1.5152	0.1606	2.2300	
1.3300	26.3158	1.5038	0.1673	2.3238	
1.3400	26.1194	1.4925	0.7464	10.3670	

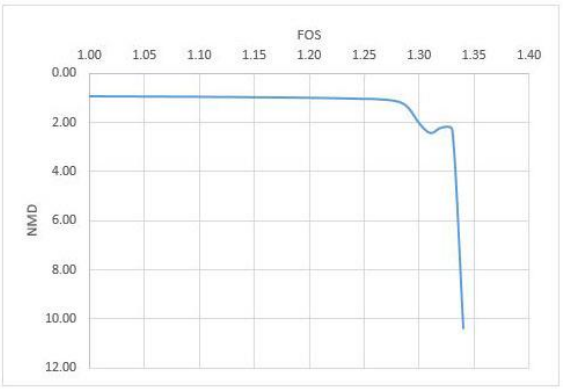

Figure B.26 FOS for general slope for Xp/X=1 & ϕ=35 degrees

For ϕ=40 Degrees

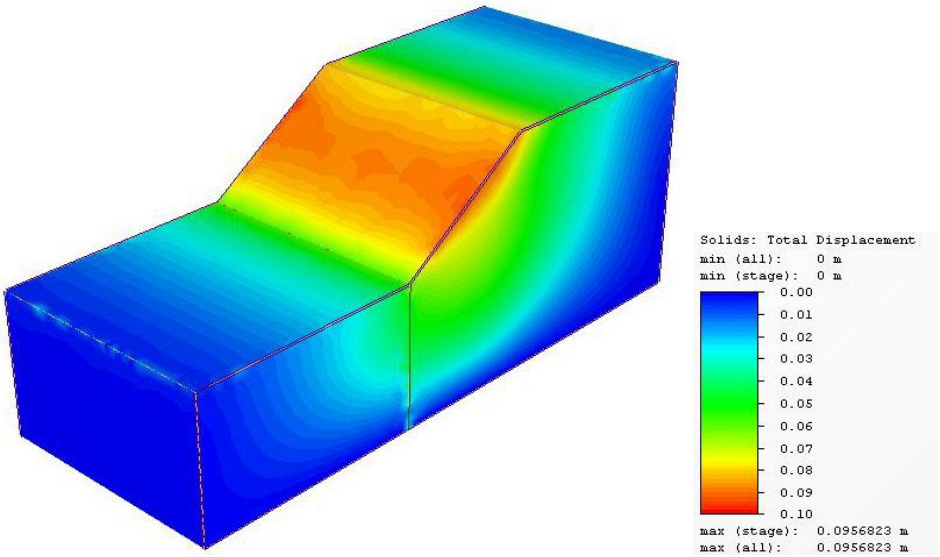

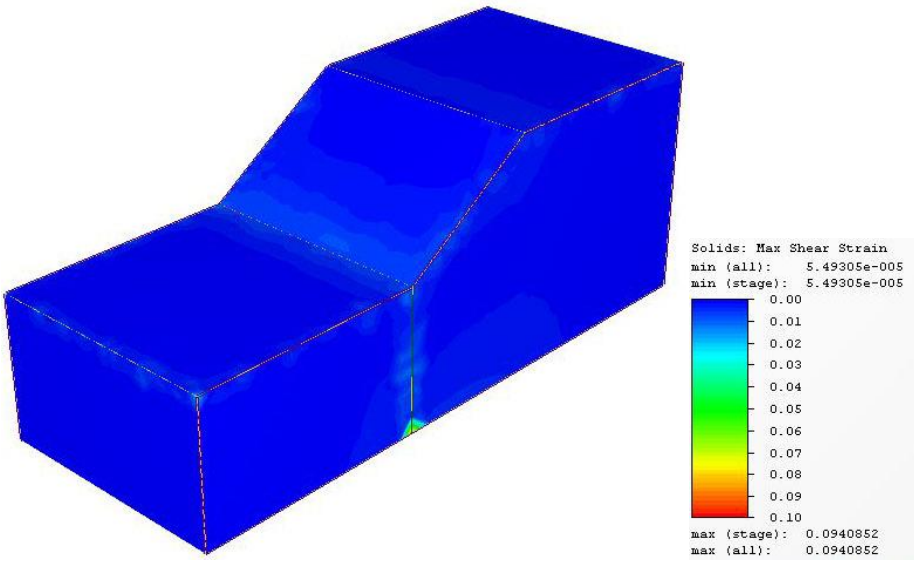

Xp=0

FOS	ϕ(Degrees)	C (KN/m^2)	δ_{max}	NMD	Remarks
1.0000	40.0000	2.0000	0.0676	0.9388	
1.1000	36.3636	1.8182	0.0692	0.9606	
1.2000	33.3333	1.6667	0.0709	0.9844	
1.3000	30.7692	1.5385	0.0736	1.0223	
1.4000	28.5714	1.4286	0.0778	1.0811	
1.4400	27.7778	1.3889	0.0843	1.1709	
1.4500	27.5862	1.3793	0.0957	1.3289	
1.4600	27.3973	1.3699	0.4717	6.5508	
1.4700	27.2109	1.3605	0.4800	6.6672	
1.5000	26.6667	1.3333	0.5501	7.6403	
1.6000	25.0000	1.2500	0.7008	9.7331	
1.6200	24.6914	1.2346	0.8392	11.6558	
1.6300	24.5399	1.2270	1.4699	20.4153	Unstable

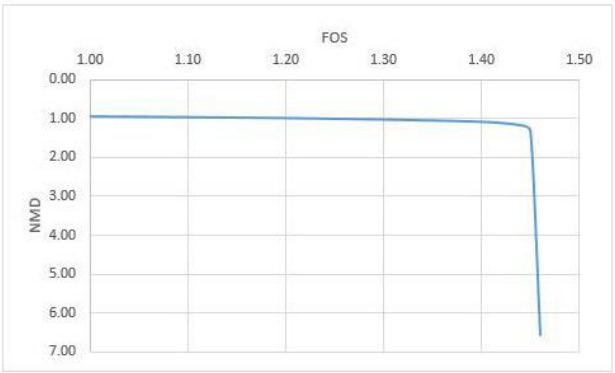

Figure B.27 FOS for general slope for Xp/X=0 & ϕ=40 degrees

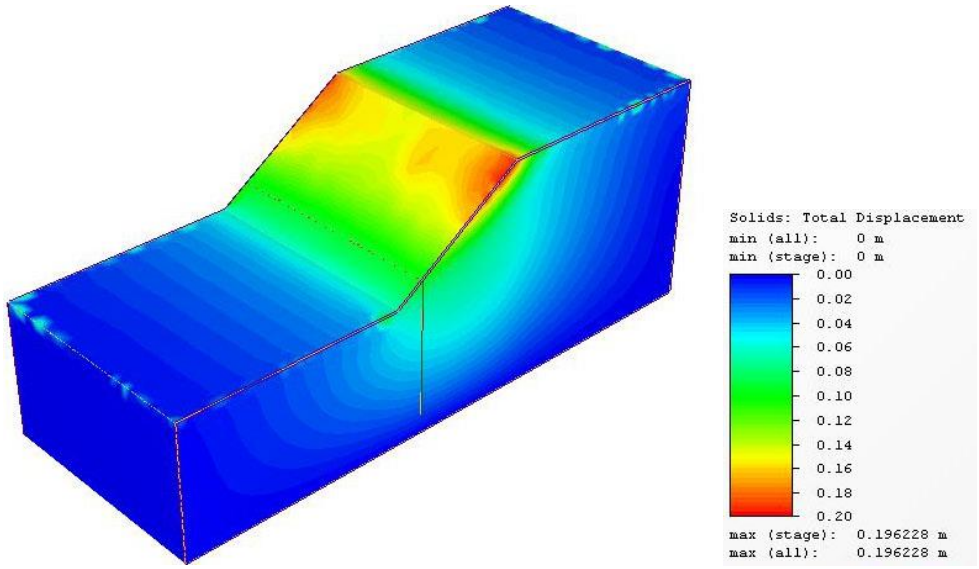

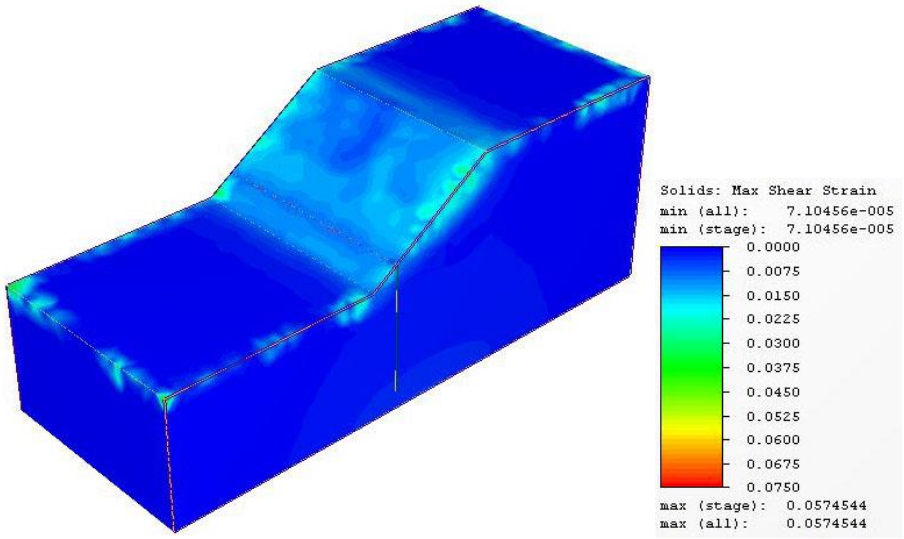

Xp=0.2

FOS	ϕ(Degrees)	C (KN/m^2)	δ_{max}	NMD	Remarks
1.0000	40.0000	2.0000	0.0680	0.9444	
1.1000	36.3636	1.8182	0.0697	0.9678	
1.2000	33.3333	1.6667	0.0711	0.9873	
1.3000	30.7692	1.5385	0.0732	1.0173	
1.4000	28.5714	1.4286	0.0777	1.0789	
1.4400	27.7778	1.3889	0.0826	1.1475	
1.4500	27.5862	1.3793	0.0866	1.2023	
1.4600	27.3973	1.3699	0.0928	1.2893	
1.4700	27.2109	1.3605	0.1116	1.5501	
1.4800	27.0270	1.3514	0.1962	2.7254	
1.5000	26.6667	1.3333	0.4046	5.6190	
1.6000	25.0000	1.2500	1.1467	15.9257	
1.7000	23.5294	1.1765	0.7524	10.4496	
1.7300	23.1214	1.1561	1.1494	15.9644	

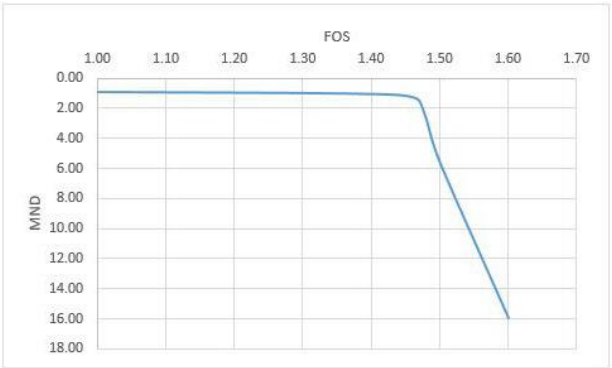

Figure B.28 FOS for general slope for Xp/X=0.2 & ϕ=40 degrees

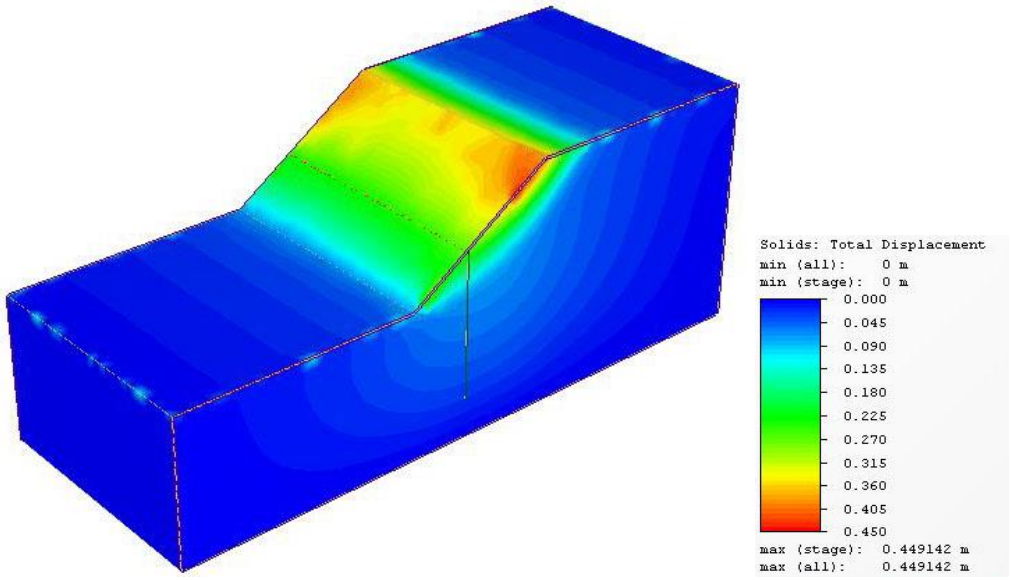

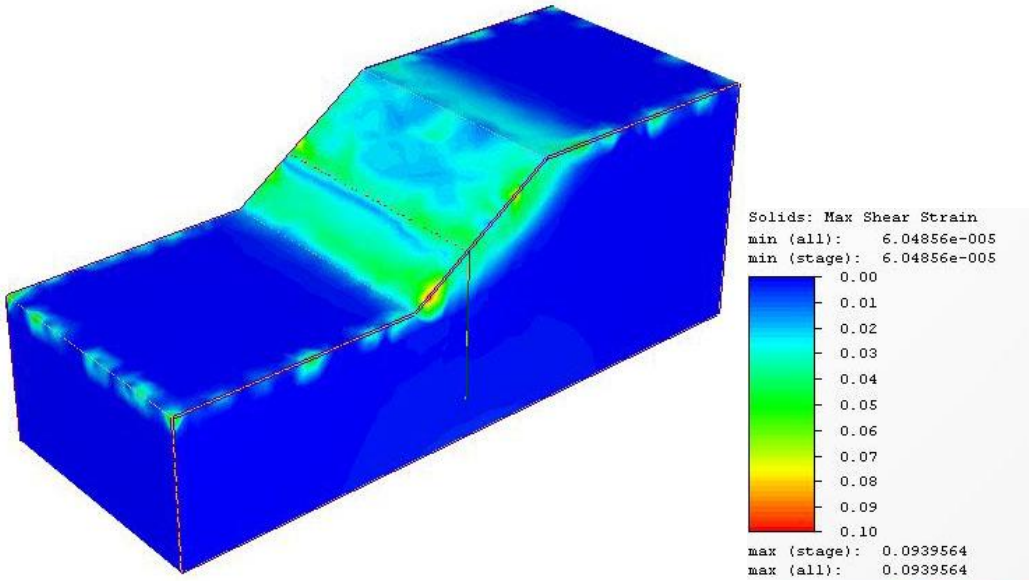

Xp=0.4

FOS	ϕ(Degrees)	C (KN/m^2)	δ_{max}	NMD	Remarks
1.0000	40.0000	2.0000	0.0680	0.9449	
1.1000	36.3636	1.8182	0.0702	0.9751	
1.2000	33.3333	1.6667	0.0726	1.0077	
1.3000	30.7692	1.5385	0.0754	1.0475	
1.4000	28.5714	1.4286	0.0804	1.1166	
1.4500	27.5862	1.3793	0.0996	1.3827	
1.4600	27.3973	1.3699	0.1280	1.7775	
1.4700	27.2109	1.3605	0.2233	3.1016	
1.5000	26.6667	1.3333	0.2596	3.6061	
1.6000	25.0000	1.2500	0.4491	6.2381	
1.6100	24.8447	1.2422	0.7557	10.4960	
1.6300	24.5399	1.2270	0.8056	11.1895	
1.6500	24.2424	1.2121	1.0592	14.7114	
1.7000	23.5294	1.1765	1.5346	21.3132	
1.8000	22.2222	1.1111	1.8358	25.4974	
1.9000	21.0526	1.0526	2.0485	28.4518	
1.9500	20.5128	1.0256	4.2036	58.3838	

Figure B.29 FOS for general slope for Xp/X=0.4 & ϕ=40 degrees

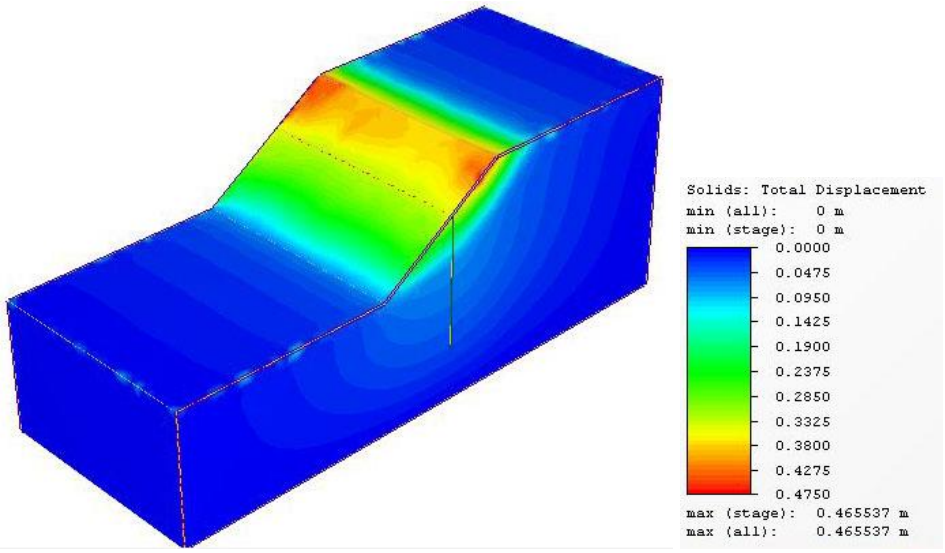

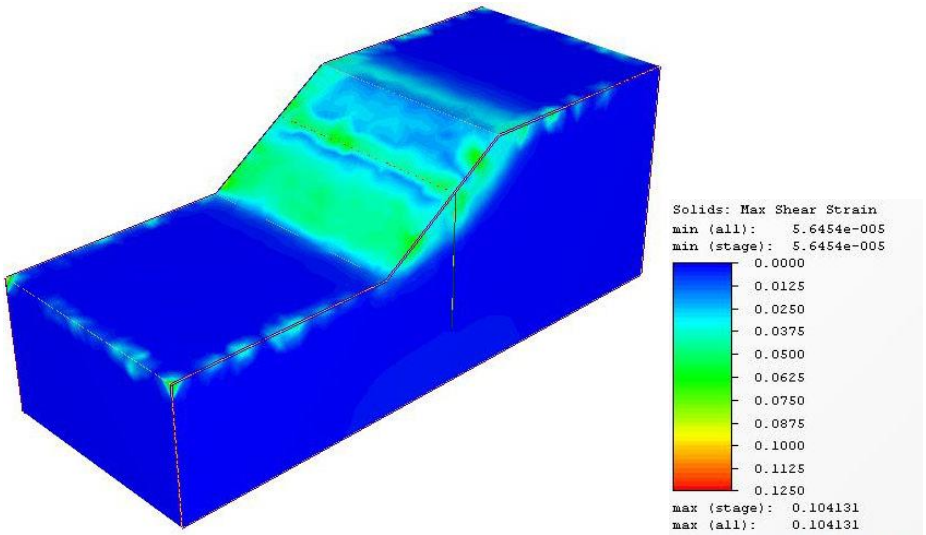

Xp=0.6

FOS	ϕ(Degrees)	C (KN/m^2)	δ_{max}	NMD	Remarks
1.0000	40.0000	2.0000	0.0672	0.9333	
1.1000	36.3636	1.8182	0.0688	0.9555	
1.2000	33.3333	1.6667	0.0702	0.9752	
1.3000	30.7692	1.5385	0.0731	1.0150	
1.4000	28.5714	1.4286	0.0774	1.0744	
1.4500	27.5862	1.3793	0.0958	1.3311	
1.4600	27.3973	1.3699	0.1142	1.5858	
1.4700	27.2109	1.3605	0.1571	2.1816	
1.4800	27.0270	1.3514	0.2120	2.9448	
1.4900	26.8456	1.3423	0.2474	3.4357	
1.5000	26.6667	1.3333	0.2243	3.1148	
1.6000	25.0000	1.2500	0.4136	5.7446	
1.6100	24.8447	1.2422	0.4655	6.4658	
1.6200	24.6914	1.2346	0.7125	9.8962	
1.6300	24.5399	1.2270	0.8614	11.9635	
1.6500	24.2424	1.2121	0.5930	8.2367	

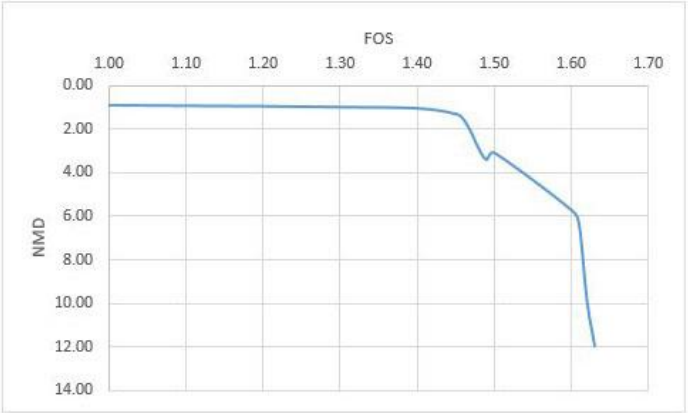

Figure B.30 FOS for general slope for Xp/X=0.6 & ϕ=40 degrees

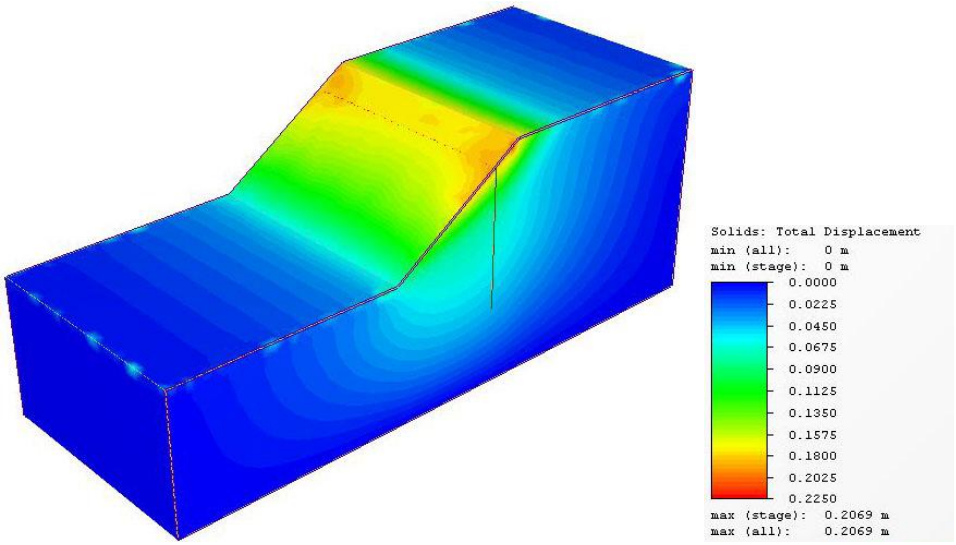

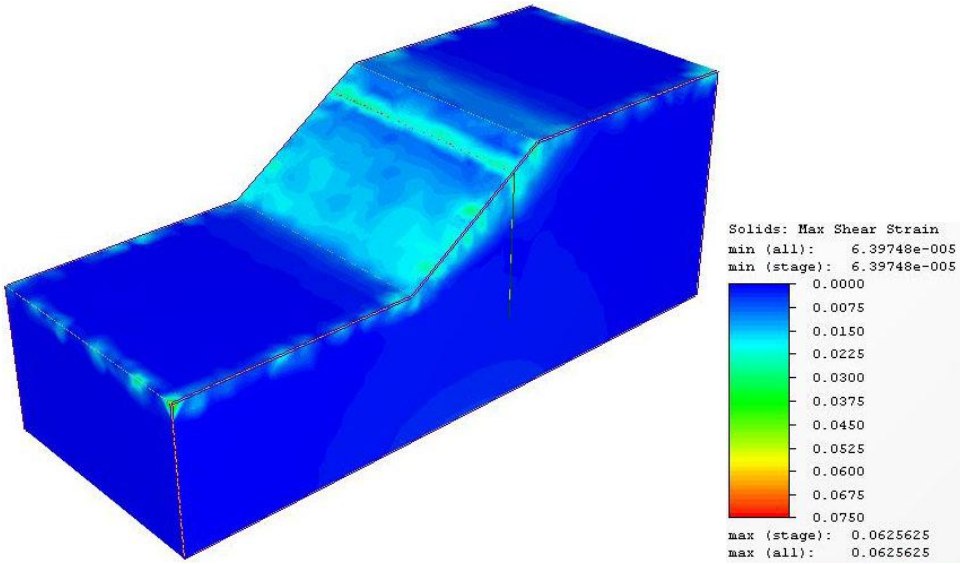

Xp=0.8

FOS	ϕ(Degrees)	C (KN/m^2)	δ_{max}	NMD	Remarks
1.0000	40.0000	2.0000	0.0672	0.9331	
1.1000	36.3636	1.8182	0.0687	0.9540	
1.2000	33.3333	1.6667	0.0701	0.9732	
1.3000	30.7692	1.5385	0.0723	1.0043	
1.4000	28.5714	1.4286	0.0766	1.0634	
1.4500	27.5862	1.3793	0.0890	1.2358	
1.5000	26.6667	1.3333	0.2432	3.3782	
1.5300	26.1438	1.3072	0.2069	2.8736	
1.5400	25.9740	1.2987	0.4340	6.0282	
1.5500	25.8065	1.2903	0.5422	7.5307	
1.6000	25.0000	1.2500	0.8301	11.5293	
1.7000	23.5294	1.1765	1.0729	14.9017	

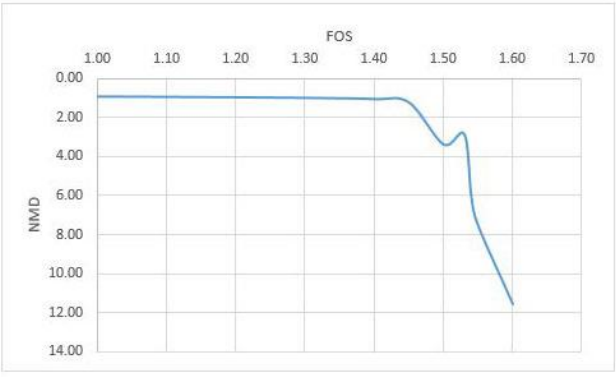

Figure B.31 FOS for general slope for Xp/X=0.8 & ϕ=40 degrees

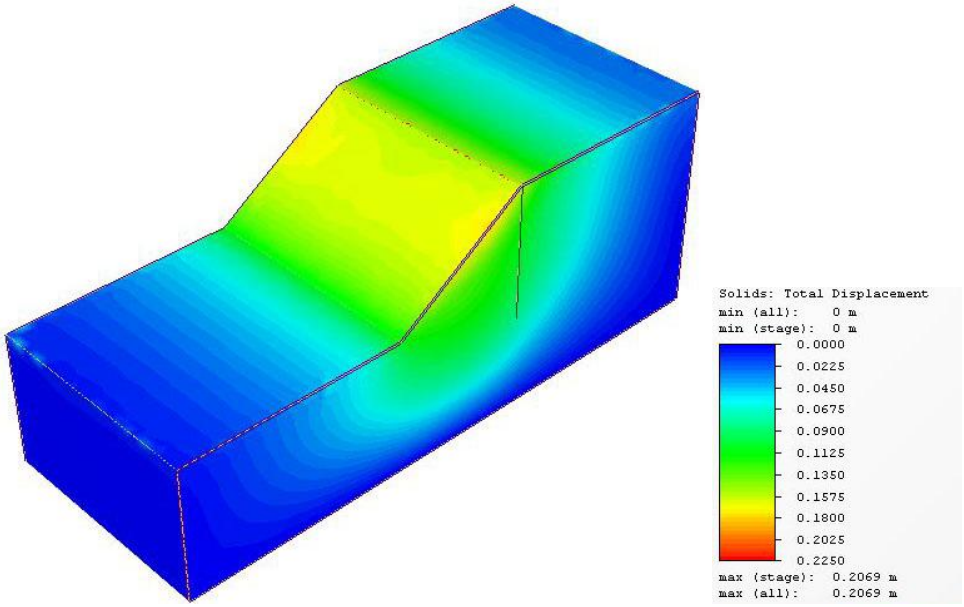

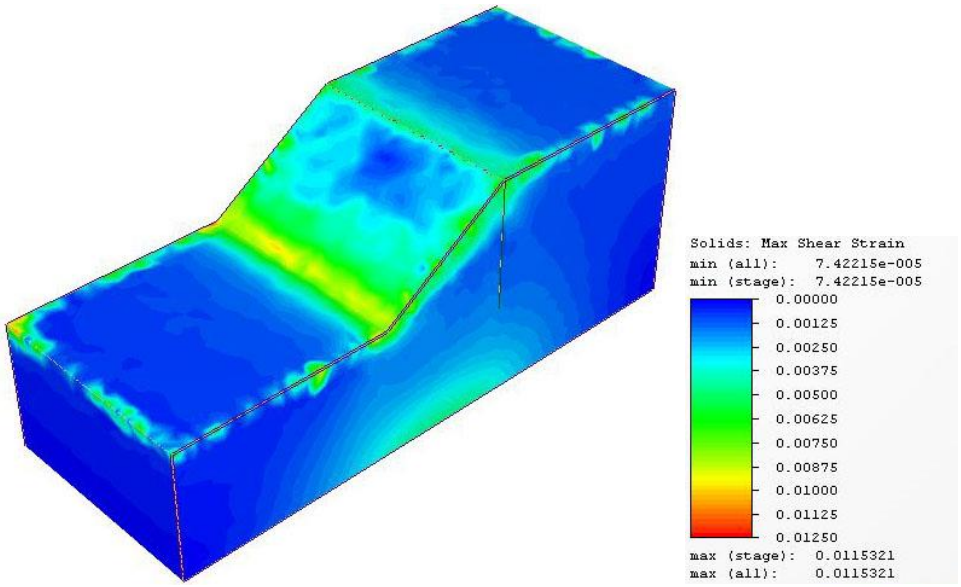

Xp=1

FOS	ϕ(Degrees)	C (KN/m^2)	δ_{max}	NMD	Remarks
1.0000	40.0000	2.0000	0.0671	0.9313	
1.1000	36.3636	1.8182	0.0684	0.9502	
1.2000	33.3333	1.6667	0.0696	0.9674	
1.3000	30.7692	1.5385	0.0715	0.9928	
1.4000	28.5714	1.4286	0.0749	1.0396	
1.4100	28.3688	1.4184	0.0761	1.0569	
1.4200	28.1690	1.4085	0.0766	1.0642	
1.4300	27.9720	1.3986	0.0780	1.0837	
1.4400	27.7778	1.3889	0.0796	1.1062	
1.4500	27.5862	1.3793	0.0859	1.1936	
1.4600	27.3973	1.3699	0.1004	1.3950	
1.4700	27.2109	1.3605	0.1731	2.4043	
1.4800	27.0270	1.3514	0.1949	2.7073	
1.4900	26.8456	1.3423	0.2071	2.8761	
1.5000	26.6667	1.3333	0.3164	4.3949	
1.6000	25.0000	1.2500	0.5581	7.7516	
1.6500	24.2424	1.2121	0.9454	13.1308	

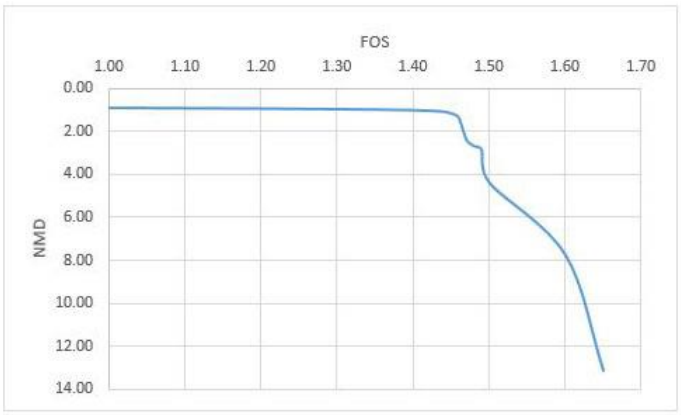

Figure B.32 FOS for general slope for Xp/X=1 & ϕ=40 degree

ANNEX C

Verification of Results

- **Verification of slope stability results for general slope without piles** *(Plaxis-3D Foundation)*

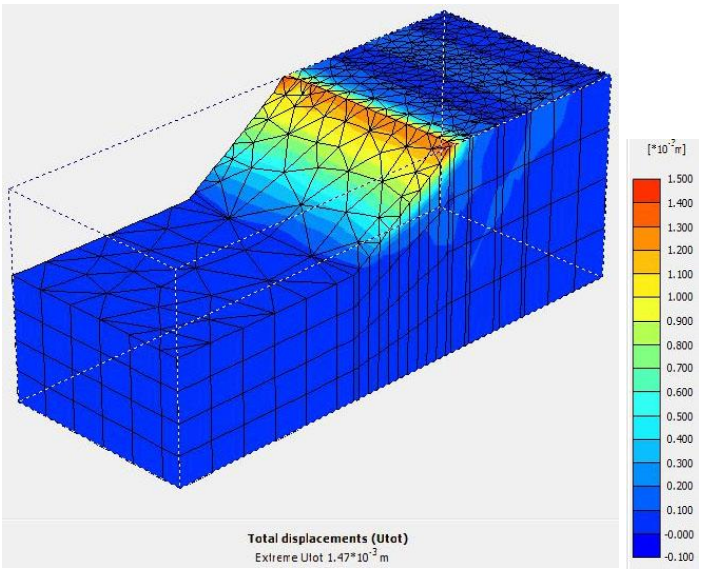

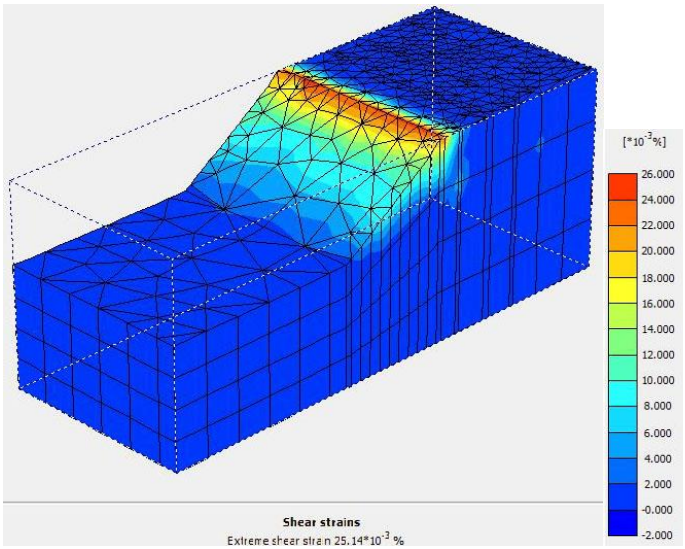

SRF	ϕ (Degrees)	C (KN/m^2)	δmax	Remarks
1	30.000	2.000	0.000186	
1.09	27.523	1.835	0.000564	
1.1	27.273	1.818	0.000642	
1.11	27.027	1.802	0.000763	
1.12	26.786	1.786	0.000933	
1.13	26.549	1.770	0.00105	
1.14	26.316	1.754	0.00119	
1.15	26.087	1.739	0.00133	
1.16	25.862	1.724	0.00147	
1.17	25.641	1.709	0.00588	
1.19	25.210	1.681	1.81	Unstable
1.2	25.000	1.667	1.69	Unstable

Figure C.1 FOS for general slope without piles for ϕ=30 degrees

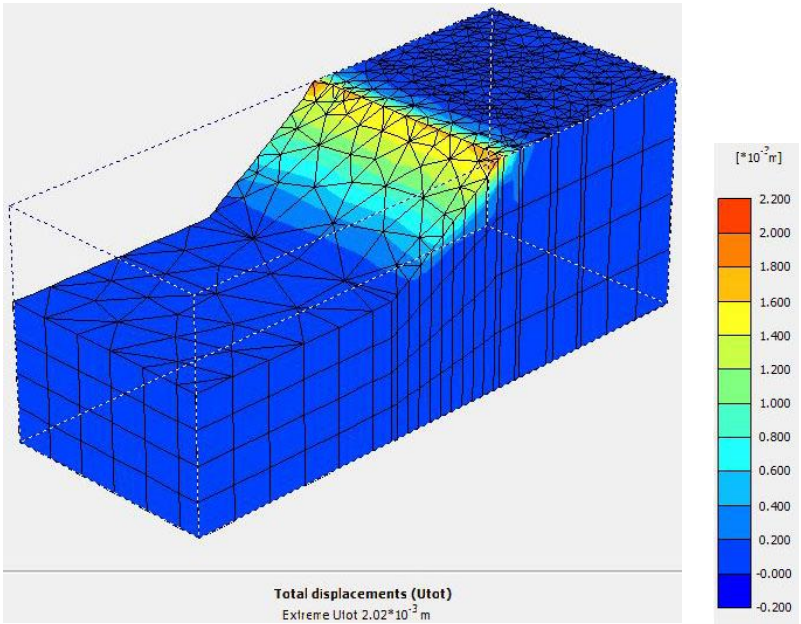

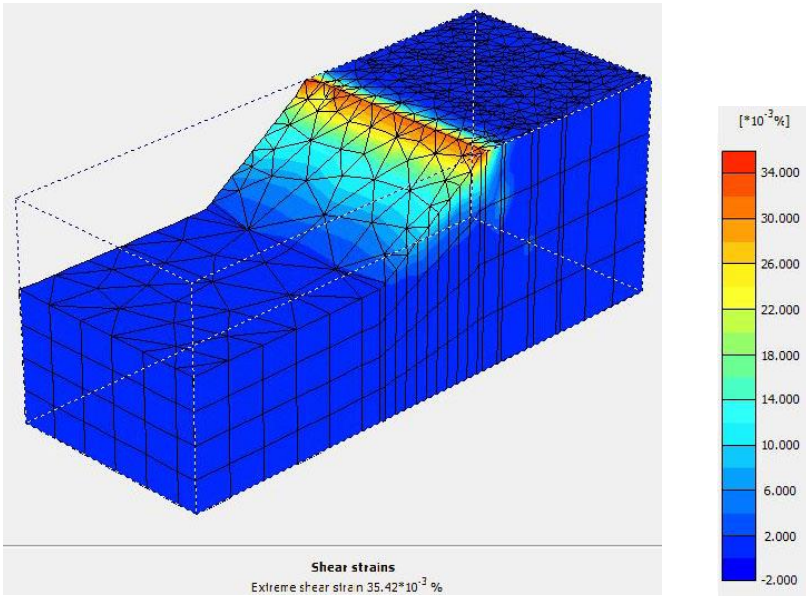

SRF	ϕ (Degrees)	C (KN/m^2)	δmax	Remarks
1	35.000	2.000	0.00013	
1.05	33.333	1.905	0.00013	
1.1	31.818	1.818	0.00012	
1.15	30.435	1.739	0.00014	
1.2	29.167	1.667	0.00201	
1.25	28.000	1.600	0.00166	
1.3	26.923	1.538	0.00108	
1.32	26.515	1.515	0.00132	
1.33	26.316	1.504	0.00202	
1.34	26.119	1.493	1.73000	
1.35	25.926	1.481	1.73000	Unstable

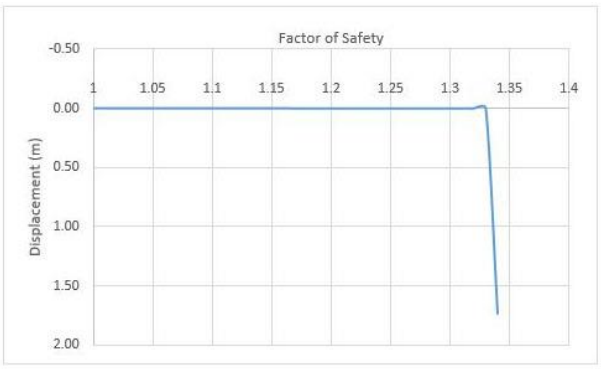

Figure C.2 FOS for general slope without piles for ϕ=35 degrees

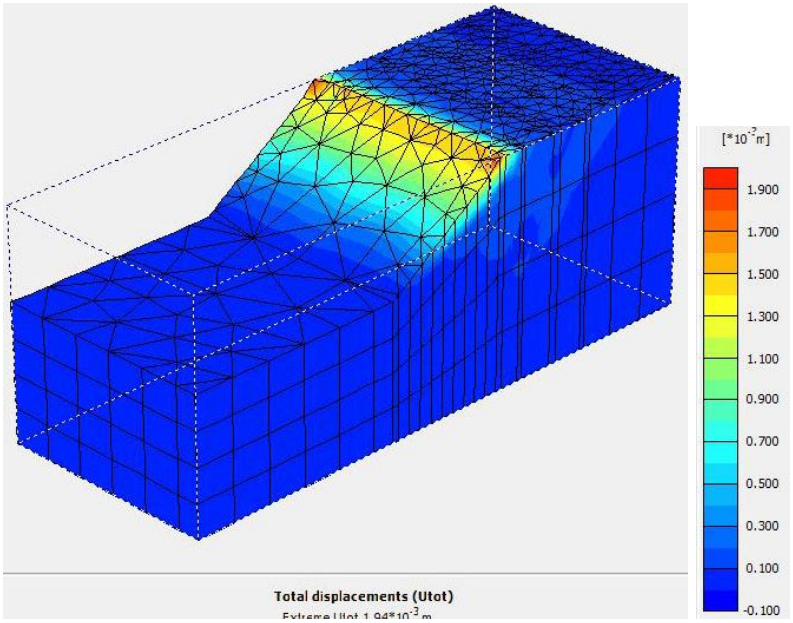

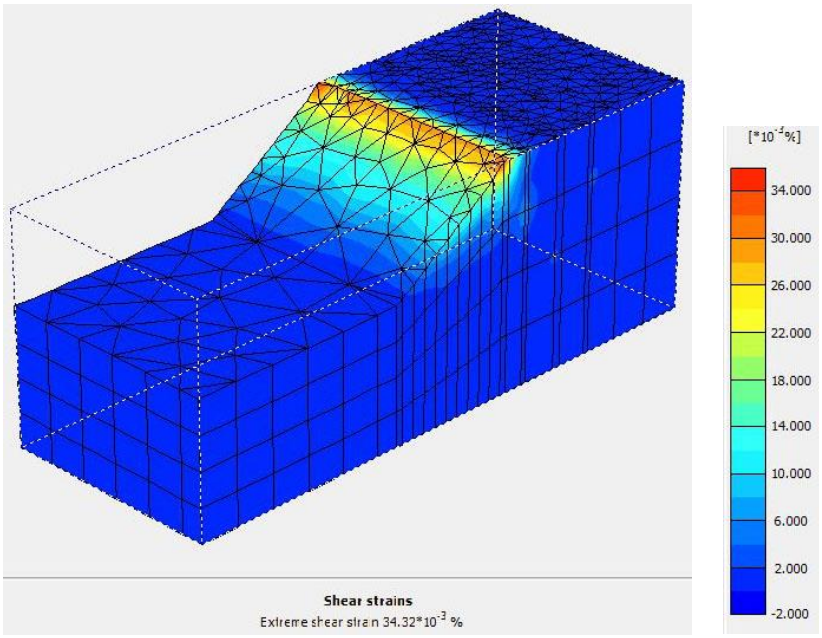

SRF	ϕ	c	δmax	Remarks
1	40.0000	2.0000	0.00013	
1.1	36.3636	1.8182	0.00015	
1.2	33.3333	1.6667	0.00010	
1.3	30.7692	1.5385	0.00012	
1.4	28.5714	1.4286	0.00645	
1.5	26.6667	1.3333	0.00194	
1.51	26.4901	1.3245	1.41	Unstable
1.55	25.8065	1.2903	2.04	Unstable

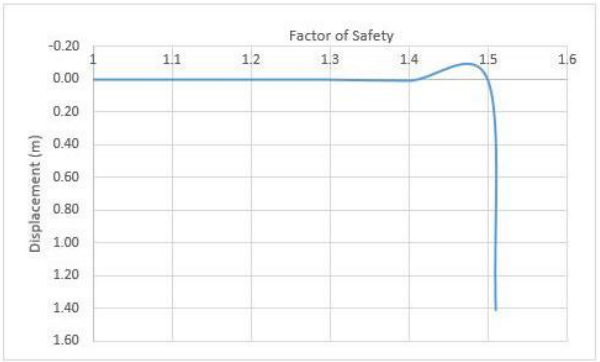

Figure C.3 FOS for general slope without piles for ϕ=40 degrees

- **Verification of parametric studies results**

(Gandhi & Ilamparuthi, 2012)

Results of Plot Digitizer for Variation of Position of Piles

Table C.1 Variation of FOS with respect position of pile for different types of sandy soil (Gandhi & Ilamparuthi, 2012)

ϕ = 30 Degrees

Xp/X	FOS
0	1.12427
0.111557	1.13975
0.185056	1.16168
0.27471	1.20889
0.398446	1.28765
0.468408	1.35708
0.498906	1.38865
0.547261	1.35684
0.642172	1.28688
0.762173	1.21684
0.896507	1.14359
1.00397	1.0831

ϕ = 35 Degrees

Xp/X	FOS
0	1.26359
0.134977	1.25999
0.186967	1.27882
0.285594	1.33867
0.387834	1.427
0.452434	1.50911
0.499077	1.55646
0.570706	1.50241
0.656667	1.44198
0.765918	1.37514
0.891295	1.30509
1.00772	1.24139

ϕ = 40 Degrees

Xp/X	FOS
0	1.44089
0.14949	1.43408
0.203276	1.45608
0.318058	1.5412
0.395192	1.61378
0.465174	1.70221
0.506438	1.74641
0.56375	1.7114
0.637159	1.64467
0.741024	1.56836
0.868193	1.4983
1.00434	1.44088

Results of Plot Digitizer for Variation of Length of Piles

Table C.2 Variation of FOS with respect length of pile for different types of sandy soil (Gandhi & Ilamparuthi, 2012)

ϕ= 30 Degrees

L/H	FOS
0	1.11399
0.24744	1.2035
0.460751	1.27063
0.635666	1.31259
0.797782	1.35455
0.959898	1.37972
1.10068	1.39091
1.43345	1.3965
1.79181	1.3965
2.12457	1.3965
2.49573	1.3993

ϕ= 35 Degrees

L/H	FOS
0.004266	1.28462
0.174915	1.35734
0.375427	1.43846
0.511945	1.48042
0.648464	1.51119
0.776451	1.53077
0.942833	1.54755
1.16468	1.55035
1.38652	1.55035
1.71075	1.54755
2.10751	1.54476
2.48294	1.55035

ϕ= 40 Degrees

L/H	FOS
0	1.47762
0.127986	1.52517
0.255973	1.57552
0.401024	1.63147
0.537543	1.66224
0.691126	1.7014
0.861775	1.72937
1.00256	1.74056
1.2628	1.74615
1.63396	1.74336
1.99659	1.74336
2.33788	1.74336
2.49573	1.74056

➢ **Verification of slope stability results of Ghurmi Slope**

(Plaxis-3D Foundation)

Without piles

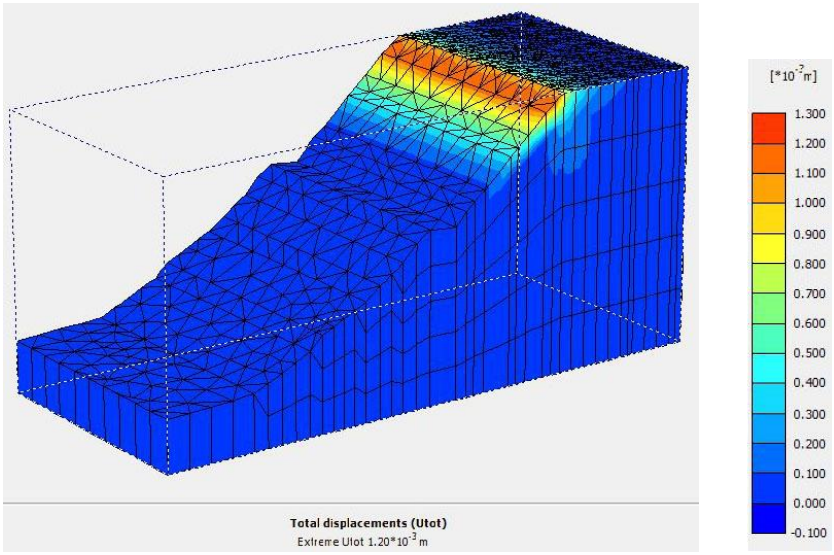

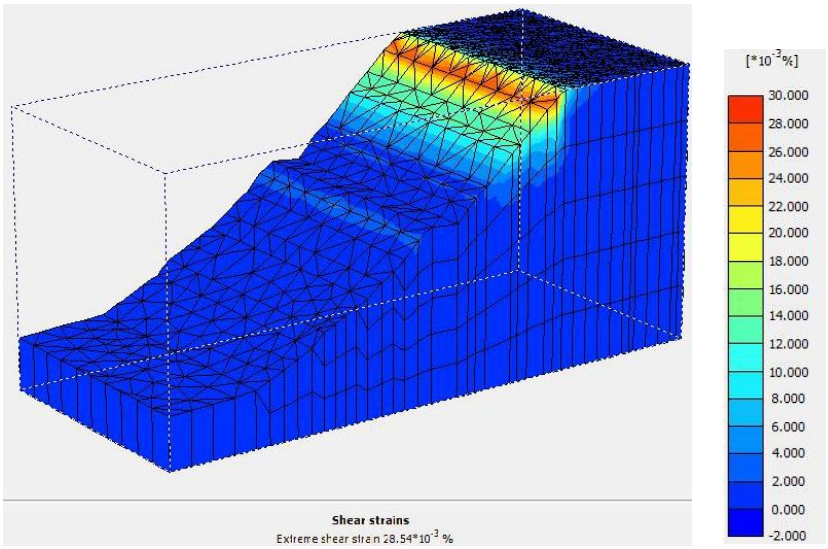

FOS	ϕ (Degrees)	C (KN/m^2)	δ_{max}	Remarks
1	36.000000	2.000000	0.000168	
1.01	35.643564	1.980198	0.000196	
1.02	35.294118	1.960784	0.000205	
1.03	34.951456	1.941748	0.000198	
1.04	34.615385	1.923077	0.000391	
1.05	34.285714	1.904762	0.001200	
1.06	33.962264	1.886792	0.092930	Unstable
1.07	33.644860	1.869159	0.041150	Unstable

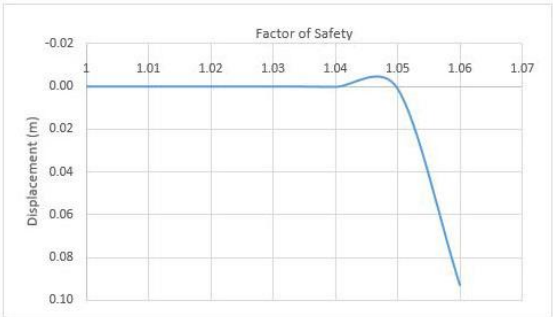

Figure C.4 Slope stability analysis of Ghurmi slope without piles

With Piles

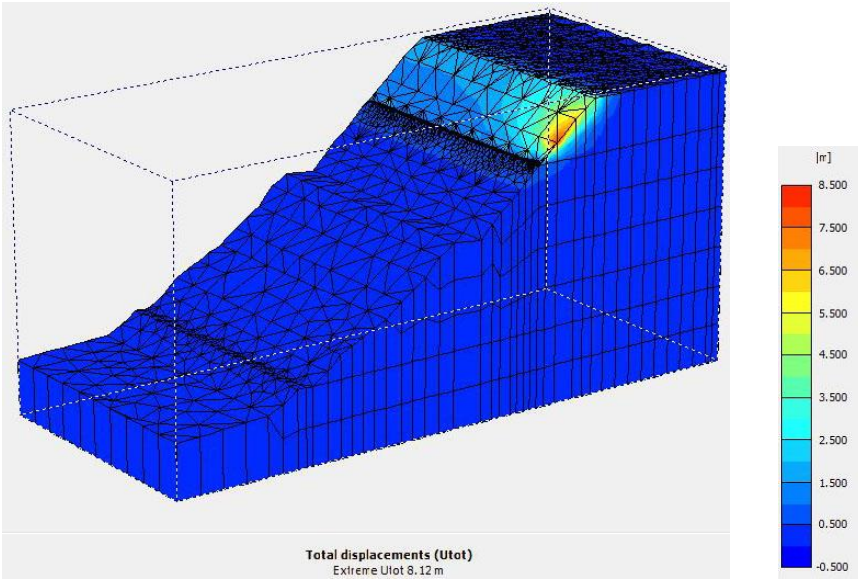

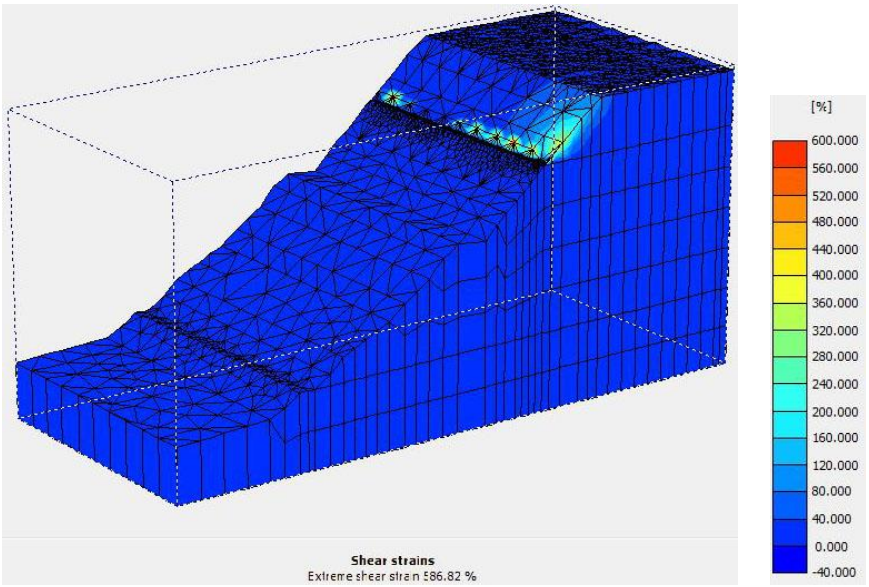

FOS	ϕ (Degrees)	C (KN/m^2)	δ_{max}	Remarks
1	36.00	2.00	0.00012	
1.05	34.29	1.90	0.202	
1.07	33.64	1.87	0.417	
1.1	32.73	1.82	6.430	
1.11	32.43	1.80	8.120	
1.12	32.14	1.79	40.920	Unstable

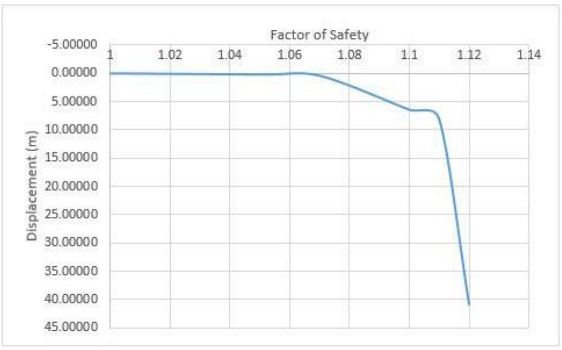

Figure C.5 Slope stability analysis of Ghrumi slope with piles